UNIVERSITÁ DEGLI STUDI DI MILANO-BICOCCA

Facoltà di Scienze Matematiche Fisiche e Naturali

Dipartimento di Biotecnologie e Bioscienze

Dottorato di ricerca in Biologia, XXVI ciclo

Regulation of cytokinesis in Saccharomyces cerevisiae

Corinne Cassani

Anno Accademico 2012-2013

UNIVERSITÁ DEGLI STUDI DI MILANO-BICOCCA

Facoltà di Scienze Matematiche Fisiche e Naturali

Dipartimento di Biotecnologie e Bioscienze

Dottorato di ricerca in Biologia, XXVI ciclo

Regulation of cytokinesis in Saccharomyces cerevisiae

Corinne Cassani

Anno Accademico 2012-2013

Regulation of cytokinesis in Saccharomyces cerevisiae

Corinne Cassani
Matricola 071794

TUTOR: DOTT.SSA ROBERTA FRASCHINI

DOTTORATO DI RICERCA IN BIOLOGIA XXVI CICLO

Università degli Studi di Milano-Bicocca
Piazza dell'Ateneo Nuovo 1, 20126, Milano

Dipartimento di Biotecnologie e Bioscienze
Piazza dela Scienza 2, 20126, Milano

Ai miei genitori e ai miei nonni,

cui devo tutto quel che sono

“Credo di poter affermare che nella ricerca scientifica né il grado di intelligenza né la capacità di eseguire e portare a termine il compito intrapreso siano fattori essenziali per la riuscita e per la soddisfazione personale. Nè l'uno nè l'altro contano maggiormente della totale dedizione e del chiudere gli occhi davanti alle difficoltà: in tal modo possiamo affrontare i problemi che altri, più critici e più acuti, non affronterebbero.”

-- **Rita Levi Montalcini**--

Index

Abstract

- Abstract **Pag. 1**

Riassunto

- Riassunto **Pag. 4**

Introduction

- The regulation of mitotic exit **Pag. 7**
- The cytokinesis **Pag. 11**
- The Dma proteins in Saccharomyces cerevisiae **Pag. 17**
- The NoCut pathway **Pag. 21**
- Vhs2 and actin **Pag. 26**
- Septins in budding yeast **Pag. 28**

Results

Saccharomyces cerevisiae Dma proteins participate in cytokinesis by controlling two different pathways

- Dma2 impairs a parallel cytokinesis pathway with respect to Hof1 **Pag. 31**
- Dma2 overproduction impairs AMR contraction and Tem1-Iqg1 interaction **Pag. 36**
- PS formation and Cyk3 localization at the bud neck are inhibited by Dma2 excess **Pag. 40**
- Tem1 ubiquitylation and the Dma proteins **Pag. 43**
- The lack of the Dma proteins impairs primary septum formation **Pag. 45**

Tem1 ubiquitylation role in AMR contraction

- Mutations in putative Tem1 ubiquitylation sites improves AMR contraction of *GAL1-DMA2* cells. **Pag. 47**

Dma1 and Dma2 role in the NoCut pathway

- The lack of the Dma proteins forces cytokinesis in *ndc10-1* cells. **Pag. 53**
- Dma1 and Dma2 proteins are involved in the NoCut pathway. **Pag. 55**
- The contemporary lack of Dma proteins and of Boi1 and Boi2 causes missegregation of chromosomes. **Pag. 57**

Search for new players in cell division control

- Vhs2 characterization **Pag. 60**
- The lack of Vhs2 causes septin ring instability **Pag. 62**

- Vhs2 levels and phosphorylation **Pag. 68**

Discussion

- *Saccharomyces cerevisiae* Dma proteins participate in cytokinesis by controlling two different pathways **Pag. 73**
- Tem1 ubiquitylation role in AMR contraction **Pag. 77**
- Dma1 and Dma2 role in the NoCut pathway **Pag. 80**
- Search for new players in cell division control **Pag. 83**

Material and methods

- Material mand methods **Pag. 87**

References

- References **Pag. 102**

Abstract

Abstract

Cytokinesis is the spatially and temporally regulated process by which, after chromosome segregation, eukaryotic cells divide their cytoplasm and membranes to produce two daughter cells independent of each other.
In the budding yeast *Saccharomyces cerevisiae* cytokinesis is driven by tightly regulated pathways that coordinate cell division with nuclear division to ensure the genetic stability during cell growth. These ways promote actomyosin ring (AMR) contraction coupled to plasma membrane constriction and to centripetal deposition of the primary septum, respectively. These pathways can partially substitute for each other, but their concomitant inactivation leads to cytokinesis block and cell death.
In animal cells, the division plane is defined by the central spindle positioning and cytokinesis occurs through the contraction of the AMR, followed by the membrane furrowing. In *S. cerevisiae*, the first step towards cytokinesis is the assembly of a rigid septin ring, which forms at the bud neck concomitantly with bud emergence as soon as cells enter S phase and marks the position where constriction between mother and daughter cell will take place at the end of mitosis. The septin ring acts as a scaffold for the recruitment other proteins, among which Myo1, the heavy chain of the type II miosin. Myo1 forms a ring at the site of bud emergence at the onset of S phase in a septin-dependent manner. At the end of anaphase, an actin ring overlaps with that of Myo1 and the resulting contractile actomyosin ring drives primary septum deposition. The septin ring also recruits Iqg1 which is important, together with Bni1, for actin recruitment at the bud neck, Cyk3, required for proper synthesis of the septum, and Hof1, which is phosphorylated in telophase and colocalizes with the actomyosin ring during cytokinesis. The subsequent degradation of Hof1 allows efficient AMR contraction and cell separation. During mitotic exit, Chs2 localizes at the cell division site, where it drives synthesis of the primary septum, composed of chitin, simultaneously with actomyosin ring contraction. Afterwards the secondary septum, which has a similar composition to yeast cell wall, is produced on both the mother and the daughter side of the bud neck. The subsequent degradation of the primary septum from the daughter-side is ensured by the RAM pathway

that is activated only in the bud. At this point mother and daughter cell separate permanently from each other leaving a chitin disk, that is the primary septum residue, called “bud scar", on the mother cell surface.
In the first chapter we describe the role in cytokinesis of the functionally redundant FHA-RING ubiquitin ligases Dma1 and Dma2, that belong to the same ubiquitin ligase family as human Chfr and Rnf8 and *Schizosaccharomyces pombe* Dma1. In particular we show that both the lack of Dma1 and Dma2 and moderate Dma2 overproduction affect actomyosin ring contraction as well as primary septum deposition, although they do not apparently alter cell cycle progression of otherwise wild type cells. In addition, overproduction of Dma2 impairs the interaction between Tem1 and Iqg1, which is thought to be required for AMR contraction, and causes asymmetric primary septum deposition as well as mislocalization of Cyk3, a positive regulator of this process. In agreement with these multiple inhibitory effects, a Dma2 excess that does not cause any apparent defect in wild-type cells leads to lethal cytokinesis block in cells lacking the Hof1 protein, which is essential for primary septum formation in the absence of Cyk3. Altogether, these findings suggest that the Dma proteins act as negative regulators of cytokinesis.
In the second chapter we show that the Ras-like GTPase Tem1 ubiquitylation is involved in AMR contraction regulation. Tem1 is not required for the actomyosin ring assembly but is required for its dynamics. In the first chapter we show how this protein undergoes cell cycle-regulated ubiquitylation, in particular the amount of ubiquitylated Tem1 decreases concomitantly with cells undergoing AMR contraction. Interestingly, high levels of Dma2 induce Tem1 ubiquitylation as well as inhibit AMR contraction. Analyzing the kinetics of AMR contraction in cells that express high levels of Dma2 and different Tem1 K-R variants (in which lysine residues were replaced by arginine residues, thus becoming not ubiquitylable), we show that Tem1 ubiquitylation seems to be important for Dma2’s AMR contraction inhibition. In particular lysines 112, 133 and 219 are mostly implicated in this regulation. Altogether, these findings suggest that the Dma proteins act as negative regulators of AMR contraction by indirectly influencing Tem1 ubiquitylation.

In the third chapter we show that Dma1 and Dma2 are involved in the NoCut pathway, a checkpoint whose activation prevents chromosome breakage during cell division. The lack of Dma proteins affects checkpoint activation in the presence of mutations that cause chromatin persistance at the division site or spindle midzone damage. Moreover, the lack of Dma1 and Dma2 causes cell growth defect in combination with the deletion of genes involved in the NoCut pathway or in the mechanisms that permit DNA breaks repair generated when the checkpoint is not totally functional. Furthermore the lack of Dma proteins, although they do not apparently alter cell cycle progression, when combined with the lack of Boi proteins (that work as abscission inhibitors in the NoCut pathway) causes a growth defect due to an increase in chromosome missegregation. Altogether, these findings suggest that the Dma proteins act in the NoCut pathway.

In the last chapther we describe the functional characterization of a new player in cell division control: Vhs2. Despite it is not essential for cells viability, we show how this protein is implicated in septins stabilizaton. The lack of Vhs2 causes cell growth defect in combination with several mutants that affect septin structure. Moreover *vhs2Δ* cells *per se* have a defect in septin stability, in fact these cells show a typical phenotype: the septins disappear from the division site before mitotic spindle disassembly, while in wild type cells septins remain until the end of cytokinesis. We also show that Vhs2 is subject to phosphorylations that decrease at the beginning of cytokinesis and that is regulated by Cdc14 phosphatase.

Riassunto

Riassunto

La citochinesi è quel processo regolato nel tempo e nello spazio tramite cui, dopo la segregazione dei cromosomi, le cellule eucariotiche dividono il loro citoplasma e le membrane per formare due cellule figlie indipendenti l'una dall'altra. Nel lievito gemmante *Saccharomyces cerevisiae* la citochinesi è promossa da vie finemente regolate che coordinano la divisione cellulare con la divisione nucleare al fine di garantire la stabilità genetica di cellule in crescita. Queste vie promuovono la contrazione dell'anello di actomiosina (AC) accoppiandola rispettivamente con la costrizione della membrana plasmatica e con la deposizione centripeta del setto primario (SP). Le vie che portano alla citochinesi sono parzialmente ridondanti e la loro contemporanea inattivazione causa un blocco della citochinesi e morte cellulare.

Nelle cellule animali, il piano di divisione è specificato dal posizionamento del fuso mitotico e la citochinesi avviene grazie alla contrazione dell'anello di actomiosina, seguita dall'invaginazione della membrana plasmatica. In *S. cerevisiae*, il primo passo verso la citochinesi è l'assemblaggio di un anello rigido di septine attorno al collo della gemma contemporaneamente all'emissione della stessa, non appena le cellule entrano in fase S, definendo la posizione in cui avrà luogo la costrizione tra la cellula madre e la figlia in seguito all'uscita dalla mitosi.

L'anello di septine funge da piattaforma di legame, al collo della gemma, per diverse proteine tra cui la catena pesante della miosina di tipo II, Myo1. Myo1 forma un anello al sito di emissione della gemma all'inizio della fase S in modo dipendente dalle septine. Alla fine dell'anafase un anello di actina si sovrappone con quello di Myo1 a generare il risultante anello di actomiosina la cui contrazione è strettamente accoppiata alla deposizione del setto primario. L'anello di septine permette la localizzazione anche di Iqg1 che, insieme a Bni1, è importante per il reclutamento dell'actina al collo della gemma, di Cyk3, richiesto per la corretta formazione del setto primario, e di Hof1, che colocalizza con l'anello di actomiosina durante la citochinesi. La successiva degradazione di Hof1 permette l'efficiente contrazione dell'anello di actomiosina e la separazione cellulare.

Durante l'uscita dalla mitosi, la chitina sintasi Chs2 si localizza al sito di divisione e sintetizza il setto primario, composto di chitina, evento cha

avviene in contemporanea con la contrazione dell'AC. Infine il setto secondario, che ha composizione simile a quella della parete di lievito, è deposto da entrambi i lati, della madre e della figlia, del setto primario. La successiva degradazione del setto primario dal solo lato della cellula figlia è garantita dal RAM pathway il quale viene attivato solo all'interno della gemma. A questo punto la cellula madre e la cellula figlia si separano definitivamente e questo processo lascia un disco di chitina (bud scar), residuo del setto primario, sulla superficie della cellula madre.

Nel primo capitolo è stato descritto il ruolo delle ubiquitine ligasi Dma1 e Dma2 nella citochinesi. Queste proteine, a funzione almeno parzialmente ridondante, appartengono alla stessa famiglia FHA-RING ubiquitina ligasi di Chfr e Rnf8 umane e di Dma1 di *Schizosaccharomyce pombe*. In particolare abbiamo dimostrato che sia la mancanza di Dma1 e Dma2 che la moderata sovraproduzione di Dma2, nonostante non causino alterazioni nella progressione del ciclo cellulare, inficiano la contrazione dell'anello di actomiosina e la deposizione del setto primario. Inoltre, la moderata sovraproduzione di Dma2 impedisce l'interazione tra Tem1 e Iqg1, la quale è richiesta per la contrazione dell'AC, e causa la deposizione asimmetrica del setto primario nonché la delocalizzazione di Cyk3, un regolatore positivo di questo processo. Nell'insieme queste scoperte suggeriscono che le proteine Dma agiscono come dei regolatori negativi della citochinesi.

Nel secondo capitolo è stato mostrato che l'ubiquitinazione della GTPasi Ras-like Tem1 è coinvolta nella regolazione della contrazione dell'anello di actomiosina. Tem1 non è richiesta per l'assemblaggio dell'AC ma per la sua dinamica. Nel primo capitolo abbiamo mostrato come questa proteina venga sottoposta ad ubiquitinazione ciclo-cellulare dipendente, in particolare la quantità di Tem1 ubiquitinata decresce quando le cellule iniziano a contrarre l'anello di actomiosina. In particolare, alti livelli di Dma2 inducono l'ubiquitinazione di Tem1, come anche l'inibizione della contrazione dell'AC. Analizzando le cinetiche di contrazione dell'AC in cellule che esprimono alti livelli di Dma2 e diverse varianti di Tem1 K-R (in cui i residui di lisina sono stati sostituiti con arginine, rendendo così la proteina non ubiquitinabile), abbiamo dimostrato che l'ubiquitinazione di Tem1 sembra essere importante per l'inibizione Dma-dipendente della contrazione dell'anello di actomiosina. In particolare le lisine 112, 133 e

219 sembrano essere maggiormente implicate in questo processo. Nell'insieme questi dati suggeriscono che le proteine Dma agiscono come regolatori negativi della contrazione dell'AC influenzando in modo indiretto l'ubiquitinazione di Tem1.
Nel terzo capitolo è stato mostrato come Dma1 e Dma2 sono coinvolte nel NoCut pathway, un checkpoint la cui attivazione previene la rottura dei cromosomi durante la divisione cellulare. La mancanza delle proteine Dma inficia l'attivazione del checkpoint in presenza di mutazioni che causano la permanenza di cromatina a livello del sito di divisione o danni alla zona centrale del fuso. Inoltre, la mancanza di Dma1 e Dma2 causa difetti di crescita se combinata con la delezione di geni coinvolti nel NoCut pathway o nei meccanismi che permettono la riparazione delle rotture del DNA che si vengono a generare quando il checkpoint non è perfettamente funzionante. Inoltre la mancanza delle proteine Dma, nonostante non sembra alterare la progressione del ciclo cellulare, quando combinata con la mancanza delle proteine Boi (le quali agiscono da inibitori dell'abscissione nel NoCut pathway) causa difetti di crescita dovuti ad un aumento della missegregazione cromosomica. Nell'insieme questi dati suggeriscono che le proteine Dma sono coinvolte nell'attivazione del NoCut pathway.
Nell'ultimo capitolo è illustrata l'analisi della funzione di un nuovo fattore che regola la divisione cellulare: Vhs2. Nonostante questa proteina non sia essenziale per la vitalità cellulare, abbiamo dimostrato la sua implicazione nella stabilizzazione delle strutture generate dalle septine. La mancanza di Vhs2 causa difetti di crescita se combinata con diversi mutanti che affliggono la stabilità di queste strutture. Inoltre le cellule *vhs2Δ* mostrano *per se* un difetto nella stabilità delle septine infatti queste cellule mostrano un fenotipo tipico: le septine spariscono dal sito di divisione prima che il fuso venga disassemblato, mentre nelle cellule selvatiche le septine permangono fino alla fine della citochinesi. Abbiamo inoltre mostrato che Vhs2 è una proteina fosforilata e la sua fosforilazione decresce all'inizio della citochinesi ed è regolata dalla fosfatasi Cdc14.

Introduction

The regulation of mitotic exit

Mitosis is the phase of the cell cycle that leads to the balanced subdivision of the duplicated genome in two nuclei of an eukaryotic cell, this event allows the mother cell to give rise to two daughter cells that are genetically identical to each other. In order to be stably transmitted during cell division, the replicated chromosomes must be partitioned equally between the two progeny cells during each round of mitosis. This is accomplished by the segregation of sister chromatids in opposite directions, followed by physical division of the cell between the two chromosome sets. So, in order to maintain genetic stability, exit from mitosis and cytokinesis must be coupled with nuclear division.

In budding yeast chromosomal segregation occurs across a narrow constriction (called bud neck) between the mother and the bud. Spindle assembly and elongation begin in the mother cell while the bud grows; then one of the spindle poles is 'dragged' across the bud neck and the spindle adopts an orientation roughly parallel to the mother-bud axis. In this way, elongation of the spindle leads to segregation of duplicated chromosomes to the opposite sides of the bud neck. Only afterwards spindle disassembly and cytokinesis can occur.

The key event that promotes mitotic exit in *Saccharomyces cerevisiae* is the sustained activation of Cdc14, a phosphatase that targets cyclin-dependent kinase (CDK) substrates for reversal of their phosphorylated state. The major role of Cdc14 in the completion of anaphase is to dephosphorylate Cdh1, required for the degradation of the mitotic cyclins, and Sic1, an inhibitor of the yeast cyclin-dependent kinase Cdc28 (Visintin et al., 1998; Zachariae et al., 1998). These events lead to inactivation of CDKs, the ultimate event required for mitotic exit (Sullivan et al., 2007). Cdc14 remains inactive in the nucleolus by the interaction with its inhibitor Cfi1/Net1 (Weiss 2012). After anaphase onset, two signaling pathways sequentially control Cdc14 release: the FEAR network induces the partial release and afterwards the mitotic exit network (MEN) allows the complete release of Cdc14 from the nucleolus throughout the cell, bringing about mitotic exit (Bosl et al., 2005). Given the crucial role of Cdc14 in Cdh1 and Sic1 dephosphorylation, cells rely on the mitotic exit network to undergo cytokinesis and enter the next cell cycle.

As shown in figure 1A, activation of the MEN cascade is controlled by Tem1, a small GTPase localized to the spindle pole body (SPB), the yeast equivalent of animal centrosome. Tem1 is downregulated by Bub2-Bfa1, a two-component GTPase-activating protein (GAP) that stimulates hydrolysis of Tem1-bound GTP. This GAP is controlled by two kinases acting antagonistically. Phosphorylation of Bfa1 by the polo kinase Cdc5 inhibits the GAP, rendering Tem1 active (Weiss 2012). A second kinase confined to the mother cell, Kin4, antagonizes Cdc5 action, thus indirectly inhibiting Tem1 (Weiss 2012). Moreover the protein phosphatase PP2A, in complex with its regulatory subunit Rts1, is required both for Kin4's localization and Cdc5 inhibition (Chan and Amon 2010). Additionally, the bud neck localized protein kinase Elm1 activates Kin4 by phosphorilation (Weiss 2012) (Fig. 1A).

By contrast Lte1, a Tem1 positive regulator, is restricted to the bud cortex (Fig. 1B). Furthermore, correct spindle alignment instructs Bub2–Bfa1 asymmetric binding at the SPB destined for the bud. In this way, the SPB can sense negative and positive signals compartmentalized in the mother cell or the bud, respectively, as it transits through the bud neck. This surveillance system is known as the spindle position orientation checkpoint (SPOC) (Caydasi et al., 2010). Once the SPB enters the bud (dSPB), Tem1 escapes Kin4 inhibition and is activated by Lte1, although the precise mode of activation is unclear, so position-dependent Tem1 activation is an elegant way of ensuring that cells only exit mitosis and initiate cytokinesis when one of spindle pole bodies is in the bud (Fig. 1B).

Active GTP-bound Tem1 recruits MEN components to the SPB, starting with the kinase at the top of the cascade, Cdc15. This is followed by activation of the kinase Dbf2-Mob1, partly responsible for the release of Cdc14 from the nucleous to the cytoplasm, the hallmark of MEN activation (Segal 2011) (Fig. 1A). The subcellular localization of MEN components is critical for their activation and function in response to proper spindle position and it is largely accomplished throught their association with the centriolin-related SPB protein Nud1 (Luca et al., 2001; Yoshida et al., 2002).

Work over the past few years showed that MEN conponents and Cdc14 also concentrate at the cytokinesis site just prior to actomyosin ring contraction and septation and have a direct role in promoting cytokinesis by acting upon components of the AMR and cell separation machineries (Fig. 1B).

With the drop of mitotic Cdk1 activity, MEN kinases including Cdc15, Dbf2-Mob1 and Dbf20-Mob1 accumulate at the bud neck (Caydasi at al., 2010; Hwa Lim et al., 2003). The analysis of peculiar MEN mutants that are permissive for mitotic exit, revealed abnormalities in cytokinetic events related to septin and AMR behavior (Menssen et al., 2001; Luca et al., 2001; Lippincott et al., 2001). In fact Dbf2-Mob1 and Cdc5 kinases act on different cytokinetic proteins like Hof1 and Chs2 in order to regulate their activity (Meitinger et al., 2013; Oh et al., 2012). Furthermore Tem1 was shown to be implicated in AMR contraction signalling by interacting with the GAP-related domain of Iqg1 (Shannon et al., 1999). Moreover activation of Cdc14 result in the reorganization of the actin cytoskeleton toward the bud neck maybe by regulating the formins Bnr1 and Bni1. This actin binding proteins are partially redundant and are required for the formation of the actin ring during cytokinesis (Vallen et al., 2000). In addition Cdc14 also dephosphorylates the chitin sintase Chs2 in order to allow its relocalization from the ER to the bud neck by reverting Cdk1 phosphorilation (Meitinger et al, 2012).
It is important to point out that MEN components are highly conserved in other yeast species and higher eukaryotes; the subcellular distribution and functional analysis of the homologs are highly indicative of their functions in the control of exit from mitosis and/or cytokinesis (Meitinger et al, 2012).

A

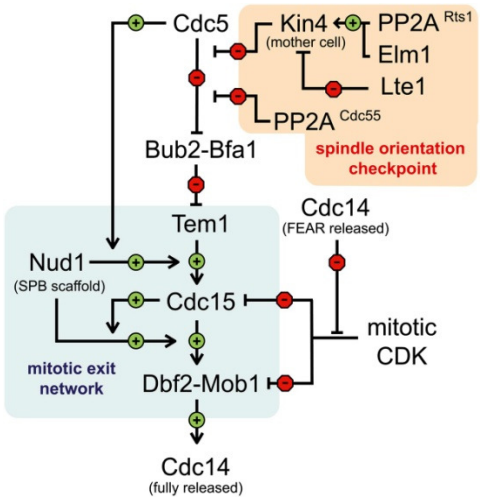

B

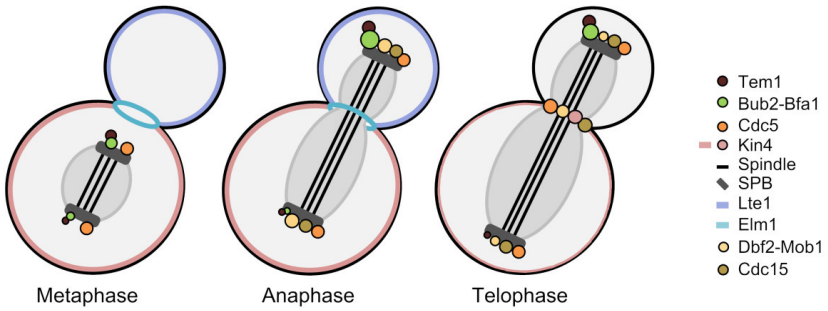

Figure 1. Localization of SPOC and MEN proteins.
(**A**) positive interactions in the MEN pathway are indicated as pointed arrows, and negative ones as block arrows. See text for details (Picture from Weiss 2012). (**B**) Localization of indicated SPOC and MEN proteins are shown in different phases of mitosis. Bfa1-Bub2 and Tem1 mainly localize at the dSPB (daughter SPB). Cdc15, Dbf2-Mob1 and Cdc5 are recruited to both SPBs during late anaphase and relocate to the bud neck in late telophase. Lte1 localizes to the bud-cortex and cytoplasm from G1/S to M phases. However in telophase, shortly before cytokinesis, Lte1 diffuses into the cytoplasm of the daughter and mother cells equally. Kin4 localizes to the mother cell cortex throughout the cell cycle and to the mSPB (mother SPB) in anaphase for a short time, and accumulates at the bud neck in telophase. Elm1 localizes to the bud neck in mitosis but dissociates from there during telophase. (Picture from Caydasi, Ibrahim and Pereira; 2010)

The cytokinesis

Cytokinesis is the spatially and temporally regulated process by which, after chromosome segregation, eukaryotic cells divide their cytoplasm and membranes to produce two daughter cells. Not all cells type divide symmetrically. Indeed, asymmetric division is widespread in nature and generates daughter cells different from mother cells in shape and/or in fate (Fig. 2).

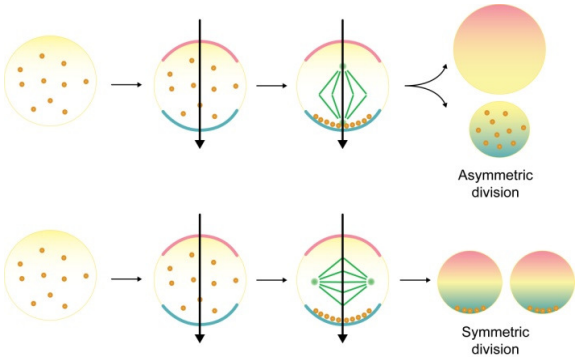

Figure 2. Relationship between the mitotic spindle orientation and the asymmetric outcome of a cell division.
To make an asymmetric cell division, the position of the mitotic spindle has to be tightly coordinated with the cortical polarity, so that daughter cells will be properly positioned within the tissue, will inherit unequal sets of fate determinants and follow differential fates. See text for details.
(Picture from http://www.ifom-ieo-campus.it/research/mapelli.php)

This mode of division is typical of many unicellular organisms both prokaryotic (*Caulobacter crescentus*) and eukaryotic (*Saccharomyces cerevisiae*), and it is also very important for the development of the embryo of multicellular eukaryotes. Moreover, staminal cells of adult organisms divide asymmetrically in order to generate daughter cells destined to differentiate, while the mother cells retain the ability to divide in an undifferentiated way. The proper execution of asymmetric divisions is also crucial in generating tissue diversity during development, as well as for tissue homeostasis and regeneration in adult organisms. During asymmetrical division, the cells determine cell polarity locating unevenly specific factors in certain positions in the cell. Subsequently, the mitotic spindle is positioned along the axis of polarity, specifying the division plane (Fig. 2). In this way, the factors that determinate the fate of a cell segregate

in only one of the two cells arising from division, making it different from the other. Also *Saccharomyces cerevisiae*, well known as an excellent model organism for studies on the cell cycle, divides asymmetrically producing a daughter cell that originates as a bud from the body of the mother cell and that, at the time of the division, is smallest than the mother cell (Fig. 3B). Unlike in the multicellular eukaryotic cells, where the division site and the type of division (symmetrical or asymmetrical) is estabilished by the central spindle positioning (Fig. 3A), the axis of polarity in budding yeast is established during the G1 phase of the cell cycle through the localization of factors that determine the bud emergency site, which is also the site where cell division will take place. Since the bud site selection occurs before SPBs duplication and spindle assembly, in order to ensure the proper segregation of chromosomes, the mitotic spindle must then be correctly positioned along the mother-bud axis before nuclear division.

A

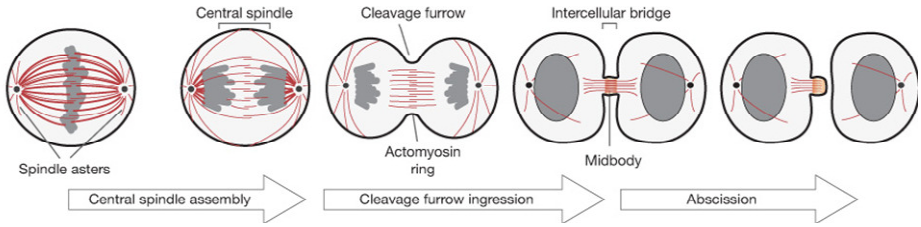

B

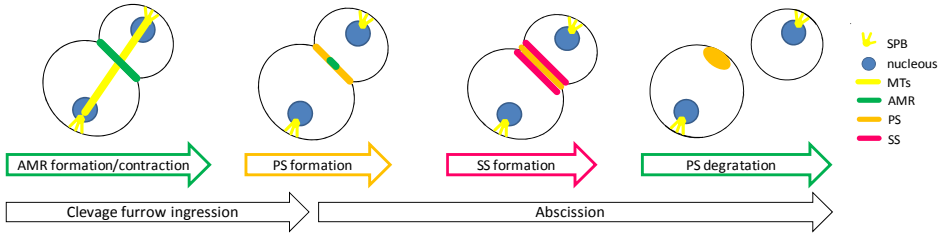

Figure 3. Cytokinesis in animal and budding yeast cells.
(**A**) Cytokinesis in animal cells requires the formation of an actomyosin ring (AMR) below the plasma membrane, as well as its contraction that allows clevage furrow ingression. The contraction continues until the reaching of the midbody structure, then the intercellular bridge is cut in order to allow separation. (Picture from Fededa and Gerlich 2012). (**B**) In *S. cerevisiae* the cytokinesis requires the formation of an AMR below the plasma membrane at the bud neck, as well as its contraction coupled with primary septum (PS) deposition. After PS deposition secondary septum (SS) synthesis occurs. At the end, degradation of PS from the daugther side allows cell separation. See text for details.

Although cytokinesis modes appear to be different among species, several cytokinesis factors and mechanisms are evolutionarily conserved. Cytokinesis in the budding yeast involves the same broadly conserved cleavage furrow mechanism that is found in metazoans, where contraction of an actomyosin ring (AMR) leads to membrane furrowing and subsequent cell division (Pollard et al., 2010). While in animal cells the AMR contraction proceeds reaching the midbody structure (central region of the intracellular bridge where the overlapping antiparallel bundles of microtubules are covered by an elecrton-dense matrix), and the postmitotic sister cells remain connected by an intracellular bridge that is subsequentially cut during abscission (Fig. 2A); in *S. cerevisiae* the AMR contracts completely and this process is tightly coupled with primary septum (PS) deposition. PS is the first physical barrier that is deposed between the mother and the daughter cell, then the abscission is accomplished by the secondary septum (SS) formation. Then, physical separation of cells is completed by PS degradation only from the daughter side. This process leaves a chitin scar, called bud scar, on mother cell surface (Fig. 2B).

The subcellular localization of the components of the budding yeast cytokinetic machinery is tightly controlled and follows a hierarchical order of assembly to the mother-bud neck during the cell cycle (Fig. 4).

The first step is the assembly of a rigid, hourglass shaped septin structure, which forms at the bud neck concomitantly with bud emergence as soon as cells enter S phase, thus marking the position where constriction between mother and daughter cell will take place at the end of mitosis. The septin ring, which appears to be essential for cytokinesis in both fungal and animal cells (Longtine et al., 1996) serves as a scaffold for recruiting other proteins at the bud neck (See the last paragraph for details). Among them, the chitin synthase Chs3 builds a chitin ring, which is important for the integrity of the division site around the neck of the emergent bud (Shaw et al., 1991). Septins also recruit the only *S. cerevisiae* type II myosin, Myo1, which forms a ring at the presumptive bud site during early S phase, and whose localization depends on septins-binding protein Bni5 before cytokinesis, while it is controlled by the essential light chain (ELC) of myosin-II protein Mlc1 and by the IQ-GTPase activating protein (GAP) Iqg1 during cytokinesis. (Lee et al., 2002; Epp and Chant, 1997; Lippincott and Li, 1998; Fang et al., 2010).

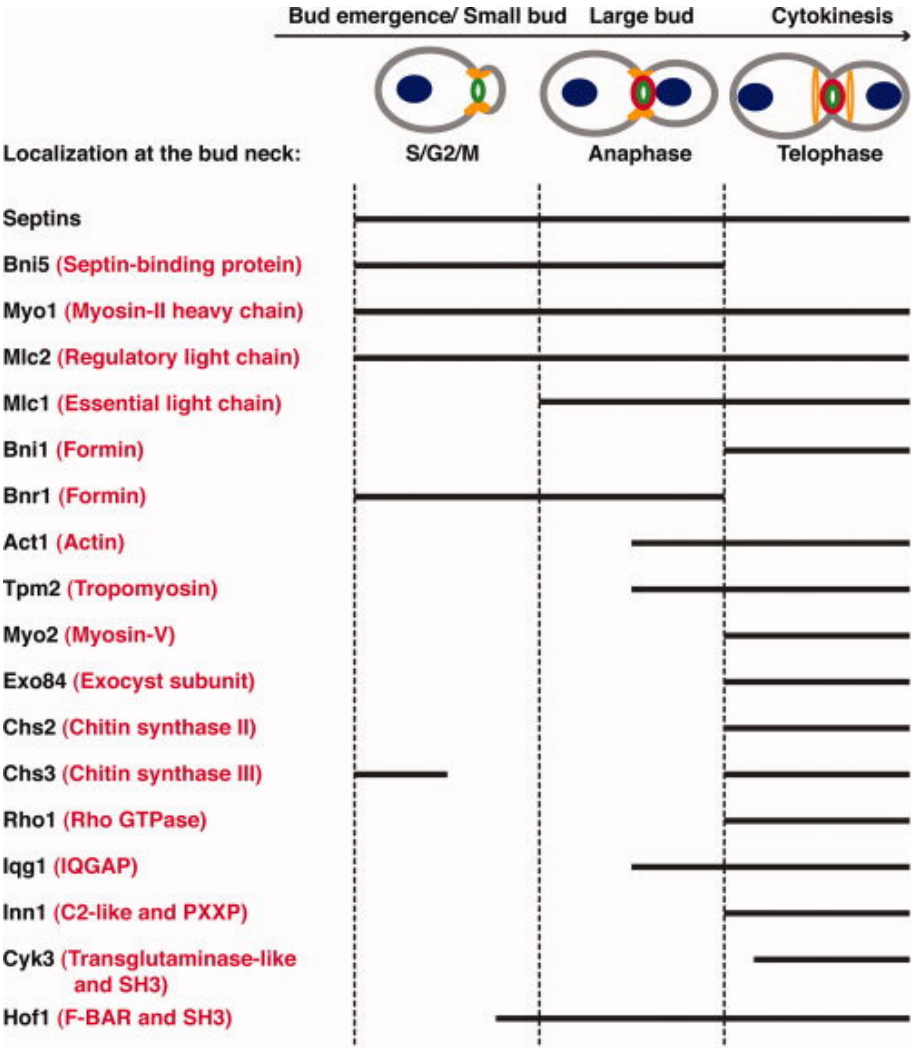

Figure 4. Localization of core cytokinesis proteins during the cell cycle.
The generic names of the proteins or their key domains/motifs are indicated in red in the parentheses. For the cell diagrams, blue, nucleus; orange, septin hourglass or rings; green, Myo1; and red, actin ring. See text for details. (Picture from Wloka and Bi., 2012)

The Myo1 ring persists at the motherbud neck until the end of anaphase, when a coincident F-actin ring assembles by capture of actin filaments by the CHD of Iqg1 (Wloka and Bi 2012). The resulting AMR contracts symmetrically, after the rigid septin hourglass has split into two rings, thus accomplishing centripetal septum formation (Bi et al., 1998; Lippincott et

al., 1998). In budding yeast, the targeting of vesicle not only increases the surface area at the division site but also delivers enzymatic cargoes such as Chs2 (Bi and Park, 2012). Indeed, after mitotic exit, chitin synthase Chs2 is recruited to the neck to build the PS (Chin et al., 2012), which is mostly made of chitin. Once the cytokinetic apparatus is fully assembled, AMR contraction, membrane invagination, and PS synthesis all begin almost immediately. At either side of the completed PS structure secondary septa, which are made of the same components as the cell wall (1,3-β-D-glucans and mannoproteins), are then synthetized by the action of enzymes like glucan synthase (Lesage et al., 2005). Once cytokinesis is complete, the separation between mother and daughter cell is accomplished by the action of the endochitinase Cts1 and several glucanases. The daughter cell-specific transcriptional factor Ace2 controls the expression of both chitinase and endoglucanases. The asymmetric localization and activation of Ace2 depends in the RAM pathway, a conserved signaling network known to play a role in polarized cell growth and separation (Colman-Lerner et al., 2001; Nelson et al., 2003; Mazanka et al., 2008). This asymmetric localization allows the degradation of the PS only from the daughter side (Yeong et al., 2005).

The complex pathways leading to cytokinesis completion in budding yeast appear to be tightly interconnected and partially redundant. Indeed, the AMR is involved in constricting the plasma membrane at the division site to complete closure (Bi et al., 1998; Lippincott et al., 1998), and AMR contraction is coupled to the centripetal growth of the PS. However, AMR contraction is not essential for cytokinesis and Myo1 is not essential for cell viability in some yeast strains but is required for efficient cytokinesis and cell separation (Bi et al., 1998). In its absence, cytokinesis can be completed by AMR-independent pathways, which likely lead to an asymmetric remedial septum deposition that allows cell separation and survival (Bi et al., 1998). While Iqg1 and the formins Bni1 and Bnr1 are all required for AMR construction, the Hof1 and Cyk3 factors appear to function in a parallel pathway that coordinates septum formation (Bi et al., 2001; Lippincott et al., 1998; Vallen et al., 2000). Hof1, which is a member of the evolutionarily conserved PCH protein family, can associate with septin ring from G2 to anaphase; it is phosphorylated at telophase and colocalizes with the AMR during cytokinesis (Vallen et al., 2000; Meitinger et al., 2011). Efficient AMR contraction and cell separation are allowed by

subsequent degradation of Hof1 by the SCF (Grr1) complex, which thus functions as an adaptor linking the septum synthesis machinery to the actomyosin system (Blondel et al., 2005). On the other hand, the SH3-domain protein Cyk3 was identified as a high-dosage suppressor of lethality caused by deletion of either *IQG1* (Korinek et al., 2000) or *MYO1* (Ko et al., 2007), and Cyk3 has been recently shown to be a strong activator of Chs2 *in vivo* (Oh et al., 2012). Moreover, Hof1 and Cyk3 function redundantly in Myo1- and Iqg1-independent recruitment to the bud neck in telophase of Inn1, an essential protein which is required for chitin synthase activation, leading to PS formation (Sanchez-diaz et al., 2008; Jendretzki et al., 2009; Nishihama et al., 2009). Notewhorthy, localization at the bud neck of Inn1, which is essential for cytokinesis completion, takes place independently of AMR in cells overexpressing *CYK3* (Jendretzki et al., 2009), indicating a central role for Cyk3 in a cytokinesis rescue mechanism in the absence of functional AMR.

As described in the first paragraph, in the last years several MEN components have been implicated in the regulation of cytokinesis at different levels. In particular they can regulate some key proteins of cytokinesis process. In this context, during PS depositon, Dbf2 localizes to the division site as PS synthesis proceeds and appears to enhance Chs2's synthesis of chitin. The phosphorylation of Chs2 by Dbf2 kinase is also important for efficient dissociation of Chs2 from division site, suggesting that Dbf2's enhancement of PS synthesis ultimately helps to turn the process off (Oh et al., 2012). Coordinated phosphorylations by MEN kinases Mob1-Dbf2 and Cdc5, together with mitotic CDK, control the localization of Hof1 before AMR contraction (Meitinger et al., 2010-2011). The overall effect of this regulation is to shift Hof1 from septin-bound pool to an AMR association. As result, Inn1 and Cyk3 promote the localized activity of Chs2 and thus growth of the PS in concert with AMR contraction. This interaction requires Cdc14, which removes mitotic CDK phosphorylations on Inn1 that block its interaction with Cyk3's SH3 domain (Palani et al., 2012).

The Dma proteins in Saccharomyces cerevisiae

The modifications of proteins by the covalent attachment of ubiquitin is a regolatory process that exists in all eukaryotic cells. The different fates of ubiquitylated proteins are defined by the nature of ubiquitin modifications; a single ubiquitin is often insufficient to target the substrate to degradation but it is used as regulation signal, whereas substrates linked to a poly-ubiquitin chain can be preferentially targeted to degradation by the proteasome. Ubiquitin is usually attached to lysine residues of the target protein. Ubiquitin itself has seven lysines, all of which can be conjugated to a second ubiquitin molecule. For example, usually, Lys48-linked chains are critical for protein degradation, whereas Lys63-linked chains are used as regulation signal (Finley et al., 2012).

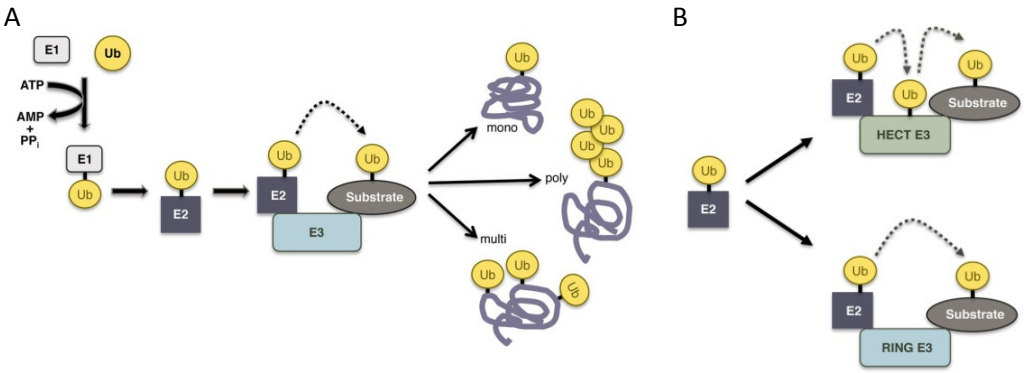

Figure 5. Protein ubiquitilation.
(**A**) Model that explain ubiquitylation mechanism in all eukaryotes. (**B**) Mechanisms of work of HECT E3 ligase and RING E3 ligase. See text for details (Pictures from Finley et al., 2012)

Ubiquitin is typically linked to substrates trough an isopeptide bond between the amino-group of a substrate lysine residue and the carboxyl terminus of ubiquitin. Ubiquitylation process involves a cascade of three class of enzymes called E1, E2 and E3. The reaction, as rappresented in figure 5A, starts by the action of ubiquitin-activating enzyme E1 (Uba1). Activated ubiquitin is transferred to the ubiquitin-conjugating enzyme E2. Finally the E3 ligase enzyme catalyzes the formation of the isopeptide bond. In yeast there is only one E1, eleven E2 and from sixty to hundred E3 enzymes. There are several types of ubiquitylation: mono-ubiquitylation is the attachment of a single ubiquitin molecule to a substrate protein,

whereas the attachment of more that one ubiquitin is called poly-ubiquitylation or multi-ubiquitylation (Fig. 5A). Poly-ubiquitylation is the attachment of a chain of lysines to a single acceptor lysine of the substrate protein. Multi-ubiquitylation is the attachment of multiple single ubiquitin molecules to several acceptor lysine residues in one protein. While poly-ubiquitylation represents the characteristic degradation signal, mono- or multi-ubiquitylation often, but not always, mediate proteasome-indipendent functions such as protein binding, subcellular localization, intracellular trafficking and modulation of substrate activity.

Ubiquitin ligases (E3) confer selectivity to the process. They bind the E2 and the substrate proteins to facilitate substrate-specific ubiquitylation. Many E3 enzymes were identified and all fall into two major classes: RING domain E3 and HECT domain E3. These two domain act by distinct mechanisms of catalysis (Fig. 5B). While HECT domain forms a thioester intermediate with ubiquitin received from E2 prior to its transfer to the substrate, RING domain do not forms thioester intermediates. They facilitate ubiquitin transfer by positioning the charged E2-Ub in proximity to the acceptor lysine of the substrate. In addition, RING domain ligases seem to activate E2 to facilitate ubiquitylation.

The budding yeast open reading frames *YHR115c* and *YNL116w*, renamed *DMA1* and *DMA2* based on the homology of their gene products with that of the fission yeast *DMA1* gene (Fraschini et al., 2004), encode for Dma1 and Dma2 E3-RING ubiquitin ligases. The 58% of aminoacid sequence identity between these two proteins suggests a gene duplication event during evolution. Moreover, orthologs of Dma1 and Dma2 proteins exist in several eukaryotes like *S. pombe* (Dma1) and *Homo Sapiens* (Chfr and Rnf8) (Fig. 6).

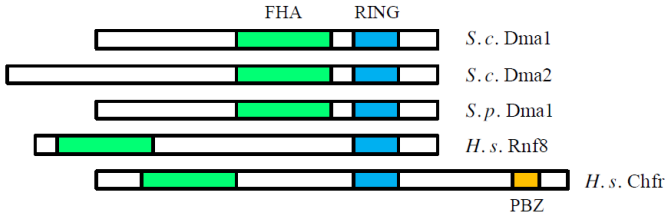

Figure 6. Domain structure of FHA-RING ubiquitin ligases.
Dma proteins and their homologues share two main domains: an FHA domain (green) and a RING domain (blue) See text for details. Moreover *H. s.* Chfr has a C-terminal PBZ domain (poly(ADPribose)-binding zinc finger). See text for details. (Picture from Brooks et al., 2008)

Schizzosaccharomyces pombe Dma1 is required for SIN (Septation Initiation Network, homologous to *S. cerevisiae* MEN) inhibition in the presence of spindle damage in order to prevent PS formation and premature mitotic exit (Murone and Simanis, 1996; Guertin et al., 2002) and it is homologous, like *S. cerevisiae* Dma1 and Dma2, to human Chfr, which is missing or unproperly expressed in several cancer cell lines and has ben shown to be a component of a stress-induced mitotic checkpoint (Scolnick and Halazonetis, 2000). Dma1 and Dma2 proteins are also homolog to human Rnf8, wich is involved in DMA-damage response contributing to arrest the cell cycle at the G2-M transition in the presence of DNA DSBs (Double-Strand DNA Breaks), and promoting the assembly of DNA repair complex at the damaged site (Kolas et al., 2007; Huen et al., 2007; Mailand et al., 2007). Rnf8 also localize at the spindle midbody and its absence cause failure to arrest the cell cycle in responce to nocodazole treatment (Tuttle et al., 2007). Moreover, *RNF8* overexpression causes a cytokinesis delay that is frequently followed by an aberrant mitosis (Plans et al., 2008).
All these proteins, which appear to control different aspects of the mitotic cell cycle, share a forkhead-associated domain (FHA) and a ring finger motif (RF). While the FHA domain is important for the binding with phosphorylated proteins, in particular on phospho-threonine, the RF motif is typical of RING domain E3 ligase (Fig. 5B; Jozeiro and Weissman, 2000). Intact FHA and RING domains are required for the function of all characterized FHA-RING ubiquitin ligases. In particular, point mutation in either the FHA or the RING domain of *S. cerevisiae* Dma1 and Dma2 are sufficient to cause a complete loss of their activity (Bieganowsky et al., 2004).
Dma1 and Dma2 of *S. cerevisiae* have a partially redundant function, indeed the single deletion of *DMA1* or *DMA2* has no phenotype while the simultaneous deletion of the two genes causes slight defect in the mitotic spindle positioning and in the checkpoint that regulates this process called SPOC (Fraschini et al., 2004), in the regulation of cellular morphogenesis and nuclear division in response to replicative-stress (Raspelli et al., 2011) and in the septin ring dynamics (Merlini et al., 2012).
Despite their involvement in a lot of processes important for cell cycle progression and regulation, the *in vivo* ubiquitylation mechanisms and targets of *S. cerevisiae* Dma1 and Dma2 are still unknown. *In vitro* ubiquitin ligase activity of Dma1 and Dma2 has been described for these proteins

(Loring et al., 2008), that appear to be able of auto-ubiquitylate theirselves and to associate with two E2 enzymes, Ubc4 and Ubc13, required for their function in G1 and G2 respectively (Loring et al., 2008). Dma1 and Dma2 proteins were shown to be invoved in the *in vivo* ubiquitylation of the Cdk1 inhibitor Swe1 (Raspelli et al., 2011) as well as of septins (Chahwan et al., 2013), but their functions and targets in cytokinesis control are still undefined.

The NoCut pathway

As described in the second paragraph, the cytokinesis is the last step of the cell cycle that leads to physical separation of the mother from the daughter cell. During this process, both in animal and in yeast cells, invagination of the membrane allows the correct partition of cytoplasm and organelles preparing the cell to the physical separation that takes place during the last part of cytokinesis: the abscission. In many cell types, while the invagination of the membrane starts when the nuclear division is not yet complete, the abscission must take place only after the complete partition of sister chromatids.

In order to ensure the genomic stability of the cells, cytokinesis must be closely coordinated with nuclear division. In fact, if cytokinesis occurs before the complete separation of sister chromatids can lead to deleterious consequences for the cell, such as damage or breakage of chromosomes that remain on the plane of division (lagging chromosomes).

This event can cause cell death, if essential genes are lost, or generation of cells containing a large amount of chromosomal fragments that can cause gross chromosomal rearrangements such as translocations, inversions and deletions, all characteristics frequently observed in cancer cells.

In the fission yeast *S. pombe* several mutants show a phenotype called 'Cut', in which cytokinesis is completed despite the inability to properly divide the genome (Yanagida, 1998). Significant data were also obtained in the budding yeast *S. cerevisiae*. In this organism, defects in the spindle midzone or the presence of chromatin at the site of division cause a delay or block in cytokinesis progression. In these conditions the contraction of actomyosin ring (AMR) is not perturbed and invagination of the membrane occurs normally, while the process of abscission, which leads to the complete separation of the cytoplasm, is delayed or inhibited and this delay require Ipl1 function (Norden et al., 2006 , Mendoza et al., 2009).

In budding yeast, Ipl1 (homologous to human Aurora B) and its cofactors Sli15, Nbl1 and Bir1 (respectively homologous to human INCENP, Borealin and Survivin) form the CPC complex: Chromosome Passenger Complex (van der Waal et al., 2012). This complex takes its name from the peculiarity of their localization during the cell cycle (Fig. 7). In animal cells CPC localization follow this order: in prophase, the CPC is found on chromosome arms. It is involved in the release of arm cohesion and mitotic

chromosome structure. During this phase it accumulates at centromeres where the maturation of kinetochores begins and continues through prometaphase. The CPC is required for the formation of a bipolar spindle and its stability from prophase/prometaphase to anaphase. In metaphase, it localizes at centromeres, where it has a central role in centromeric cohesion and the regulation of kinetochore-microtubule attachments. It controls the correct alignment of chromosomes on the spindle equator and the spindle checkpoint. In anaphase, the CPC translocates to the spindle midzone and appears at the cell cortex; it is involved in the formation of the central spindle. In telophase, the CPC concentrates at the cleavage furrow and, subsequently, at the midbody, where it is required for completion of cytokinesis (Van der Waal et al., 2012).

In *Saccharomyces cerevisiae*, the subcellular localization of the CPC is similar to that observed in animal cells except for the fact that in late anaphase the complex did not localizes to the midbody (since this structure does not exist in yeast) but follows the plus ends of the depolymerizing microtubules (Buvelot 2003).

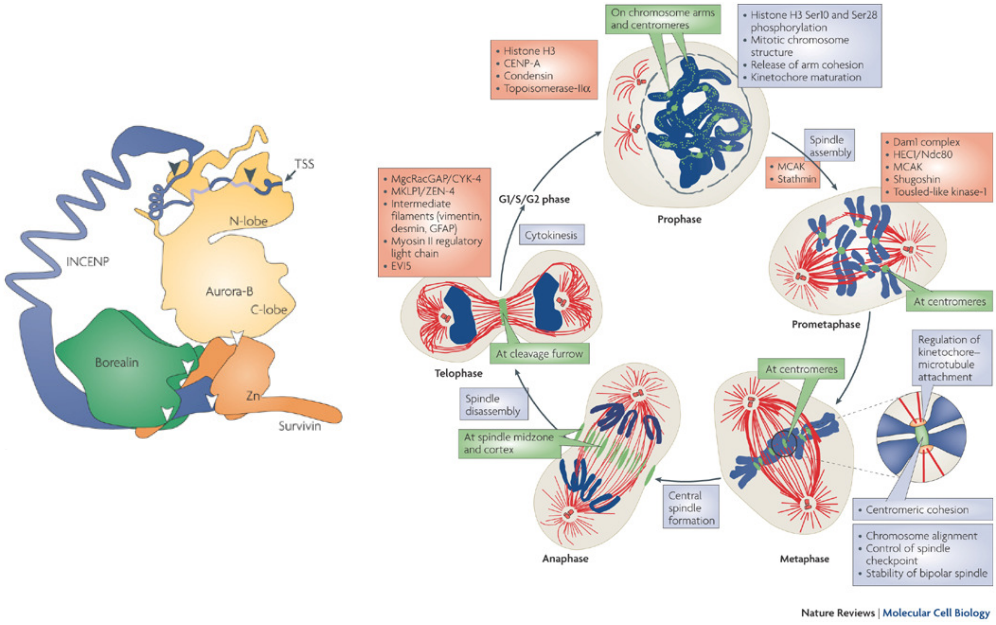

Figure 7. CPC complex composition, localization and functions.
Schematic representation of the chromosomal passenger complex localization (green) correlated with its multiple functions (grey boxes) and principal targets (red boxes) during the different phases of mitosis relative to tubulin and chromosome dynamics. Chromosomes are blue; tubulin is red; nuclear envelope is grey.
See text for details. (Picture from Ruchaud et al., 2007)

Mendoza and collaborators demonstrated that in *S. cerevisiae* there is a checkpoint that coordinates chromosome segregation with the cytokinesis progression (Fig. 8). Ipl1 kinase is primarily involved in the activation of this checkpoint called "NoCUT pathway", and performs this function, at least in part, thanks to anillin-related Boi1 and Boi2 proteins (Norden et al., 2006).
In wild type cells Boi proteins localized in the nucleus of G1 cells and then to the bud cortex. During anaphase they are translocated to the division site and then disappear during cytokinesis.
In cells with spindle midzone defects or lagging chromosomes, Boi1 and Boi2 remain localized to the division site where they seem to have a function in abscission inhibition (Norden et al., 2006).
Ipl1 does not localizes at the division site but inhibits abscission acting upstream of Boi proteins by controlling their translocation to the bud neck during each anaphase. This, together with the data that the lack of Boi proteins causes a decrease in the abscission timiming even during an unperturbed cell cycle, indicates that the NoCut pathway is active during each division (Fig. 8A) (Norden et al., 2006).

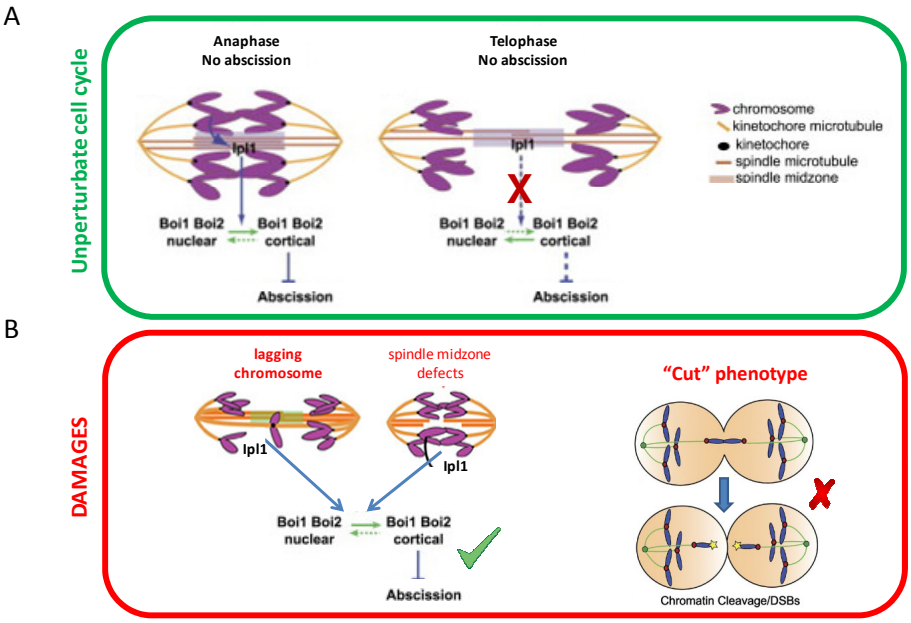

Figure 8. The NoCut pathway.
(**A**) Abscission is inhibited during every anaphase by the NoCut pathway and permitted during thelophase, when the chromosome are fully segregated. See text for details. (**B**) abscission is inhibited by the presence of lagging chromosome or spindle midzone defect (left); the inactivation of NoCut pathway impairs the coordination between copletition of cytokinesis and chromosome segregation and leads to cut phenotype (right). See text for details.

Although it is known that the NoCut inhibits abscission in yeast, the final targets of this inhibition are still obscure. In budding yeast abscission occurs due to the deposition of the primary septum (PS) and the contribution of the new membrane material thanks to vesicular traffic.
Many data demonstrate the physiological importance of NoCut pathway. It has been shown that the inactivation of this pathway in cells which have spindle midzone defects or lagging chromosomes causes the accumulation of DSBs (Norden et al. 2006; Mendoza et al., 2009). This demonstrates that the chromosome segregation delay requires a corresponding abscission delay. Indeed, in the absence of such coordination, the not completely segregated chromosomes are damaged and/or broken during the process of division. It was also demonstrated that the NoCut pathway can be activated by the presence of lagging chromosomes indipendently of the presence of spindle midzone defects (Mendoza et al., 2009). These suggests that the abscission is inhibited in response to different situations (Fig. 8B).
The existance of "cut" phenotype mutants has long been interpreted as an indication of a lack of coordination between nuclear division and cytokinesis. In light of the data obtained in *S. cerevisiae*, however, it was demonstrated that these mutants can be altered both in chromosome segregation and in NoCut pathway function and then divide despite the inability to complete the nuclear division.
For example, the termo sensitive alleles *esp1-1* of *S. cerevisiae* show a 'cut' phenotype. It has been demonstrated that Esp1 separase is required for the properly separation of sister chromatids and even for the CPC localization at the spindle midzone, and then for proper NoCut pathway.
It’s possible therefore to conclude that coordination between nuclear division and cytokinesis exists and it is controlled by a checkpoint that appears to be evolutionarily conserved. In fact, studies in animal cells showed that the presence of chromosome bridges due to an incomplete separation of sister chromatids inhibits abscission (Meraldi et al., 2004).
Moreover, recently it has been shown that Aurora B, the homologue of Ipl1 in vertebrates, is involved in a checkpoint that prevents the tetraploidization in the case of chromosome segregation defect in human cells (Steigemann et al., 2009). In particular, it has been proposed that Aurora B functions as sensor of the presence of chromatin in the division

plane and thus controls abscission in order to prevent the tetraploidization of cells by regressing the membrane invagination (Steigemann et al., 2009). Therefore, a checkpoint mechanism that responds to the spindle midzone defect and improper chromosome segregation is present in various eukaryotic organisms, including humans, where it helps to inhibit the formation of genetic abnormalities and the development of tumors. So it seems that the NoCut pathway is a conserved mechanism during evolution and that it has a fundamental role in the maintenance of genomic integrity.

Vhs2 and actin

Vhs2 is a protein of 436aa encoded by *YIL135c* ORF. It is a cytoplasmic protein (Huh et al., 2003) of unknown function, identified as a high-copy number suppressor of the synthetic lethality of a *sis2 sit4* double mutant (Munoz et al., 2003), suggesting a role in G1/S phase progression. Vhs2 was found also as a high-copy number suppressor of the synthetic lethality of *gic1 gic2* double mutant (Gandhi et al., 2006), suggesting a role in actin cytoskeleton polarization regulation in a parallel pathway respect to *GIC1* and *GIC2*. *VHS2* has a paralog, *MLF3*, that arose from the genome duplication (Byrne and Wolfe, 2005). Their primary sequences share 30% identity and 42% of similarity (Ghandi et al., 2006). However, the functions of Vhs2 and Mlf3 have not been characterized and their sequences provide no obvious clues regarding their cellular functions.

All cells undergo rapid remodeling of their actin cytoskeleton, required for important processes like endocytosis, cell polarity and cell morphogenesis. The remodeling is driven by the coordinated activities of different conserved proteins. Monomeric actin polymerizes into filamentous actin (F-actin) that forms different structures in the cells: cortical spots (patches), long fibers (cables) and bands (rings), all detectable by the use of fluorochrome-labeled drugs (rhodamine phalloidine) and anti-actin antibodies. In unbudded cells there was often a concentration of fluorescence near one pole. In small budded cells the fluorescence is concentrated in the bud as a cluster of individual spots. In cell with medium-sized bud there was tipically a higher concentration of fluorescent spots in the bud than in the mother cell. Cells with a very large buds often showed a concentration of fluorescence in the neck region, sometimes apparently as cluster of spots and sometimes apparently as a band (Fig. 9). Fibers were seen coursing trough the cells generally in a direction roughly parallel to the long axis of the cell.

The filamentous actin (F-actin) structures found in *S. cerevisiae* have different physiological function: actin patches mediated endocytosis and maybe exocytosis (Moseley and Goode, 2006), cables must provide tracks for continuous myosin-dependet transport of cargos to the bud neck and tip required for polarized endocytosis, rings is the second principal component of AMR ant therefore is involved in cytokinesis (Bi and Park, 2012).

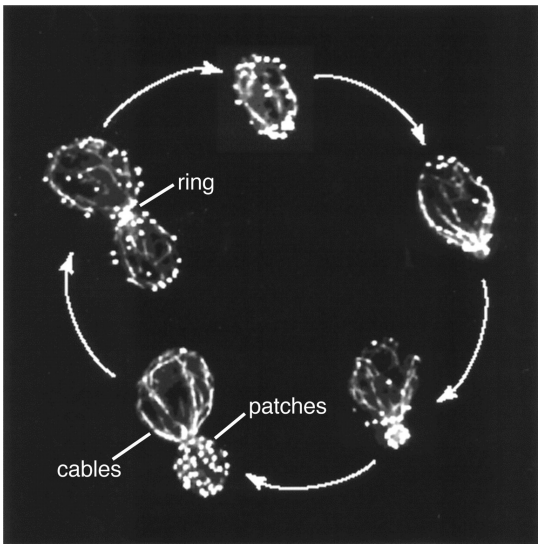

Figure 9. Cell cycle-regulated organization of the *S. cerevisiae* actin cytoskeleton.
Yeast cells at different stage in the cell cycle contain three visible F-actin structures. Cortical actin patches polarized actin cables and cytokinetic actin ring. While patches and cables are visible troughout the cell cycle, the ring is visible shortly before and during citokinesis. Shown here are actively growing cells from an asynchronous colture that were chemically fixed and stained with rodamine phalloidin to visualize filamentous actin structure. See text for details. (Picture from Moseley and Goode, 2006)

Septins in budding yeast

Septins are conserved GTP-binding proteins discovered in the 1970s in *S. cerevisiae* as 'neck filaments' surrounding the bud neck.
These proteins are conserved from yeast to human but are absent in plants (Pan et al., 2007). The number of septin genes varies widely between different organisms, the budding yeast have seven septins: Cdc3, Cdc10, Cdc11, Cdc12, Shs1 (expressed during the mitotic cell cycle), Spr3 and Spr28 (expressed specifically during meiosis where they replace Cdc12 and Shs1 respectively) (De Virgilio et al., 1996; Fares et al., 1996). These proteins can form hetero-oligomeric complexes which are then assembled into different higher-order structures that variate during different phases of the cell cycle. These structures are associated with other cytoskeletal structure (actin or tubulin) or localize to discrete region of the plasma membrane where they act as scaffold or diffusion barrier to mediate several processes including cytokinesis, mitosis, exocytosis and several checkpoint pathways (Oh and Bi, 2011).
All septins share a basic structure: a variable N-terminal region, a polybasic region that binds to phospholipids, and a conserved GTP-binding domain. Most septins also contain a predicted coiled-coil region in C-terminal. Septins form rod-shaped hetero-oligomeric complexes, which polymerize end-to-end into long paired linear filaments. These filaments are further assembled into other higher-order structures such as rings or hourglasses (Oh and Bi, 2011).
In budding yeast, at the beginning of a new cell cycle, septin ring is assembled at the presumptive bud site. This ring is dynamic as indicated by FRAP analysis (Fig. 10) (Oh and Bi, 2011). Coincident with bud emergence, or shortly after, the septin ring expands into a stable hourglass that surrounds the bud neck. At the onsent of cytokinesis the septin hourglass is split into two dynamic rings that sandwich the cytokinesis machinery (Fig. 10B). In *S. cerevisiae* CDKs, polarity factors and post-translational modifications of septins (phosphorylation and SUMOylation) are involved in septin organization and dynamics.

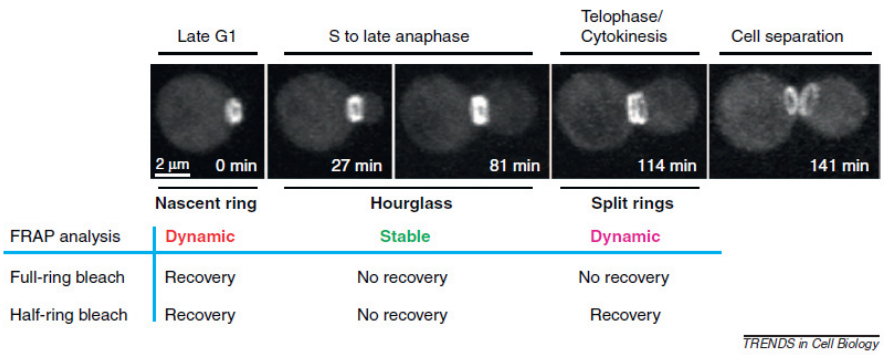

Figure 10. Septin organization and dynamics during cell cycle in *S. cerevisiae*.
During G1-S transition the new septin ring is assembled at the presuntive bud site. After bud emergence, in S phase, the septin ring is converted into a stable hourlass structure that is mantained until late anaphase (from 27 to 81 min) at the onset of cytokinesis. The septin hourglass is split into two dynamic cortical rings. The two ring are then disassembled after cell division while the new rings are assembled into the mother and daughter cells at the presuntive bud site. See text for details. (Picture from Bi, 2011)

In *S. cerevisiae* the small Rho-family GTPase Cdc42 control polarized localization of both actin and septin ring assembly at the incipient bud site. The newly recruited septins are usually present in disorganized clouds or patches. Also G1 CDK play a dual role in septin ring assembly. One role is indirect and is mediated by Cdc42, the other role is by direct phosphorylation of septins (Oh and Bi, 2011). Moreover PAK kinase Cla4, an effector of Cdc42, also regulates septin ring assembly by directly phosphorylating a subset of septin. Once recruited, septin complexes associate with the PM via interactions between septin poly-basic motifs and plasmamembrane phospholipids.
During bud emergence, septin ring is converted into a stable hourglass. The mechanisms underlying this transformation remains unknown, but involves the kinases Cla4, Elm1 and Gin4, and the septin associated proteins Bni5 and Nap1 (Oh and Bi, 2011). Afterwards, the septin hourglass splitting is controlled by MEN activity (Oh and Bi, 2011). The inactivation of mitotic CDK at the end of mitosis is essential for the septin hourglass-to-ring transition in different organisms.
After cytokinesis and cell separation the old septin ring at the division site is disassembled and the new septin ring is formed adjacent to the old ring (Oh and Bi, 2011). The timing of old septin ring disassembly is important for the assembly and function of the new septin ring because the subunits of the old ring are recycled in order to form the new ring during successive divisions (Oh and Bi, 2011). Disassembly of the old septin ring appear to be

regulated by dephosphorylation events driven by the protein phosphatase $PP2A^{Rts1}$ (Oh and Bi, 2011). In addition, septins are major targets of SUMOylation during mitosis in *S. cerevisiae* (Oh and Bi, 2011). However, notwhistanding inhibition of Shs1, Cdc11 and Cdc3 SUMOylation causes septin rings stabilization, the significance of this modification remains unclear (Oh and Bi, 2011).

In the end two non-mutually-exclusive models have been proposed to explain the diverse functions of the septins. The “scaffold model” explains that septin-based structures serve as a scaffold for permits the localization of several proteins at the bud neck to perform their specific functions (Oh and Bi, 2011). The “diffusion-barrier model” explains that the septin-based structures function as a diffusion barrier at a discrete region of the plasma membrane and prevent membrane and membrane-associated proteins from crossing these regions (Oh and Bi, 2011). Some *S. cerevisiae* mutants are unable to assemble or mantain a double septin ring during cytokinesis but they are nonetheless capable of dividing efficently, suggesting that a septin-ring based diffusion barrier is not required for cytokinesis in this organism (Wloka et al., 2011).

Results

Saccharomyces cerevisiae Dma proteins participate in cytokinesis by controlling two different pathways

Cell Cycle 12:17, 2794–2808; September 1, 2013; doi: 10.4161/cc.25869, © 2013 Landes Bioscience.

Corinne Cassani[1], Erica Raspelli[1], Nadia Santo[2], Elena Chiroli[3], Giovanna Lucchini[1], and Roberta Fraschini[1].

1Università degli Studi di Milano-Bicocca; Dipartimento di Biotecnologie e Bioscienze; Milano, Italy; 2Università degli Studi di Milano; Centro Interdipartimentale di Microscopia Avanzata; Milano, Italy; 3IFOM - Istituto FIRC di Oncologia Molecolare; Milano, Italy

Saccharomyces cerevisiae Dma proteins participate in cytokinesis by controlling two different pathways

Dma2 impairs a parallel cytokinesis pathway with respect to Hof1

We previously implicated the Dma proteins in the control of mitotic progression. In order to gain insights into the molecular mechanism of this event, we studied genetic interactions between the Dma proteins and other factors involved in cytokinesis. The concomitant lack of *DMA1* and *DMA2*, which does not cause growth defects in otherwise wild-type cells (Fraschini et al., 2004), did not affect viability or growth of meiotic segregants lacking either *HOF1* or *CHS2* or expressing the temperature sensitive (ts) allele *iqg1-1* at the permissive temperature (Table 1).

Table 1. Genetic interactions between the Dma proteins and other factors involved in cytokinesis

Genotype	Phenotype at 25 °C on YEPD	Phenotype at 25 °C on YEPRG
dma1Δ dma2Δ chs2Δ	Healthy	ND
dma1Δ dma2Δ iqg1-1	Healthy	ND
dma1Δ dma2Δ cyk3Δ	Sick/slow growth	ND
dma1Δ dma2Δ hof1Δ	Healthy	ND
GAL1-DMA2 chs2Δ	Healthy	Healthy
GAL1-DMA2 iqg1–1	Healthy	Sick/slow growth
GAL1-DMA2 cyk3Δ	Healthy	Healthy
GAL1-DMA2 hof1Δ	Healthy	Lethal
GAL1-DMA1 hof1Δ	Healthy	Lethal

Strains carrying *DMA1* and *DMA2* deletions or expressing *GAL1-DMA2* or *GAL1-DMA1* were crossed with the *chs2Δ, iqg1-1, cyk3Δ*, and *hof1Δ* mutants. The resulting diploids were induced to sporulate and meiotic segregants were assayed for their ability to grow on rich medium containing glucose (YEPD) or galactose (YEPRG) at 25°C. Only the phenotypes of meiotic segregants with the indicated genotypes are shown, the meiotic segregants with all the other possible genotypes all showed healthy phenotypes. ND, not determined.

On the other hand, *cyk3Δ dma1Δ dma2Δ* meiotic segregants formed smaller colonies than *cyk3Δ* or *dma1Δ dma2Δ* meiotic segregants (Table 1), and this phenotype correlated with a partial cytokinesis defect (see below). In addition, galactose-induced *DMA2* overexpression from a single copy of a *GAL1-DMA2* fusion integrated in the genome, which we previously showed not to cause any growth defect in otherwise wild-type cells (Fraschini et al., 2004), was used to evaluate the possible effects in the same mutants described above of this moderate Dma2 overproduction. These same *GAL1-DMA2* moderate overexpression conditions were used also for all the subsequent experiments. As shown in Table 1, *GAL1-DMA2* overexpression did not affect the growth of *chs2Δ* and *cyk3Δ* meiotic segregants, but it caused poor growth of *igq1-1* meiotic segregants at the permissive temperature, likely due to a partial cytokinesis defect (our unpublished observation). Moreover, overexpression of either *GAL1-DMA2* or *GAL1-DMA1* was lethal in the absence of the cytokinesis protein Hof1 (Table 1), further indicating redundancy between the two Dma proteins. We therefore performed more detailed analyses using only moderate *GAL1-DMA2* overexpression. In agreement with the synthetic lethal effect observed in meiotic segregants, the ability of *GAL1- DMA2 hof1Δ* cells to form colonies on galactose-containing plates was strongly reduced compared with wild-type, *GAL1-DMA2,* or *hof1Δ* cells (Fig. 11A), which all formed colonies with similar efficiency under the same conditions. In order to reveal the terminal phenotype of *GAL1-DMA2 hof1Δ* cells, we synchronized wild-type, *hof1Δ*, *GAL1-DMA2,* and *GAL1-DMA2 hof1Δ* cell cultures in G1, followed by release into cell cycle in the presence of galactose to induce Dma2 overproduction. After the release, the kinetics of DNA replication (Fig. 11B), budding, nuclear division, mitotic spindle assembly (Fig. 11C and D), and septin ring formation (Fig. 11D) showed very similar profiles in wild-type, *hof1Δ* and *GAL1-DMA2* cells. By contrast, *GAL1-DMA2 hof1Δ* cells exited from mitosis, but then accumulated as chains of cells with more than 2C DNA content (Fig. 11B), divided nuclei, and disassembled spindles (Fig. 11C) and split the septin ring (Fig. 11D).

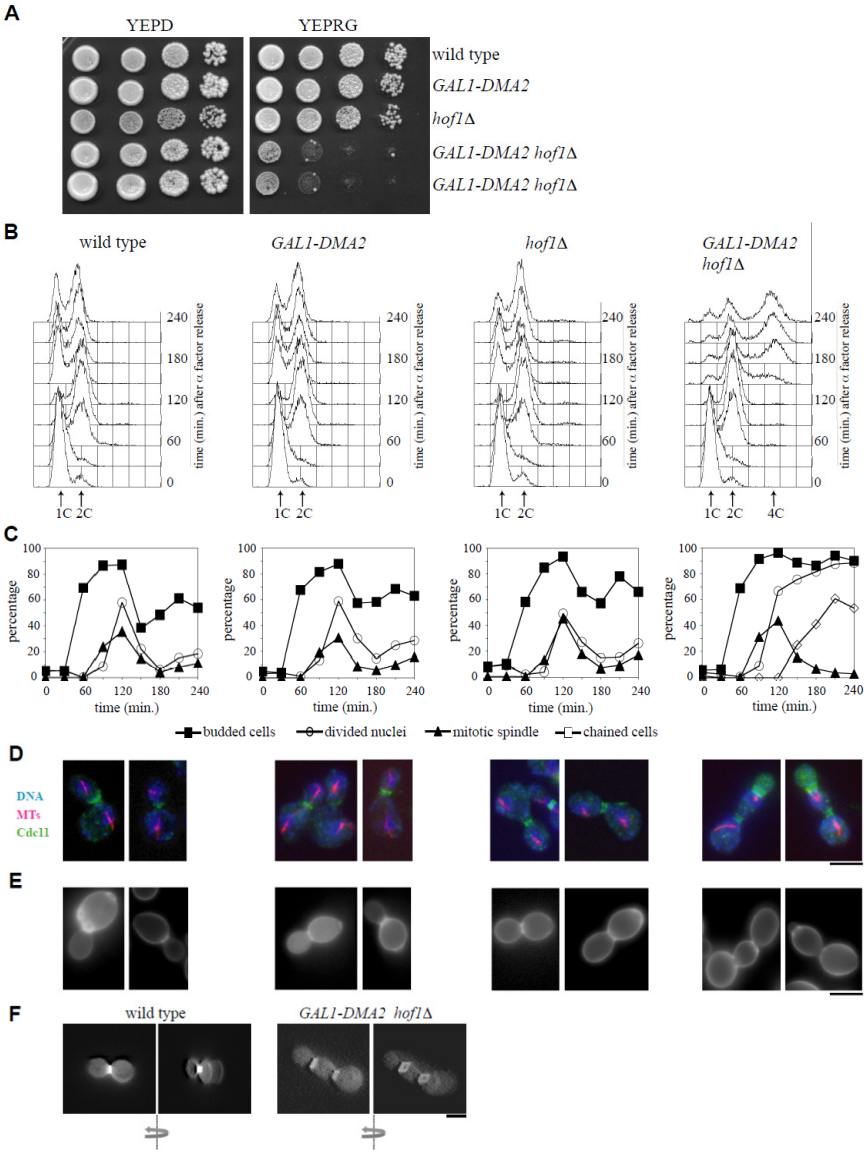

Figure 11. Dma2 excess is toxic for cells lacking Hof1.
(**A**) Serial dilutions of stationary phase cultures of strains with the indicated genotypes were spotted on YEPD or YEPRG plates, which were then incubated for 2 days at 25°C. (**B–F**) Exponentially YEPR growing cultures of wild-type, *GAL1-DMA2, hof1Δ*, and *GAL1-DMA2 hof1Δ* cells were arrested in G1 by α-factor and released from G1 arrest in YEPRG at 25°C (time 0). At the indicated times after release, cell samples were taken for FACS analysis of DNA contents (**B**), and for scoring budding, chained cells, nuclear division, and mitotic spindle formation (**C**). (**D and E**) Pictures were taken 120min after release for wild-type, *GAL1-DMA2*, and *hof1Δ* cells, or 240min after release for *GAL1-DMA2 hof1Δ* cells, to show *in situ* immunofluorescence analysis of nuclei (DNA), mitotic spindles (MTs) and septin ring deposition (Cdc11) (**D**), as well as chitin deposition analysis (**E**) by using Calcofluor White staining. (**F**) Three-dimensional reconstruction of pictures taken at different Z-stacks of wild-type and *GAL1-DMA2 hof1Δ* cells treated as in panel (**E**). The arrows indicate the direction of rotation. Wild-type cells show a complete chitin disk at the bud neck (left), while *GAL1-DMA2 hof1Δ* cells can only assemble a chitin ring (right). Bar, 5μm.

Cells in the chains were not separable by zymolyase treatment (data not shown), indicating cytokinesis failure rather than cell separation defects. Indeed, Calcofluor White staining of chitin clearly showed that *GAL1-DMA2 hof1Δ* cell chains suffered primary septum deposition defects (Fig. 11E and F and 14A). In fact, they did not show the chitin disk structure that is typical of PS-containing cells, which was instead detectable in all control cells under the same conditions, but showed a chitin ring that is built by the chitin synthase Chs3 in early S phase (Lesage et al., 2005) (Fig. 11F). Thus, although Dma2 moderate overproduction does not alter cell cycle progression in otherwise wild-type cells, it leads to cytokinesis inhibition in the absence of Hof1, suggesting that Dma2 might impair a parallel cytokinesis pathway with respect to Hof1.

Budding yeast can tolerate either loss of AMR in *myo1Δ* cells or partial defects in PS formation in *hof1Δ* or *cyk3Δ* cells, but not both. Indeed, *HOF1* deletion causes cell lethality in cells lacking either PS deposition proteins, like the chitin synthase Chs2 and its activator Cyk3, or proteins required for AMR formation, such as the septin regulator Bni5, the formin Bni1, and the myosin heavy chain Myo1 (Nishihama et al., 2009). If the lethal effect of moderate Dma2 excess in the absence of Hof1 were due to Dma2-dependent inhibition of some cytokinesis factor(s) acting in parallel with Hof1, high levels of the same factor(s) might be expected to rescue this effect. Strikingly, both *CYK3* and *CHS2* overexpression from high copy number plasmids partially suppressed galactose-induced *GAL1-DMA2 hof1Δ* synthetic lethality (Fig. 12A and B), indicating that the cytokinesis defect of these cells can be rescued by forcing PS formation. Conversely, high levels of the septin-binding protein Bni5 did not increase viability of galactose-induced *GAL1-DMA2 hof1Δ* cells (Fig. 12C), which, on the other hand, did not exhibit defects in septin ring structure and dynamics (Fig. 11D). Based on these data, we did not assay the effects of septin overproduction.

As MEN activity is required not only for mitotic exit but also for cytokinesis,(Lippincott et al., 2001; Hawa Lim et al., 2003; Menssen et al., 2001; Corbett et al., 2006) we instead investigated the effects of MEN hyperactivation through either the lack of its inhibitor Bub2 or the *Dbf2-1c* hyperactive allele (Geymonat et al., 2009). As shown in Figure 12D, *GAL1-DMA2 hof1Δ* cell lethality on galactose-containing plates was not rescued by either condition of MEN hyperactivation, indicating that it is not likely

due to MEN impairment. On the other hand, MEN targets for promoting cytokinesis are probably not available or not accessible in *GAL1-DMA2 hof1Δ* cells (see below).

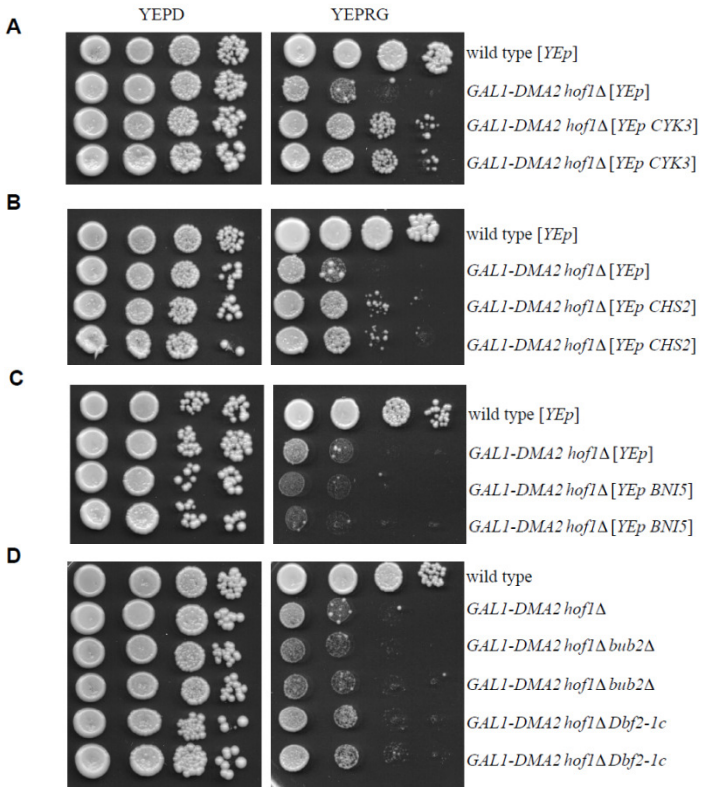

Figure 12. Toxic effects of moderate Dma2 overproduction in cells lacking Hof1 are counteracted by high Chs2 and Cyk3 levels.
(**A–D**) Serial dilutions of stationary phase cell cultures of strains with the indicated genotypes were spotted on YEPD or YEPRG plates, which were then incubated for 2 days at 25°C. With the exception of the strains carrying the *BUB2* deletion or the *Dbf2-1c* allele (**D**), which were grown in YEPD medium, cell cultures were grown to stationary phase in synthetic medium lacking leucine (**A and C**) or tryptophan (**B**) in order to maintain selective pressure for maintainance of the YEp high copy number plasmids.

Dma2 overproduction impairs AMR contraction and Tem1-Iqg1 interaction

The data above suggest that Dma2 excess can interfere with some cytokinesis-promoting pathway(s).
Nonetheless, *GAL1-DMA2* overexpression does not affect cell viability of otherwise wild-type cells (Fraschini et al., 2004) (Fig. 11A), likely because budding yeast cytokinesis is driven by parallel and partially redundant pathways.
As the localization of the cytokinetic machinery to the division site is crucial for its function, we analyzed the subcellular localization of important cytokinesis proteins in galactose induced *GAL1-DMA2* cells. In order to analyze AMR formation and contraction, we generated wild-type and *GAL1-DMA2* strains expressing a functional fluorescent variant of myosin I (Myo1-Cherry) to analyze its localization in synchronized cells. Preliminary analysis showed that Myo1-Cherry bars, which formed at the bud neck of both wild-type and GAL1-*DMA2* cells, persisted longer in Dma2-overproducing cells than in wild-type cells, where they properly contracted into a single dot and disappeared (data not shown). In order to analyze this defect in detail, we performed live-cell imaging of wild-type and *GAL1-DMA2* cells that expressed Myo1-Cherry and the mitotic spindle marker Tub1-GFP. After release from a G1 arrest, AMR contracted and disappeared from the bud neck of wild-type cells 5.6min (± 1.88, in 76 cells) after mitotic spindle breakdown, while this time was significantly longer in Dma2- overproducing cells (11.2min ± 4.4, in 98 cells) (Fig. 13A; Videos S1 and S2 (Cassani et al., 2013)). The difference between the two strains is significant (P value obtained by Wilcoxon rank-sum test P = 7.6892 10-19). This phenomenon was not due to the lack of actin localization at the bud neck, as the actin distribution patterns were very similar in wild-type and *GAL1-DMA2* cells (Fig. 13B). In addition, as shown in Figure 13C and summarized in Table 2, comparison of wild-type and *GAL1-DMA2* synchronized cells revealed that localization of an Iqg1-GFP fusion at the bud neck of late anaphase cells (large budded, binucleate) was not significantly affected by *GAL1-DMA2* overexpression.

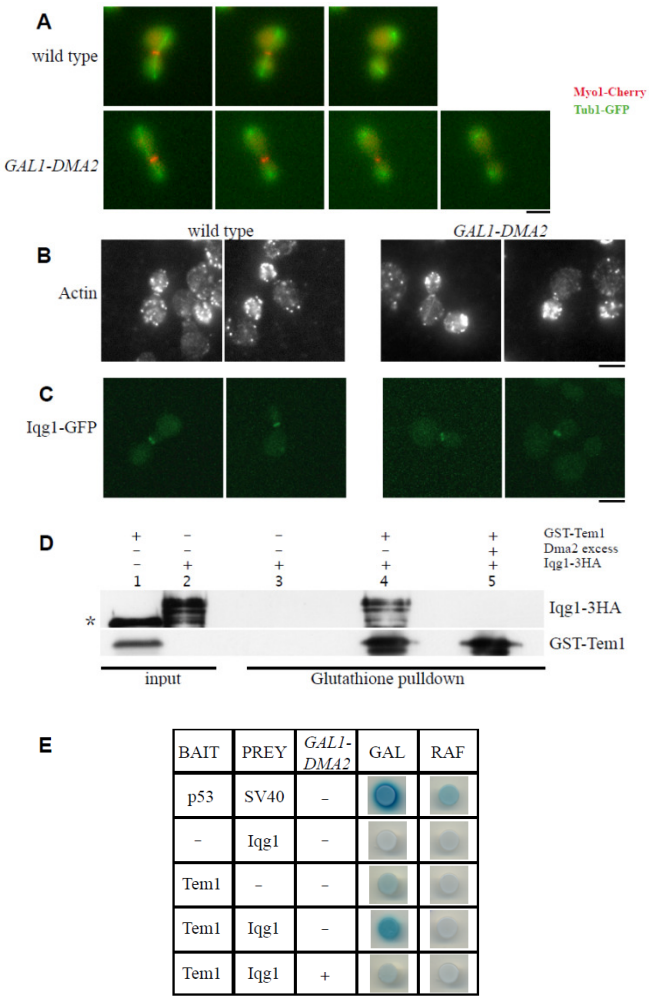

BAIT	PREY	*GAL1-DMA2*	GAL	RAF
p53	SV40	–		
–	Iqg1	–		
Tem1	–	–		
Tem1	Iqg1	–		
Tem1	Iqg1	+		

Figure 13. Dma2 excess affects AMR contraction and Tem1-Iqg1 interaction.
(**A**) Exponentially growing cultures of wild-type and *GAL1-DMA2* cells, all expressing fully functional *MYO1-Cherry* and *TUB1-GFP* fusions, were arrested in G1 by α-factor and released from G1 arrest at 25°C in raffinose–galactose synthetic medium plates for time-lapse analysis. Pictures as shown in the panel were taken every 5min for 5h and time-lapsed images were assembled to show Myo1-Cherry ring contraction (Videos S1 and S2(Cassani et al., 2013)). Bar, 5µm. (**B and C**) Exponentially growing cultures of *IQG1-GFP* and *GAL1-DMA2 IQG1-GFP* cells were arrested in G1 by α-factor and released from G1 arrest at 25°C in YEPRG medium. Pictures were taken 150min after release to show actin and Iqg1-GFP localization. Actin was visualized by *in situ* immunofluorescence analysis by using anti-actin antibodies. The percentage of late anaphase cells (large budded, binucleate) with Iqg1 localization at the bud neck is reported in Table 2. Bar, 5µm. (**D**) Glutathione beads bound to GST-Tem1 were incubated with native protein extracts prepared from either wild-type or Dma2 overproducing cells, washed, and incubated with native protein extracts containing Iqg1-3HA (glutathione pulldown). Washed and boiled beads were subjected to SDS-PAGE followed by immunoblotting with anti-HA and anti-GST antibodies. Equivalent aliquots of the lysates were also loaded on the gel (input). The asterisk marks an aspecific band. (**E**) Plasmid pEG202-Tem1 carrying the lexADB-Tem1 fusion under the *ADH* promoter (bait) and plasmid pJG4-5 carrying the B42AD-Iqg1 fusion under the *GAL1* promoter (prey) were cotrasformed with the β-galactosidase reporter

plasmid pSH18-34 in the wild-type yeast strain EGY48 (see "Materials and Methods"). To assess two-hybrid interaction, the indicated strains were spotted on 5-bromo-4-chloro-3-indolyl-β-D-galactopyranoside (X-GAL) selective synthetic plates containing either raffinose (RAF, prey not induced) or 2% galactose (GAL, prey expressed). To assess the two-hybrid interaction of Iqg1 and Tem1 in presence of Dma2 excess, we transformed the strain described above with a high copy number plasmid carrying the *GAL1-DMA2* construct. As a positive control we used the strain carrying the p53 protein as the bait and the SV40 protein as the prey.

Table 2. Iqg1, Cyk3 and Inn1 localization at the division site of large budded binucleate cells

Strain genotypes	Minutes after α-factor release	Budded cells %	Binucleate cells %	Iqg1 at bud neck % ± SEM
IQG1-GFP	150	66,7	29,2	31,8 ± 1,5
GAL1-DMA2 IQG1-GFP	150	75,7	40,0	43,4 ± 1,8
				Cyk3 at bud neck % ± SEM
CYK3-GFP	120	86,3	66,4	22,2 ± 1,2
GAL1-DMA2 CYK3-GFP	120	88,3	69,3	2,8 ± 0,9
				Inn1 at bud neck % ± SEM
INN1-GFP	165	63,2	53,2	19,9 ± 1,1
GAL1-DMA2 INN1-GFP	165	67,4	47,3	19,8 ± 1,2
GAL1-DMA1 INN1-GFP hof1Δ	165	82,9	61,3	1,0 ± 0,8

The percentages are the mean of the values obtained at the indicated time points in triplicates of the experiments described in Figure 3 (Iqg1) and Figure 4 (Cyk3 and Inn1). About 100 large budded binucleated cells were scored for protein localization in each cell culture for each experiment ± standard mean errors.

Defective AMR contraction in Dma2-overproducing cells did not appear to be due to hyperstabilization of the septin ring, because the same kinetics of AMR contraction was observed in galactose-induced *GAL1-DMA2* and *GAL1-DMA2 cdc12-1* cells, although the septin ring was destabilized in the latter cells due to the temperature-sensitive *cdc12-1* allele (Fig. S1).

We then hypothesized that defective AMR contraction in Dma2 overproducing cells might be due to specific inhibition of properly localized AMR components. AMR contraction is brought about by Iqg1 interaction with the actomyosin ring, and Iqg1 has been shown to interact with Tem1 *in vitro* (Shannon et al., 1999), leading to the proposal that its binding to Tem1 might be required for its activation.

We therefore asked whether Tem1-Iqg1 complex formation was inhibited by Dma2 excess in the previously described *in vitro* assay (Shannon et al., 1999). Glutathione pulldown analysis clearly showed Tem1-Iqg1 interaction in the absence (Fig. 13D, lane 4), but not in the presence of Dma2 excess

(Fig. 13D, lane 5). In addition, Tem1 turned out to interact with Iqg1 by a two-hybrid assay (see Material and Methods; Fig. 13E), and this interaction was impaired by *GAL1-DMA2* overexpression. Thus, Dma2 overproduction appears to impair both AMR contraction and Tem1-Iqg1 interaction.

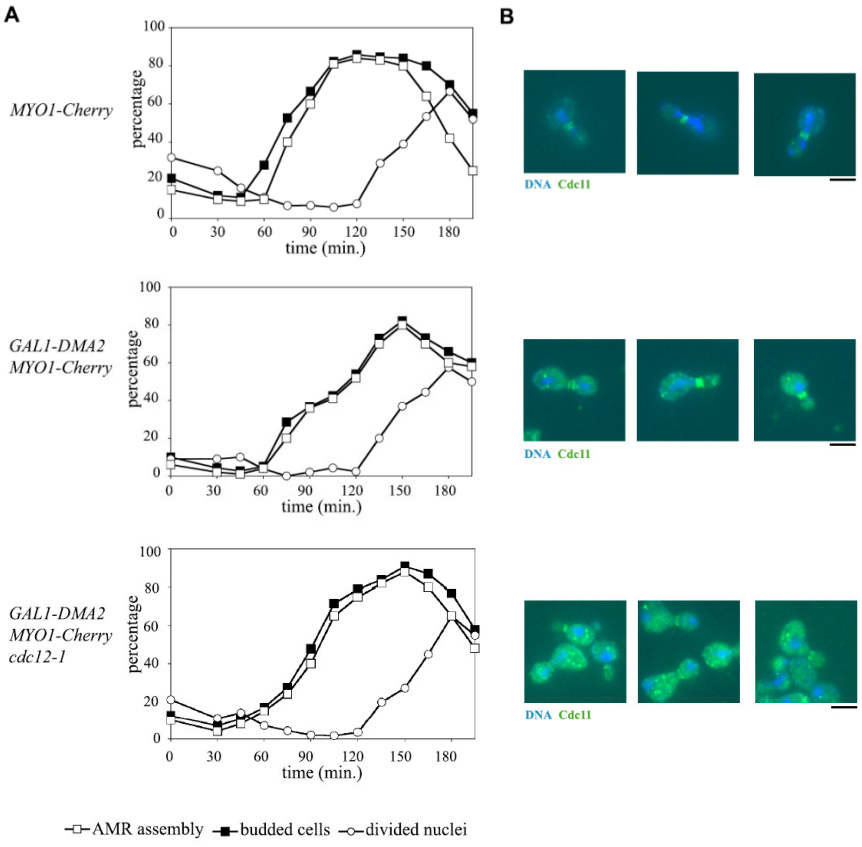

Suppl. figure 1: Septin ring destabilization does not rescue the AMR dynamic defects due to Dma2 excess.
A-B: Exponentially growing cultures of *MYO1-Cherry*, *GAL1-DMA2 MYO1-Cherry* and *GAL1-DMA2 cdc12-1 MYO1-Cherry* cells were arrested in G1 by α-factor and released from G1 arrest in YEPRG at 23°C (time 0). At the indicated times after release, cell samples were taken for scoring budding, nuclear division and AMR disassembly (**A**). Pictures were taken 120min after release to show *in situ* immunofluorescence analysis of ring deposition (Cdc11) and nuclei (DNA) (**B**). bar: 5µm.

PS formation and Cyk3 localization at the bud neck are inhibited by Dma2 excess

As shown by trasmission electron microscopy (TEM), galactose-induced *GAL1-DMA2* cells exhibited asymmetric PS deposition (Fig. 14A, middle top), which is typical of mutants impaired in AMR contraction (Vallen et al., 2000). However, these cells ultimately formed a trilaminar septum (Fig. 14A, middle bottom), and indeed they were viable (Fig. 11A). PS is synthetized by Chs2, so we compared Chs2 dynamics at the bud neck of wild-type and *GAL1-DMA2* cells that express Myo1-Cherry and Chs2-GFP by live-cell imaging on cells released from a G1 arrest. As expected, Chs2 accumulates at the bud neck after mitotic exit (Chin et al., 2012) and remains there for 9–10min in both strains (Videos S3 and S4 (Cassani et al., 2013)).

Interestingly, we observed that Chs2 contracts and disappears by endocytic removal within 4.17min after AMR contraction in wild-type cells, and this phenomenon occurs earlier in *GAL1-DMA2* cells (2.78min.; P value of Wilcoxon rank-sum test P =2.89 10−4). In addition, Chs2-GFP and AMR always constrict together and symmetrically in wild-type cells (28 of 28 cells), while they contract asymmetrically in *GAL1-DMA2* cells (33 of 36 cells) (Fig. 4B; Videos S3 and S4 (Cassani et al., 2013)), consistent with the asymmetric PS deposition observed in these cells (Fig. 14A, middle top).

We then analyzed galactose-induced *GAL1-DMA2* cells for the subcellular localization of the Cyk3 and Inn1 proteins, which are both important for PS formation. To this end, we generated wildtype and *GAL1-DMA2* strains expressing functional Cyk3-GFP and Inn1-GFP fusions that normally localized at the bud neck of both cell types in the absence of galactose (data not shown). Cell cultures of these strains were released from G1 arrest into galactose containing medium to monitor DNA replication by FACS analysis (not shown), budding, and nuclear division (Table 2) as well as protein levels (not shown) and GFP localization (Table 2 and Fig. 14C and E). Strikingly, Cyk3 was found at the bud neck of only 2.8% of late anaphase *GAL1-DMA2* cells, while it localized at the bud neck of 22.2% of late anaphase wild-type cells, as expected (Fig. 14C and Table 2). Western blot analysis showed similar Cyk3 total amounts in wild-type and *GAL1-DMA2* cells throughout the experiment (data not shown), ruling out the possibility that mislocalization of Cyk3 could be due to its degradation. Moreover,

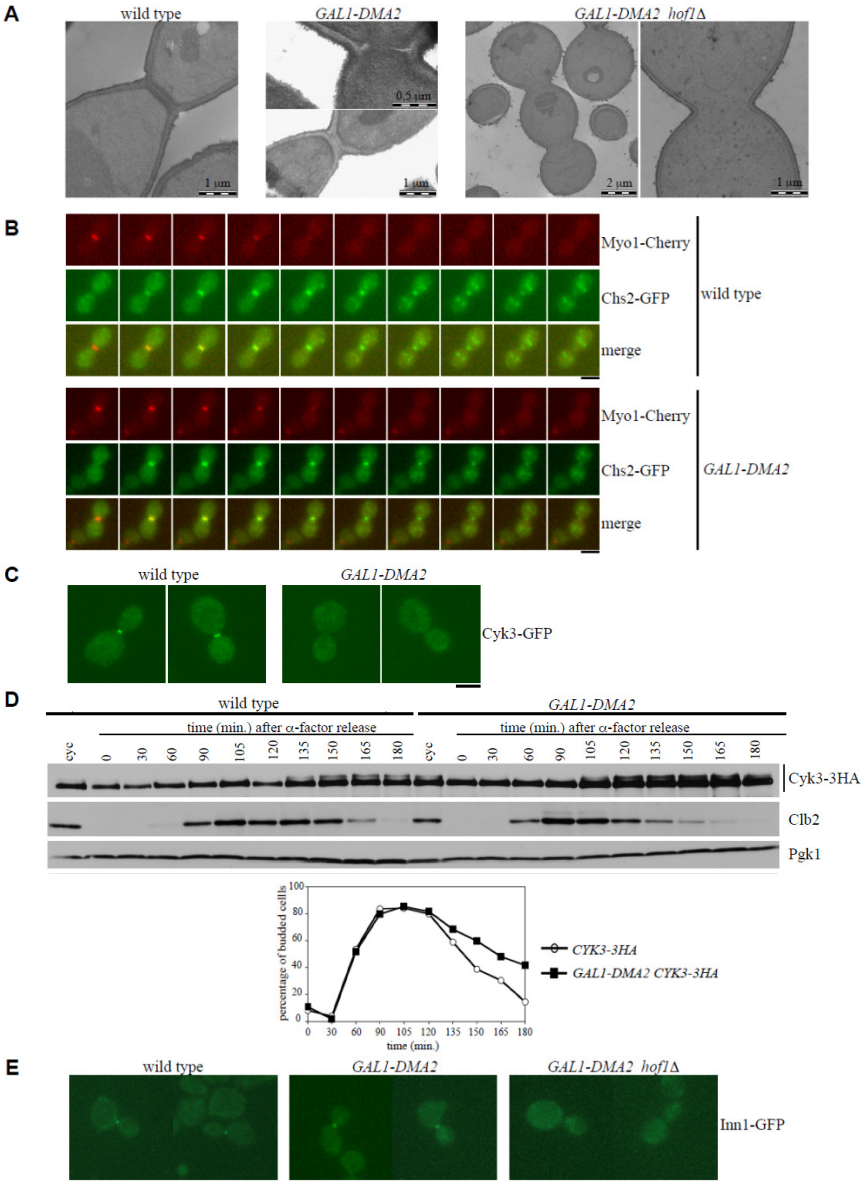

Figure 14. Dma2 overproduction affects PS formation and Cyk3 localization at the division site.
(**A**) Samples for TEM analysis were taken from exponentially growing cultures of wild-type, *GAL1-DMA2* and *GAL1-DMA2 hof1Δ* cells, which were pre-grown in YEPR medium and then incubated in YEPRG medium (1% galactose) for 4h (wild-type and *GAL1-DMA2*) or 6h (*GAL1-DMA2 hof1Δ*). The *GAL1-DMA2* top and bottom panels show cells with either defective or completed PS formation, respectively. The *GAL1-DMA2 hof1Δ* panel on the right is a magnification of the bud neck in the cell of the adiacent panel. (**B**) Exponentially growing cultures of wild-type and *GAL1-DMA2* cells, all expressing *MYO1-Cherry* and *CHS2-GFP*, were arrested in G1 by α-factor and

released from G1 arrest at 25°C in raffinose–galactose synthetic medium plates for time-lapse analysis. Pictures as shown in the panel were taken every 2min for 5h, and time-lapsed images were assembled to show Myo1 and Chs2 dynamics (Videos S3 and S4 (Cassani et al., 2013)). Bar, 5μm. (**C**) Exponentially growing cultures of *CYK3-GFP* and *GAL1-DMA2 CYK3-GFP* cells were arrested in G1 by α-factor and released from G1 arrest at 25°C in YEPRG medium. Pictures were taken 120min after release to show Cyk3-GFP localization. Bar, 5μm. (**D**) Exponentially growing cultures of *CYK3–3HA* and *GAL1-DMA2 CYK3-3HA* cells were treated as in (**B**). At the indicated times, cell samples were taken for scoring budding (graph) and for determining Cyk3 and Clb2 levels by western blot analysis with anti-HA, anti-Clb2 and anti-Pgk1 (loading control) antibodies. (**E**) Exponentially growing cultures of *INN1-GFP*, *GAL1-DMA2 INN1-GFP,* and *GAL1-DMA2 hof1Δ INN1-GFP* cells were treated as in (**B**). Pictures were taken 165min after release to show Inn1-GFP localization. Percentages of large budded binucleate cells with Cyk3 and Inn1 localization at the bud neck are reported in Table 2. Bar, 5μm.

wild-type and GAL1-DMA2 galactose-induced cell cultures released into cell cycle from G1 arrest contained very similar amounts not only of total Cyk3, but also of low electroforetic mobility Cyk3 species (Fig. 14D), indicative of Cyk3 phosphorylation (Bodenmiller et al., 2010), which is in turn required for Cyk3 recruitment to the bud neck (Meitinger et al., 2010). Thus Dma2 excess does not seem to inhibit phosphorylation of Cyk3, although it inhibits its bud neck localization. The Inn1 protein is essential for cytokinesis, as both its lack and its defective localization lead to cytokinesis failure (Sanchez-Diaz et al., 2008; Jendretzky et al., 2009; Nishihama et al., 2009). This protein is targeted to the bud neck by the concerted action of Hof1 and Cyk3 and is properly localized in both *hof1Δ* and *cyk3Δ* cells, while concomitant Hof1 and Cyk3 lack causes Cyk3 mislocalization and cell death (Jendretzky et al., 2009). Inn1-GFP localization was analyzed (Fig. 14E), and Inn1 was found at the bud neck of 19.9% late anaphase wild-type cells and of 19.8% late anaphase *GAL1-DMA2* overexpressing cells (Table 2). On the contrary, Inn1-GFP bud neck localization dropped in *GAL1-DMA2 hof1Δ* cells (1% of late anaphase cells, Table 2). These data are consistent with the observation that cytokinesis is blocked in the absence of Hof1 by moderate Dma2 overproduction (Fig. 11), which also inhibits both AMR contraction and Cyk3 localization. The same Dma2 excess by itself might allow cytokinesis completion, likely because Hof1 can promote Inn1 localization and activation also under these conditions. On the other hand, Hof1 lack in the presence of Dma2 excess results in cytokinesis block, because all pathways that could promote the final step of cell division are inactive. Indeed, *GAL1-DMA2 hof1Δ* cells completely failed to build the primary septum (100% of chained cells), as exemplified by TEM pictures in Figure 14A.

Tem1 ubiquitylation and the Dma proteins

Dma1 and Dma2 act as E3 ubiquitin ligases in vitro (Loring et al., 2008) are involved in Swe1 ubiquitylation *in vivo* (Raspelli et al., 2011) and have been recently implicated in septins' ubiquitylation (Chahwan et al., 20013), raising the possibility that they might regulate Tem1-Iqg1 interaction and Cyk3 localization by ubiquitylation. Iqg1 is known to be ubiquitylated by Cdh1/APC (Ko ert al., 2007), while no ubiquitylation data are available for Tem1 and Cyk3. We first tested Iqg1 ubiquitylation in *cdh1Δ* cells, but we could not observe any residual ubiquitylation (data not shown). Moreover, we could not obtain reproducible results for Cyk3 ubiquitylation.

In order to investigate Tem1 ubiquitylation, we produced wild-type, *TEM1-3HA*, and *TEM1-3HA GAL1-DMA2* cells containing high copy number plasmids carrying a construct expressing 6xHis-tagged ubiquitin (*YEp-CUP1-6xHIS-UBI4*) or untagged ubiquitin (*YEp-CUP1-UBI4*) from the copperinducible *CUP1* promoter (Callis et al., 2005). After purification from crude extracts of the ubiquitylated proteins by Nickel (Ni) pulldown (see "Materials and Methods"), Tem1 ubiquitylated forms were detected in the pulldown eluates by western blot analysis with anti-HA andibody.

When Ni pulldowns were performed on crude extracts from samples taken at different time points after release from G1 arrest of *TEM1-3HA* cells expressing 6xHis-tagged ubiquitin, Tem1-ubiquitylated forms began to accumulate at 105min after release (Fig. 15A), when 55% of cells were binucleate (Fig. 15B), and then decreased concomitantly with AMR contraction (Fig. 15B), suggesting that this event might require Tem1 deubiquitylation. When a similar approach was used to compare Tem1 ubiquitylation in exponentially growing wild-type and *GAL1-DMA2*-overexpressing cells, the amount of ubiquitylated Tem1 was higher in the eluates from *GAL1-DMA2*-overexpressing cells (Fig. 15C, lane 12) than in wild-type eluates (Fig. 15C, lane 10). As total Tem1 levels in *GAL1-DMA2* overproducing cells were not different from those found in wild-type cells (data not shown), Tem1 ubiquitylation in the presence of Dma2 excess does not appear to trigger its degradation. In a similar experiment, we found no difference in the amounts of Tem1 ubiquitylated forms in Ni pulldowns performed on wild-type or *dma1Δ dma2Δ* protein extacts (data not shown). Thus, although Dma2 excess increases the amount of

ubiquitylated Tem1, we found no evidence for a role of the Dma proteins in Tem1 ubiquitylation under unperturbed conditions.

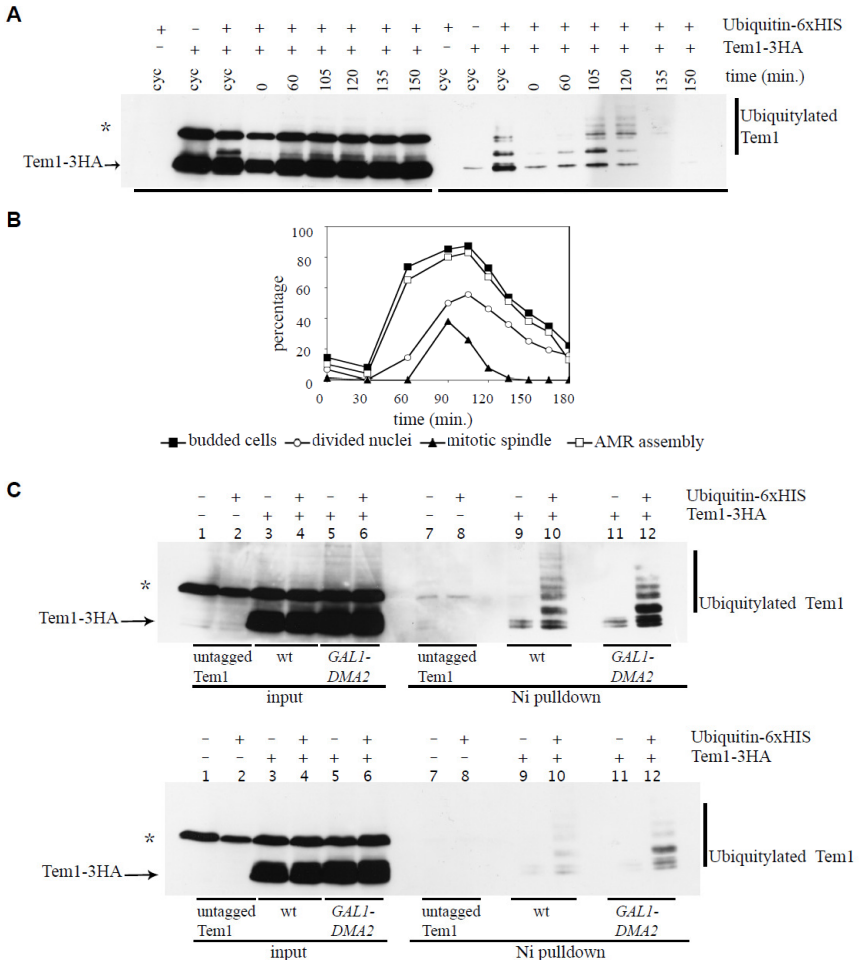

Figure 15. Tem1 undergoes cell cycle-dependent ubiquitylation.
(**A and B**) *TEM1–3HA* cells, carrying high copy number plasmids with the *CUP1-6xHISUBI4* construct and expressing the Myo1-Cherry fusion, were grown to log phase in glucose synthetic medium lacking tryptophan, arrested in G1 by α-factor and released in the cell cycle at 25°C in YEPD medium containing 250μM $CuSO_4$ (time 0). At the indicated times after release, cell samples were taken for Ni pulldowns (**A**) and for scoring budding, nuclear division, mitotic spindle formation, and AMR assembly (**B**). (**C**) Wild-type, *TEM1-3HA* and *GAL1-DMA2 TEM1-3HA* cells, carrying high copy number plasmids with the *CUP1-6xHIS-UBI4* construct or the *CUP1-UBI4* construct, were grown to log phase in raffinose containing synthetic medium lacking tryptophan and incubated in the presence of 1% galactose for 30min, followed by additional 3h incubation in the presence of 250μM $CuSO_4$. Cells were then lysed and aliquots of the lysates were incubated with Ni-NTA beads to purify the proteins bound by 6xHis-ubiquitin (Ni pulldown), followed by SDS-PAGE and western blot analysis with anti-HA antibody of the bead eluates. Equivalent aliquots of the lysates were also loaded on the gel (input). The asterisk in (**A and C**) marks an aspecific band.

The lack of the Dma proteins impairs primary septum formation

As previously reported, *dma1Δ dma2Δ* cells progress normally through the cell cycle (Fraschini et al., 2004; Merlini et al., 2012), and after exit from mitosis, they divide with kinetics similar to wild-type cells. As the effects of *DMA2* overexpression suggested that the Dma proteins might act as inhibitors of AMR contraction and PS deposition, we investigated these processes in details in the absence of the same proteins. We performed time-lapse analysis of AMR contraction in living cells by monitoring the Myo1-Cherry fusion in wild-type and *dma1Δ dma2Δ* cells that also expressed Tub1-GFP. AMR contracted and disappeared from the bud neck of wild-type cells 3.36min (± 1.56, 132 cells) after mitotic spindle breakdown, while this time was reduced in cells lacking Dma1 and Dma2 (1.8min ± 1.58, 100 cells) (Fig. 6A; Videos S5 and S6 (Cassani et al., 2013)). The difference between the 2 strains is significant (P value obtained by Wilcoxon rank-sum test P = 2.6 10-15) and indicates that the Dma proteins are involved in maintaining proper AMR contraction timing with respect to mitotic exit.

To evaluate Dma1 and Dma2 role in PS deposition, we analyzed the levels, phosphorylation, and subcellular localization of a functional Cyk3-3HA and Cyk3-GFP fusions in synchronized cell cultures. We found no differences in Cyk3-3HA total levels and phosphorylation between *CYK3-3HA* and *CYK3–3HA dma1Δ dma2Δ* strains during a synchronous cell cycle in standard YEPD medium (Fig. 16B). In addition, *CYK3-GFP* and *CYK3-GFP dma1Δ dma2Δ* synchronous cells showed very similar kinetics of recruitment of the Cyk3-GFP fusion to the bud neck (not shown). Nonetheless, the lack of Dma proteins caused Cyk3 mislocalization during cytokinesis in a small fraction of cells (6% ± 0.5 of 102 cells vs. 0% of 105 wild-type cells; Fig. 16C).

Thus, the lack of Dma proteins causes partial defects in the timing of AMR contraction and in Cyk3 localization.

Accordingly, *dma1Δ dma2Δ* cells showed abnormally shaped PS (65% of 26 cells, vs. 10% of 20 wild-type cells), as judged by TEM analysis (Fig. 16D). However, these defects do not either block cell division or impair viability of *dma1Δ dma2Δ* cells, likely due to redundancy of cytokinesis controls. Indeed, the lack of the Dma proteins caused a cytokinesis defect in *cyk3Δ* cells, as *cyk3Δ dma1Δ dma2Δ* cells grew slowly (Table 1) and accumulated as chained cells (not shown) with more than 2C DNA content (Fig. 16E).

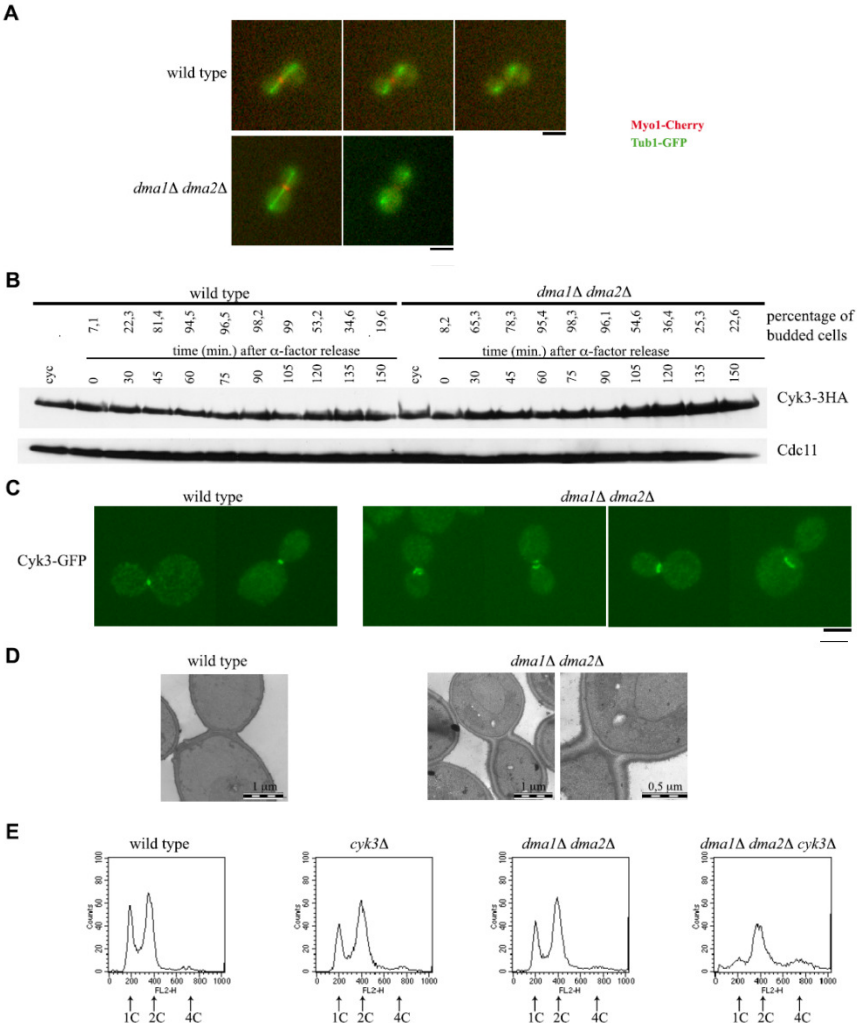

Figure 16. The lack of Dma proteins partially impairs AMR contraction and PS deposition.
(**A**) Exponentially growing cultures of wild-type and *dma1Δ dma2Δ* cells, all expressing *MYO1-Cherry*, and *TUB1-GFP* were plated on glucose synthetic medium plates at 25°C for time-lapse analysis. Pictures as shown in the panel were taken every 3min for 5h, and time-lapsed images were assembled for showing Myo1-Cherry ring contraction (Video S5 and 6 (Cassani et al., 2013)). Bar, 5µm. (**B**) Exponentially growing cultures of *CYK3-3HA* and *dma1Δ dma2Δ CYK3-3HA* cells were arrested in G1 by α-factor and released from G1 arrest at 25°C in YEPD medium (time = 0). At the indicated times, cell samples were taken for scoring budding and for determining Cyk3 levels by western blot analysis with anti-HA and anti-Cdc11 (loading control) antibodies. (**C**) Exponentially growing cultures of *CYK3-GFP* and *GAL1-DMA2 CYK3-GFP* cells were treated as in (**B**). Pictures were taken 120min after release to show Cyk3-GFP localization. Bar: 5µm. (**D**) Samples for TEM analysis were taken from exponentially growing cultures of wild-type and *dma1Δ dma2Δ* cells grown in YEPD medium at 25°C. (**E**) FACS analysis of DNA content of the indicated strains exponentially growing in YEPD medium at 25°C.

Tem1 ubiquitylation role in AMR contraction

Mutations in putative Tem1 ubiquitylation sites improves AMR contraction of GAL1-DMA2$_s$ cells.

As described in the previous chapter, we observed that Tem1 undergoes cell cycle-regulated ubiquitylation and the amount of ubiquitylated Tem1 decreases concomitantly with cells undergoing AMR contraction (Fig. 15A and B)(Cassani et al., 2013). Moreover the amount of Tem1 ubiquitylated forms increases in the presence of Dma2 excess (Fig. 15C), which inhibits AMR contraction too (Fig. 13A)(Cassani et al., 2013). Our data led us to hypothesize that ubiquitylation of Tem1 might inhibit Tem1-Iqg1 complex formation which is important for AMR contraction signalling. Subsequent Tem1 deubiquitylation would allow Tem1-Iqg1 interaction, thus promoting AMR contraction. In this scenario, unscheduled Tem1 ubiquitylation may lead to AMR contraction inhibition in Dma2 overexpressing cells.
Tem1 is a GTP-binding protein of 245 amminoacids containing 17 lysines. In order to test the importance of Tem1 ubiquitylation in AMR dynamics, we took advantage of several centromeric plasmids containing different Tem1 mutants previusly genereted in our laboratory by the use of site directed mutagenesis that modified each codon encoding for lysines (K, the residue that is used to bind ubiquitin) into codon encoding for arginine (R).
We produced *GAL1-DMA2* strains that carries the deletion of *TEM1* and plasmids expressing different Tem1 mutant alleles. These strains also expressed Myo1-Cherry fusion, to visualize AMR.
If our hypothesis is correct a Tem1 version that cannot be ubiquitylated should abrogate the effect of Dma2 excess on AMR contraction.
Cell cultures of *MYO1-Cherry*, *MYO1-Cherry GAL1-DMA2* and *MYO1-Cherry GAL1-DMA2 tem1K-R* cells were released grom G1 arrest into galactose-containing medium to monitor DNA replication by FACS analysis and AMR contraction (Fig. 17).
At first we analyzed *tem1* mutant alleles that contain two mutagenized lysines in order to exclude those strains that did not show an evident change in AMR contraction efficiency of Dma2 overexpressing cells.
Based on the dynamics of Myo1-Cherry contraction we excluded the lysines 154, 184, 206, 208 and 227 as a putative Tem1 ubiquitylation sites important for regulation of AMR contraction because their mutation did not increase the efficiency of this process (Fig. 17B). Instead we found that lysines 39, 59, 112, 133, 170, 213 and 219 could have a role in the

regulation of AMR contraction because their lack restores, in part, the AMR contraction of *GAL1-DMA2* cells (Fig. 17B).

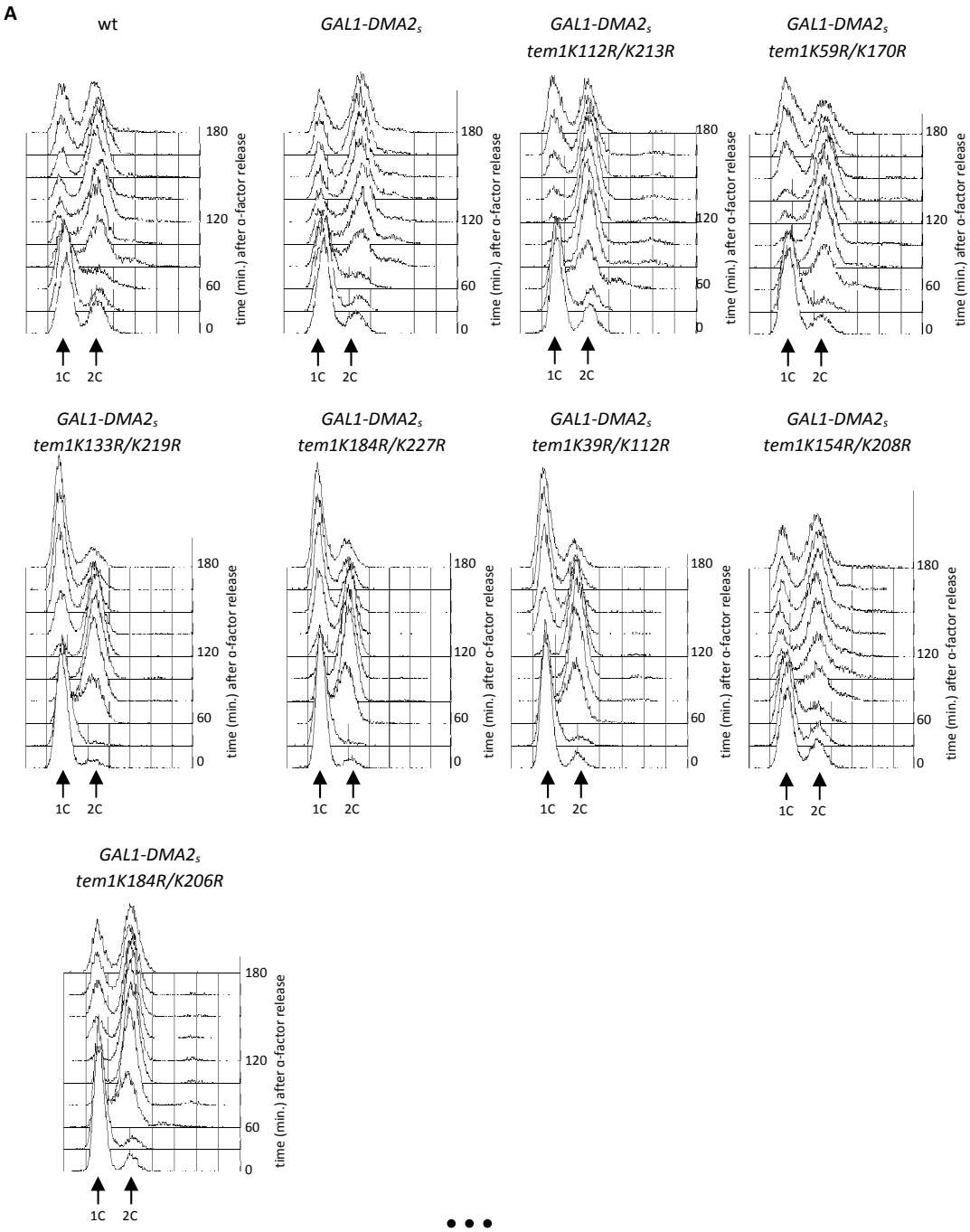

B

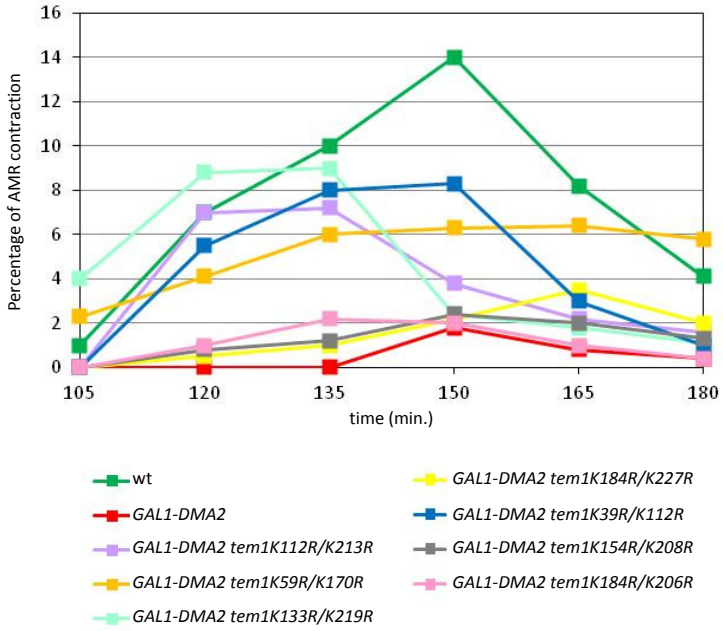

Figure 17. Several *tem1* mutant alleles that contain two mutagenized lysines restore, in part, the AMR contraction of *GAL1-DMA2* cells.
(**A–B**) Exponentially YEPR growing cultures of the indicated strains, all expressing fully functional *MYO1-Cherry*, were arrested in G1 by α-factor and released from G1 arrest in YEPRG at 25 °C (time 0). At the indicated times after release, cell samples were taken for FACS analysis of DNA contents (**A**), and for scoring AMR contraction (**B**).

Then we analyzed the effect of Tem1 variants carrying only one lysine replaced by arginine and we found that lysines 112, 133 and 219 can effectively rescue, almost completely, the AMR contraction defects of *GAL1-DMA2* cells. Also lack of lysines 39 and 47 led to a partial effect (Fig. 18). While lack of lysines 33, 59, 61, 170 caused only a slight improvement of AMR contraction (Fig. 19). We could not analyze the effect of lysines 176 and 179 because it was not possible to mutagenized these sites. In addition we not analyze the effect of the single lisyne 213 because we don't have the single mutant.
Thus, the lysines residues: 112, 133, 219 and in part also 39 and 47 appear to have an important role in AMR contraction inhibition of Dma2 overexpressing cells.

A

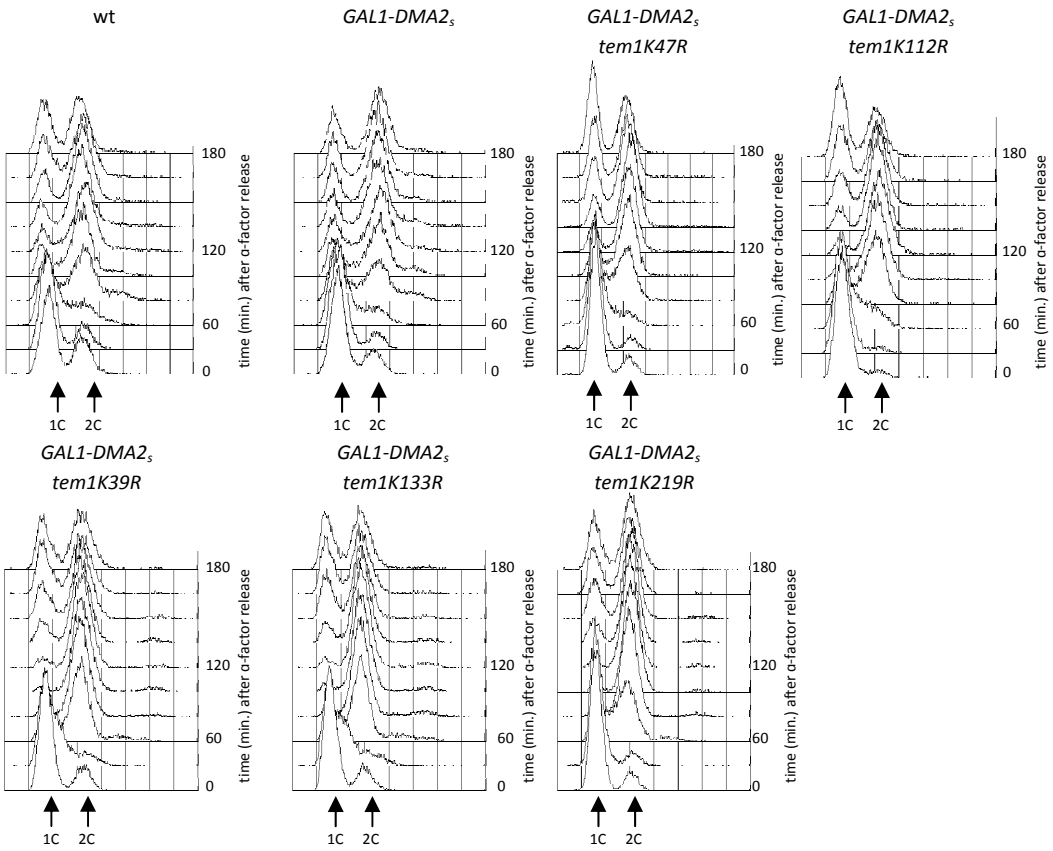
wt
GAL1-DMA2s
GAL1-DMA2s tem1K47R
GAL1-DMA2s tem1K112R
GAL1-DMA2s tem1K39R
GAL1-DMA2s tem1K133R
GAL1-DMA2s tem1K219R
180
120
60
0
time (min.) after α-factor release
1C
2C

B

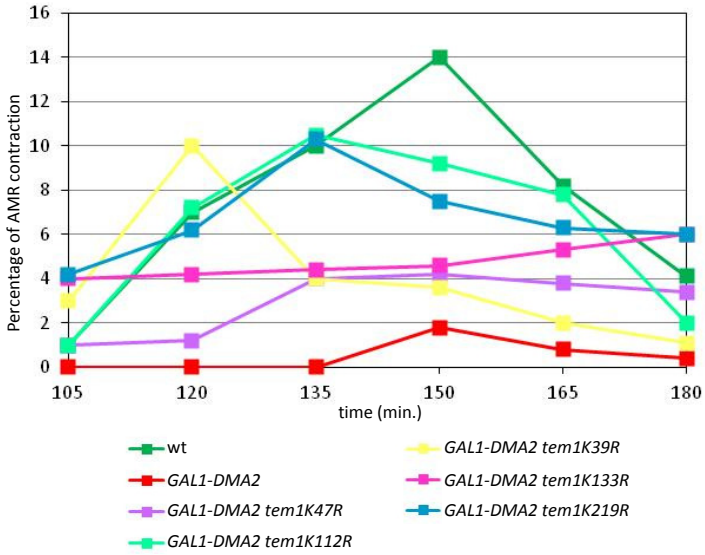
Percentage of AMR contraction
16
14
12
10
8
6
4
2
0
105
120
135
150
165
180
time (min.)
wt
GAL1-DMA2
GAL1-DMA2 tem1K47R
GAL1-DMA2 tem1K112R
GAL1-DMA2 tem1K39R
GAL1-DMA2 tem1K133R
GAL1-DMA2 tem1K219R

Figure 18. Several *tem1* mutant alleles that contain one mutagenized lysine restore almost completely the AMR contraction of *GAL1-DMA2* cells.
(**A–B**) Exponentially YEPR growing cultures of the indicated strains all expressing fully functional *MYO1-Cherry* were arrested in G1 by α-factor and released from G1 arrest in YEPRG at 25 °C (time 0). At the indicated times after release, cell samples were taken for FACS analysis of DNA contents (**A**), and for scoring AMR contraction (**B**).

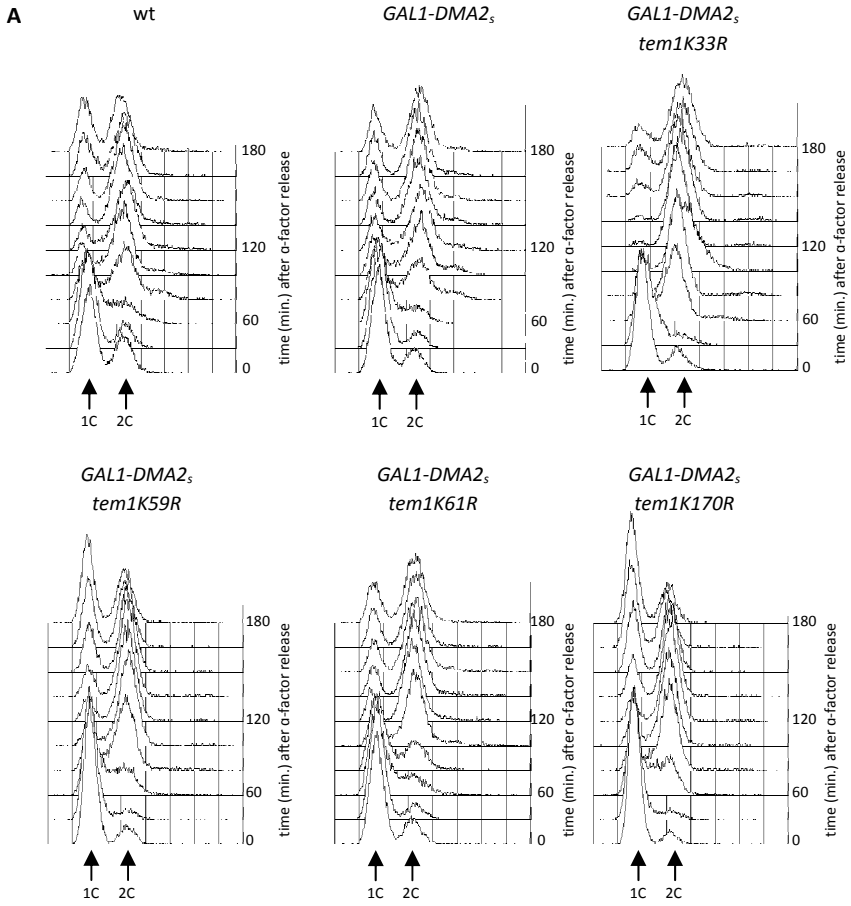

B

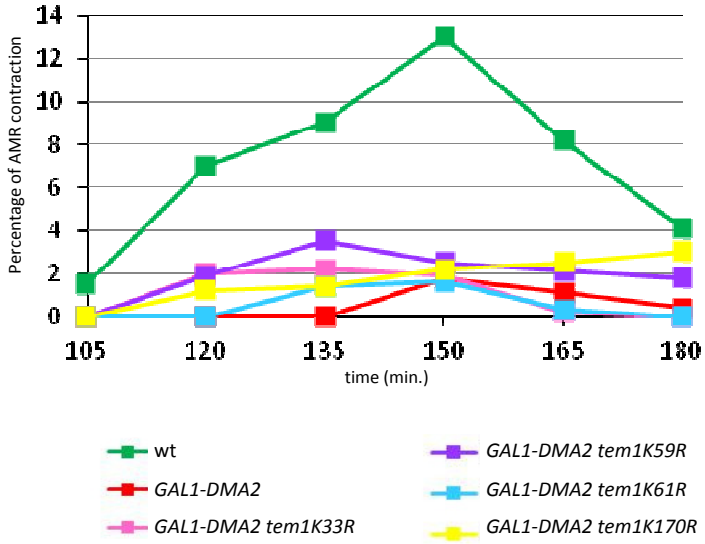

Figure 19. Several *tem1* mutant alleles that contain one mutagenized lysine do not restore the AMR contraction of *GAL1-DMA2* cells.
(**A–B**) Exponentially YEPR growing cultures of the indicated strains all expressing fully functional *MYO1-Cherry* were arrested in G1 by α-factor and released from G1 arrest in YEPRG at 25 °C (time 0). At the indicated times after release, cell samples were taken for FACS analysis of DNA contents (**A**), and for scoring AMR contraction (**B**).

Dma1 and Dma2 role in the NoCut pathway

The lack of the Dma proteins forces cytokinesis in ndc10-1 cells.

Ndc10 is a kinetochore component that localizes at the spindle midzone during anaphase. This protein is required for the correct kinetochore assembly and for the spindle midzone stability (Bouck and Bloom 2005; Buvelot et al., 2003).*ndc10-1* mutant cells, at the restrictive temperature, exhibit a spindle midzone defect that is sensed by Boi1 and Boi2. Indeed in these conditions, *ndc10-1* cells can exit from mitosis but form chains of cells that cannot be separated by zymolyase treatment, indicative of a cytokinesis defect due to inhibition of cell abscission caused by NoCut pathway activation (Norden et al., 2006). As expected, inactivation of this pathway dy deleting *BOI1* and *BOI2* induces *ndc10-1* bibudded cells to form a proper septa and to be resolved into unbudded and single-budded cells by zymolyase treatment (Norden et al., 2006).
In order to understand if Dma1 and Dma2 can function as Boi proteins in the activation of NoCut pathway, we analyzed the phenotype of the triple mutant *dma1Δ dma2Δ ndc10-1* after 240min at the restrictive temperature, 37°C. As shown in figure 20A, *ndc10-1* cells remained bi-budded while most of the triple mutant bibudded cells separated after zymolyase treatment (bibudded cells decrease from 52% to 28%). We also analyzed primary septum (PS) deposition by Calcofluor White staining in these cells and, as expected, *ndc10-1* cells showed primary septum deposition defects, due to a proper checkpoint activation, while *dma1Δ dma2Δ ndc10-1* cells complete PS deposition (Fig. 20B). These data indicate that the Dma proteins act as abscission inhibitors like Boi1 and Boi2 in the NoCut pathway.

A

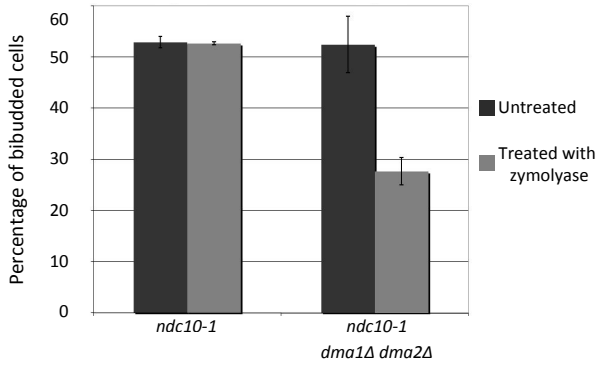

B

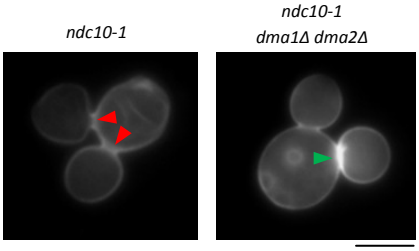

Figure 20. *ndc10-1* cells complete cytokinesis in the absence of Dma proteins.
(**A**) *ndc10-1* and *dma1Δ dma2Δ* cell coltures were grown at 25°C in YEPD until reaching the exponentially phase and then were shifted at 37°C for 240min. Cell samples were taken for scoring bibudded cells before and after the zymolyase treatment. (**B**) Pictures were taken 240min after the shift to show chitin deposition by using Calcofluor White staining. Red arrowheads show the uncomplete PS deposition. Green arrowheads show the complete PS . Bar, 5µm.

Dma1 and Dma2 proteins are involved in the NoCut pathway.

We previously implicated the Dma proteins in the regulation of cytokinesis (Cassani et al., 2013). In particular Dma1 and Dma2 appear to act as inhibitors of this process by acting on AMR contraction and PS deposition, however the regulation of the activity of these proteins is still obscure. We can hypothesize that they function in every cell cycle and/or that they are activated by specific stimuli.

Since our data indicate that the Dma proteins work in the NoCut pathway (previous paragraph) we hypothesize that, for example, they can sense spindle defects or lagging chromosomes. In order to gain insights into the role of the Dma proteins in this checkpoint, we studied genetic interactions between the Dma proteins and other factors involved in the NoCut pathway function or activation.

Since *boi1Δ boi2Δ* cells carrying mutations in the Non Homologous End Joining repair pathway (NHEJ) genes showed impaired growth due to an increased incidence of chromosome breaks during abscission (Norden et al., 2006), first we wanted to test if the lack of *DMA1* and *DMA2* caused growth defect in absence of *MRE11*, whose product is indeed involved in NHEJ. Mutant and control strains were inoculated in YEPD at 25°C and serial diluitions were spotted on YEPD plates at different temperatures. Surprisingly, the triple mutant *dma1Δ dma2Δ mre11Δ* showed a synthetic growth defect respect to the control strains (Fig. 21A) as the triple *boi1Δ boi2Δ mre11* in W303 background (Fig. 21B). These data are in agreement with our hypothesis.

So, in order to understand at which level Dma proteins work in the NoCut pathway we analyzed the genetic interactions between the Dma proteins and Boi1 Boi2 or Ipl1, all acting in the NoCut pathway. We performed a drop test as described above and we found that the contemporary deletion of *DMA1* and *DMA2* and of *BOI1* and *BOI2* caused a synthetic growth defect at 37°C (Fig. 21C). On the contrary, the lack of *DMA1* and *DMA2* in combination with the *ipl1-321* termo-sensitive allele did not have any effect at any permissive temperature (Fig. 21D). These data suggests that Dma proteins might function in a parallel pathway respect to Boi1 and Boi2, and in the same pathway respect to Ipl1.

It is known that the lack of proteins involved in spindle-midzone stability like Ase1 triggers the NoCut pathway attivation (Norden et al., 2006). So

we asked if the simultaneous loss of *DMA1* and *DMA2* could causes a synthetic growth defect in the absence of Ase1, likely due to an inefficient activation of the checkpoint. As shown in figure 21E we did not detect any effect on cell vitality of the triple mutant, indicating the existence of parallel pathways that lead to activation of the NoCut pathway, on one side by Boi proteins and on the other side by Dma proteins that act with other players.

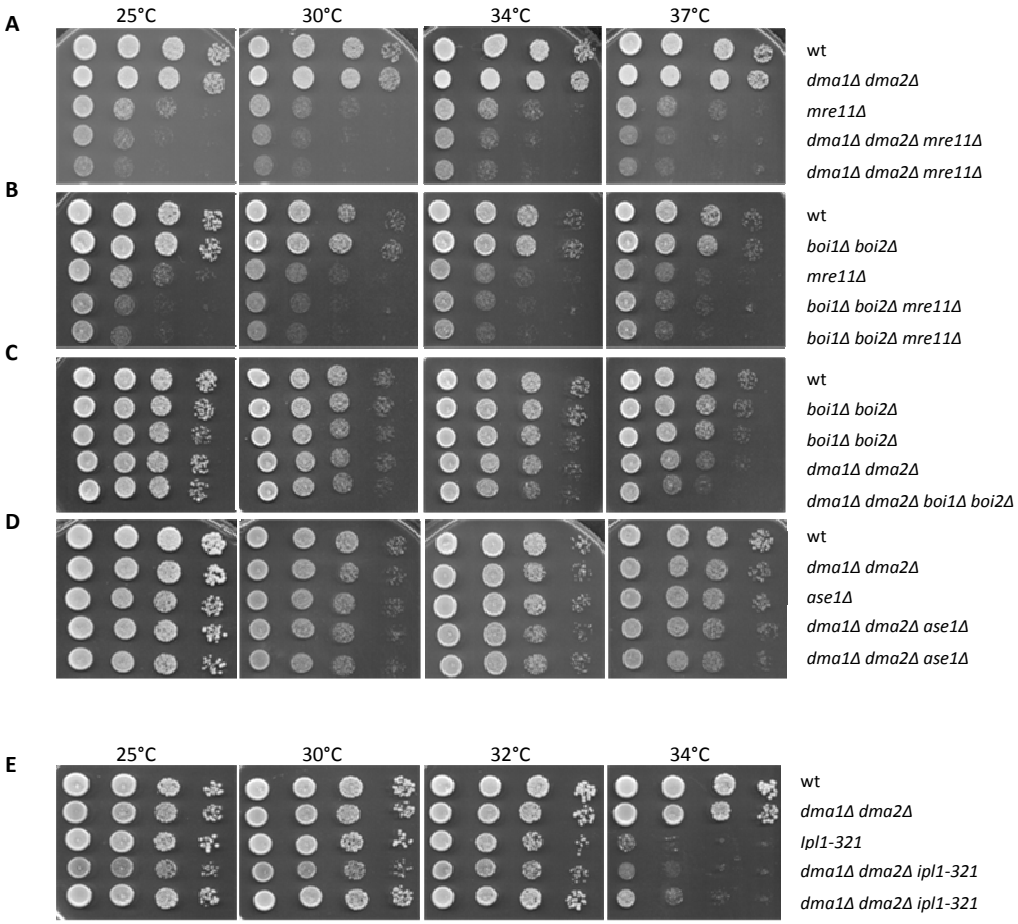

Figure 21. Genetic interactions between the Dma proteins and other factors involved in the NoCut pathway. (**A–E**) Serial dilutions of stationary phase cell cultures of strains with the indicated genotypes were spotted on YEPD plates, which were then incubated for 2 days at 25°C or for 1 day at 30, 34 and 37°C (**A-D**) with the exception of the strains carrying the *ipl1-321* allele which were incubated for 2 days at 25°C or for 1 day at 30, 32 and 34°C (**E**).

The contemporary lack of Dma proteins and of Boi1 and Boi2 causes missegregation of chromosomes.

As described above, the simultaneous lack of Dma and Boi proteins causes a synthetic growth defect at 37°C on YEPD plates (Fig. 21C).
In order to understand the cause of this phenotype, we synchronized wild-type, *dma1Δ dma2Δ*, boi*1Δ boi2Δ* and *dma1Δ dma2Δ boi1Δ boi2Δ* cell cultures at 25°C in G1 by using α-factor, followed by release into the cell cycle. When most of the cells had started to replicate their DNA (recognizable as the apperearance of budded cells), we have re-added α-factor to block cells in the following G1 phase and to better understand how efficently cells divide. We did not perform this experiment at 37°C because, from our previuous data, the phenotype of the quadruple mutant at this temperature was not clear probably due to the cytokinetic defect of *dma1Δ dma2Δ* cells (data not shown).
After the release, the kinetics of DNA replication, budding and nuclear division showed a similar profile in wt, *dma1Δ dma2Δ* and *boi1Δ boi2Δ* cells. Interestingly, the quadruple mutant showed an aberrant FACS profile with an accumulation of cells with DNA content between 1C and 2C (Fig. 22A and B). To try to explain the meaning of this FACS profile, we hypothesize that the lack of all Dma1, Dma2, Boi1 and Boi2 causes a syntetic growth defect because of unfaithful chromosome segregation that can occour spontaneously during every cell cycle.
To test if our hypothesis is correct we generated wild-type, *dma1Δ dma2Δ*, boi*1Δ boi2Δ* and *dma1Δ dma2Δ boi1Δ boi2Δ* strains carrying the TetO/TetR system to visualize sister chromatids in living cells (Michaelis et al., 1997). Briefly, 336 sequence of Tet operators are inserted adjacent to the centromere of chromosome V in cells that expresses a Tet repressor fused to GFP. The Tet operators are visible as green fluorescent dots within the nuclei of cells. In particular, they appear as a single dot when the sister chromatids are bound together by cohesin and as two dots when the cohesion between them is removed. We analyzed the percentage chromosome missegregation in *dma1Δ dma2Δ boi1Δ boi2Δ* calculated as cells that showed two separated points into the nucleus of unbudded cells or into one nucleus of anaphase cells. As shown in figure 22C wild-type, *dma1Δ dma2Δ*, boi*1Δ boi2Δ* cells showed a normal chromosome segregation at 25°C while the *dma1Δ dma2Δ boi1Δ boi2Δ* mutant showed a

little segregation defect (5%). At 37°C, while the control strains missegregated chromosomes up to 6%, the quadruple mutant defect reached 23%. All together these data indicate that the lack of Dma proteins concomitantly with the absence of Boi1 and Boi2 causes missegregation of chromosome probably due to a failure in the NoCut pathway activation.

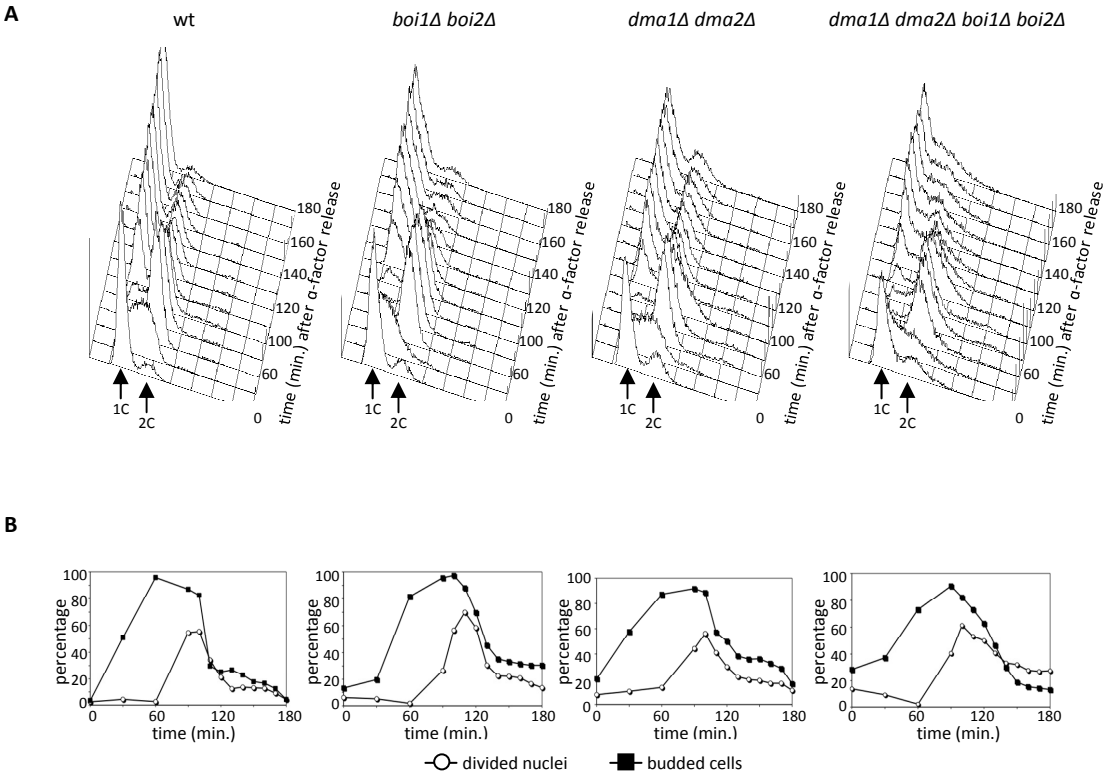

C

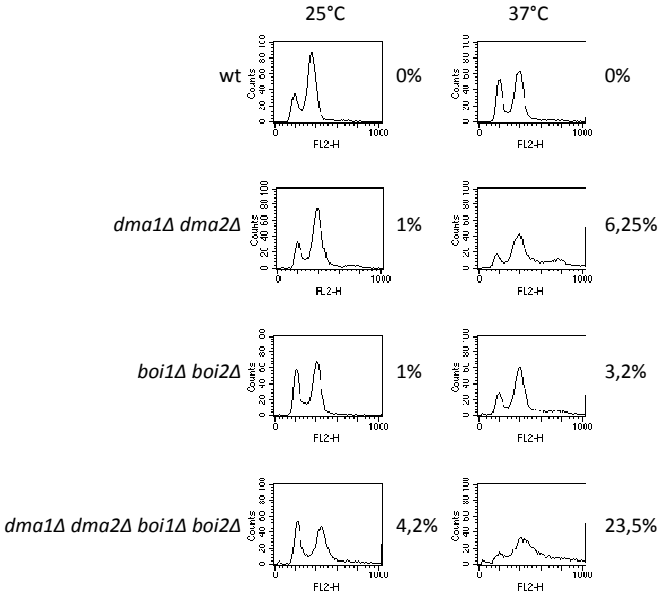

Figure 22. The lack of Dma proteins concomitantly with the absence of Boi1 and Boi2 causes chromosome missegregation.

(**A–B**) Exponentially growing cultures of wild-type, *dma1Δ dma2Δ, boi1Δ boi2Δ*, and *dma1Δ dma2Δ boi1Δ boi2Δ* cells were arrested in G1 by α-factor and released from G1 arrest at 25°C (time 0). At 90min after release α-factor was readded at 10μg/ml. At the indicated times after release, cell samples were taken for FACS analysis of DNA contents (**A**), and for scoring budding and nuclear division (**B**). (**C**) Exponentially cell coltures of the indicated strains carryng the the TetO/TetR system to visualize sister chromatids were grown at 25°C in YEPD and then shifted to 37°C for 240min. Cell samples were taken for FACS analysis of DNA contents and for scoring the percentage of chromosome missegregation.

Search for new players in cell division control

Vhs2 characterization

VHS2 ORF was found in our laboratory by a genetic screening aimed to find multicopy suppressors of the *GAL1-DMA2 hof1Δ* lethality on galactose containing plates, by transformation with a library of yeast episomic plasmids containing DNA inserts of the yeast genome. Among library plasmids that allowed the *GAL1-DMA2 hof1Δ* strain to grow on YEPRG plates, one plasmid contained a piece of chromosome IX containing several genes, among which *VHS2* seemed to be involved in the suppression phenotype.

In order to test if high Vhs2 levels can really rescue the synthetic lethality of the *GAL1-DMA2 hof1Δ* combination, we generated a centromeric and an integrative plasmid carrying the *VHS2* ORF under the *GAL1* promoter control. These plasmids were used to transform wild-type and *GAL1-DMA2 hof1Δ* cells. Several transformant were tested to verify the suppression on YEPRG plates but, with our disappointment, no transformants were able to grow in these conditions (data not shown). In parallel to this analysis we started to delete *VHS2* in wild type haploid cells in order to functionally characterize the gene product. *vhs2Δ* strain turned out to be viable and therefore suitable for further analysis. To investigate the role of Vhs2 in the yeast cell cycle we synchronized wild type and *vhs2Δ* cell colture in G1, followed by release into the cell cycle at 25°C. When about 90-95% of the cells were budded, we readded α-factor in order to analyze a single cell cycle. After the release, the kinetics of DNA replication (Fig. 23A), budding and nuclear division (Fig. 23B) showed a very similar profile in both strains. So Vhs2 doesn't seem to have a role during an unperturbed cell cycle.

We also tested if the *vhs2Δ* cells were sensitive to several kind of stress: osmotic stress (NaCl 500mM or 1M), or DNA replication stress (HU 100mM or 200mM) or mitotic spindle damage (Benomyl 10µg/ml or 15µg/ml), but *vhs2Δ* cells did not show any sensitivity (data not shown).

In addition, we also analyzed the effects of the galactose induced-overexpression of *GAL1-VHS2* from single or multiple copy integration in the yeast genome, but we observed that it does not cause evident defects on cell viability and in the cell cycle progression (data not shown).

Since *VHS2* was isolated as possible multicopy suppressor of the lethal cytokinetic defect of the *GAL1-DMA2 hof1Δ* combination, we looked for synthetic effects between the *VHS2* deletion and mutations in genes

implicated in cytokinesis. We analyzed the growth ability of different double mutants derived from meiotic segregants of the diploids obtained by crossing *vhs2Δ* cells with: *iqg1-1*, *ase1Δ*, *cyk3Δ* and *chs2Δ* cells. None of the double mutants showed a synthetic growth defect of a on YEPD plates at different temperatures (data not shown). Taken together these preliminary data suggest that Vhs2 is not involved in cytokinesis control.

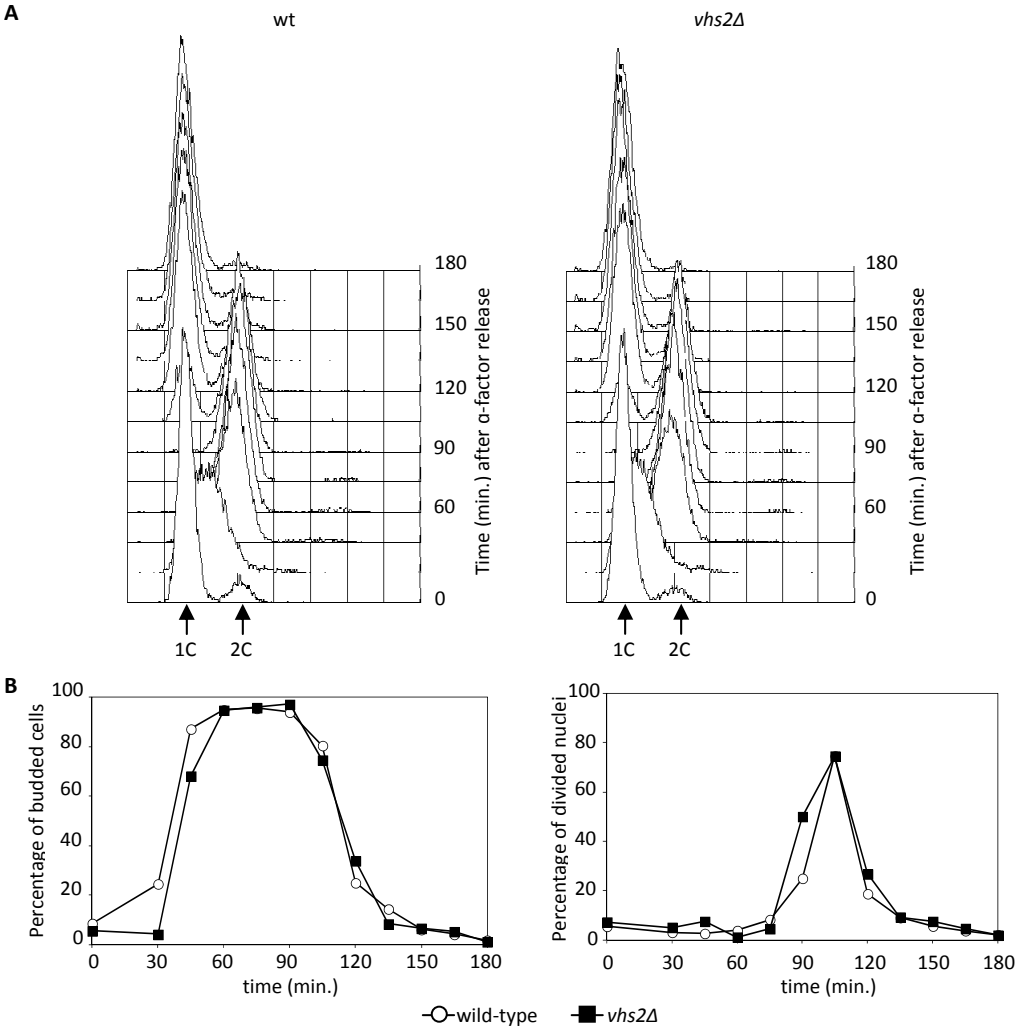

Figure 23. The lack of Vhs2 doesn't alterate cell cycle progression.
(**A–B**) Exponentially growing cultures of wild-type and *vhs2Δ* cells were arrested in G1 by α-factor and released from G1 arrest at 25°C (time 0). At 75min after release α-factor was readded at 10μg/ml. At the indicated times after release, cell samples were taken for FACS analysis of DNA contents (**A**), for scoring budding and nuclear division (**B**).

The lack of Vhs2 causes septin ring instability

Since septins are involved in cytokinesis and Vhs2 seems to interact with these proteins (by an high-throughput screening described in Costanzo et al., 2010; Addinall et al., 2008), we decided to test if *VHS2* deletion could have a synthetic effect in combination with mutations that destabilize septins structure.

Double mutants and control strains were inoculated in YEPD at 25°C and serial diluitions were spotted on YEPD plates and incubated at different temperatures (Fig. 24). Interestingly, *VHS2* deletion showed synthetic growth defects in combination with different septin mutant alleles *cdc12-6*, *shs1Δ*, *shs1-100, cdc3-1* and with the lack of Rts1, the regulatory subunit of protein phosphatase 2A involved in septin ring stability (Oh and bi, 2011) at high temperatures: (Fig. 24A, D, E and F); while it did not cause any effect when combined with *cdc10-1* or *cdc12-1* septin alleles (Fig. 24B and C). These data suggest that Vhs2 might be involved in septins structure stability.

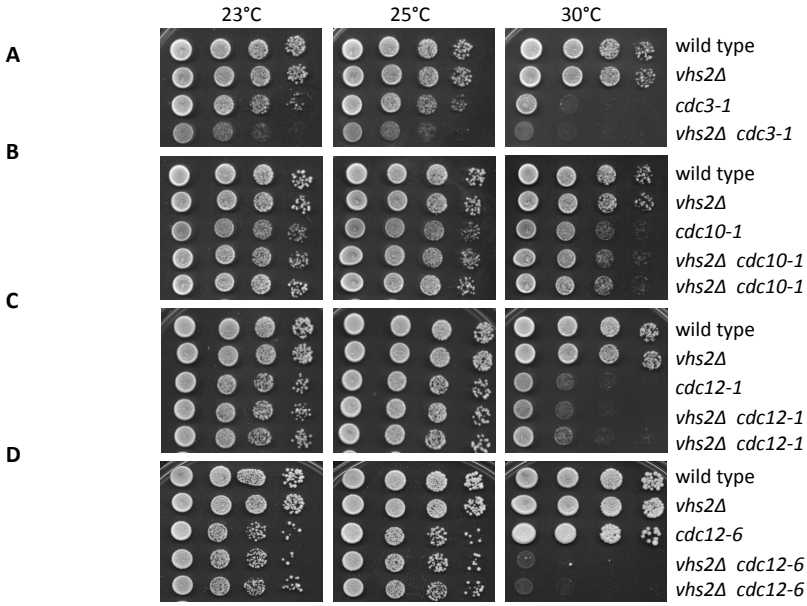

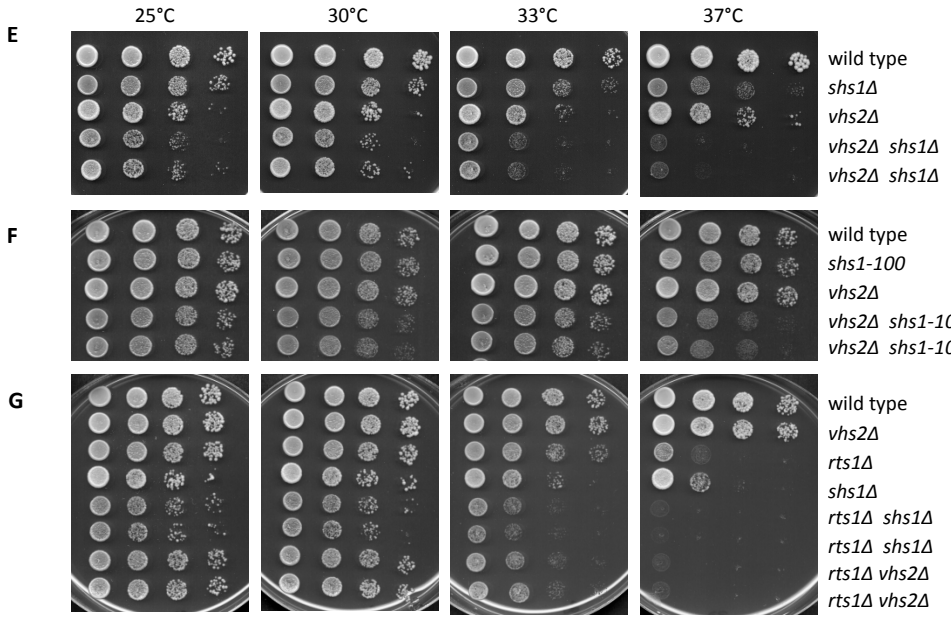

Figure 24. Genetic interactions between Vhs2 and septin mutants.
(**A–G**) Serial dilutions of stationary phase cell cultures of strains with the indicated genotypes were spotted on YEPD plates, which were then incubated for 2 days at 23 or 25°C, or for 1 day at 30°C (**A-D**) with the exception of the strains carrying the *shs1Δ*, *shs1-100* or *rts1Δ* allele which were incubated for 2 days at 25 °C or for 1 day at 30, 33 and 37°C (**E-G**).

In order to better understand the cause of the synthetic growth defect showed on YEPD plates of *vhs2Δ shs1Δ*, *vhs2Δ shs1-100, vhs2Δ cdc12-6* and *vhs2Δ cdc3-1* cells we analyzed the phenotype of synchronized cell cultures of control and mutant strains released at the respective critical temperature. From FACS analysis of DNA content of wild type, *vhs2Δ*, *shs1Δ* and *vhs2Δ shs1Δ* cells we did not find any obvious difference between the single septin mutant and the double mutant (data not shown), making it impossible to determine the cause of the synthetic growth defect.
Notwithstanding the difficult to synchronize *shs1-100, cdc12-6 and cdc3-1* mutants, we also tried to synchronize these strains and *vhs2Δ shs1-100, vhs2Δ cdc12-6* and *vhs2Δ cdc3-1* strains at 23°C and released all the strains at the respective critical temperature (37°C, 30°C and 25°C respectively). The double mutants, respect to the control strains, seemed to be defective in starting DNA replication/spindle elongation (*vhs2Δ shs1-100*), S phase progression (*vhs2Δ cdc12-6*) or starting S phase/S phase progression and

cell division (*vhs2Δ cdc3-1*) respectively (data not shown). So, further analysis will be required to better understand the molecular details of the role of Vhs2 on septins structure stability.

Since Vhs2 was implicated in actin polarization (Gandhi et al., 2006), we analyzed also the actin localization in the above mentioned double mutants that share a synthetic grow defect with *VHS2* deletion (*shs1*, *shs1-100*, *rts1*, *cdc12-6*, *cdc3-1* carring *VHS2* deletion). Double mutants and control cell cultures were inoculated in YEPD at 25°C ON and then shifted to 30°C or 37°C over night (Fig. 25). Cell samples were taken to analyze actin patch, cables and rings by using Rhodamine-phalloidine staining. We did not detected any obvious defect of cell polarization in any double mutant (Fig. 25), despite the strange shape of the cells of some of them. This finding led us to hypothesize that the growth defects of the combination of the *VHS2* deletion with septins mutants were not due to an actin polarization defect. In the same mutants we did not analyze septin ring deposition because the single septins mutants showed severe defects *per se* even at 25°C (data not shown).

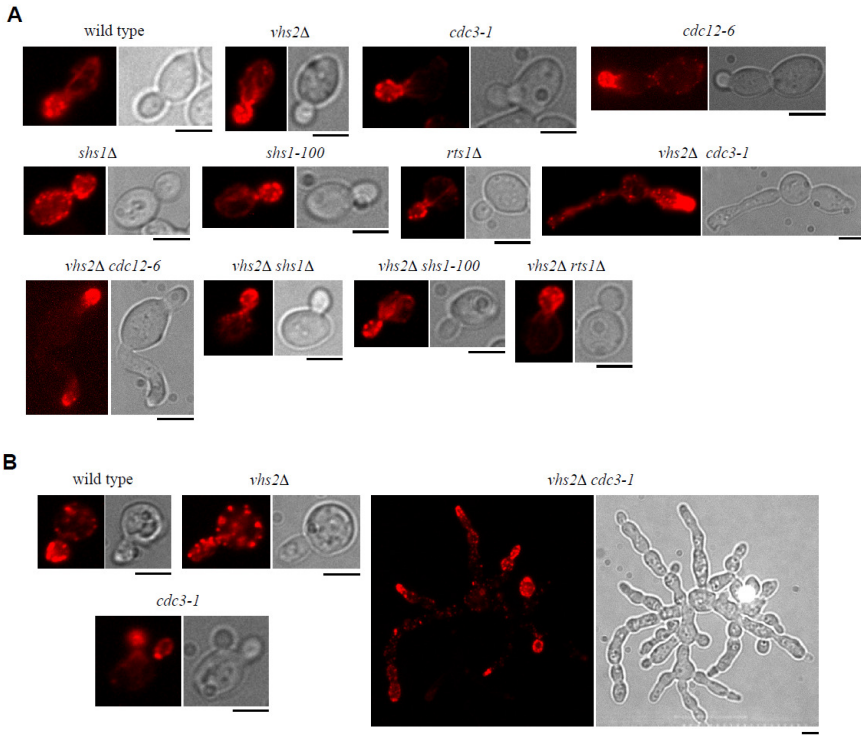

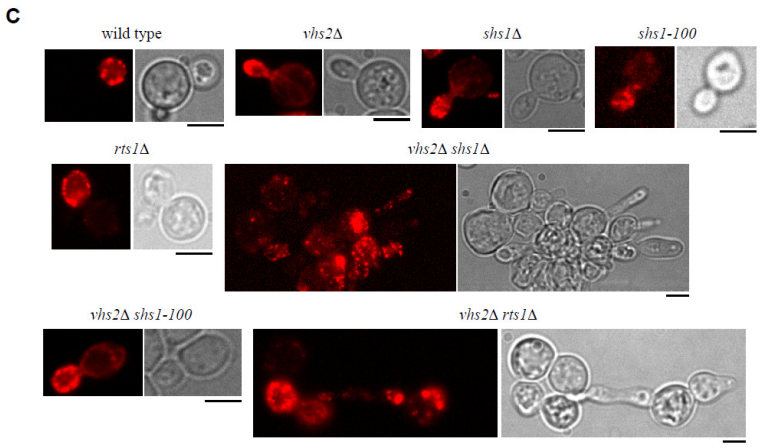

Figure 25. The synthetic grow defects between the lack of Vhs2 and septins mutants isn't due to an obvious defect of cell polarization.
(**A–C**) Exponentially growing coltures of cells with the indicated genotype were grown at 25°C in YEPD ON (**A**) and then shifted to 30°C (**B**) or 37°C (**C**) ON. Cell samples were taken to analyze actin patch, cables and rings by using Rhodamine-phalloidine staining. Bar, 5µm.

However, we carefully analyzed septin dynamics of exponentially growing *vhs2Δ* cells during an unperturbed cell cycle respect to the wild-type.
We observed that *vhs2Δ* cells undergo premature disassembly of septin ring before mitotic exit onset. Indeed 30,7% (39 of 127 large budded cells with separated nuclei) of *vhs2Δ* cells exhibited long mitotic spindle but no septin ring. On the contrary, only 11,3% (10 of 88 large budded cells with separated nuclei) of wt cells showed this defect (Fig. 26). Together, these data suggest that the lack of Vhs2 affects septin ring dynamics, in particular Vhs2 seems to stabilize the double ring structure during mitotic exit and cytokinesis.

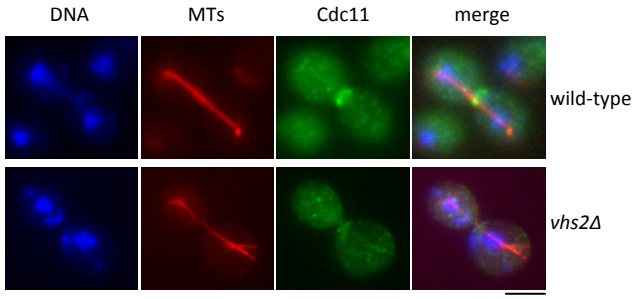

Figure 26. The lack of Vhs2 affects septin ring dynamics.
Exponentially growing cultures of wild-type and *vhs2Δ* cells were grown in YEPD at 25°C. Pictures were taken to show *in situ* immunofluorescence analysis of nuclei (DNA), mitotic spindles (MTs) and septin ring deposition (Cdc11). Bar, 5µm.

Since Shs1 dephosphorylation is important for septin ring destabilization during citokinesis (Dobbelaere et al., 2003) we asked if the lack of Vhs2 could affect this process.

In order to test this hypothesis we generated *vhs2Δ* cells containing a functional version of Shs1 tagged with HA epitope. Then *SHS1-HA* and *vhs2Δ SHS1-HA* cells were synchronized in G1 phase using α-factor and then released in fresh medium. When about 90-95% of the cells were budded, we readded α-factor in order to analyze a single cell cycle. Samples were taken at different time points after release to monitor the kinetics of DNA replication (Fig. 27A), budding, nuclear division (data not shown) and to evaluate Shs1 phophorylation by western blot analysis using anti-HA or anti-Cdc11 antibodies (loading control) (Fig. 27C). As shown in figure 27, Shs1 phosphorylated forms appearance and amount are very similar in the absence of Vhs2 respect to wild-type cells.

These data indicate that Vhs2 does not control Shs1 phosphorylation in order to regulate septin ring stability and it may act downstream of this event.

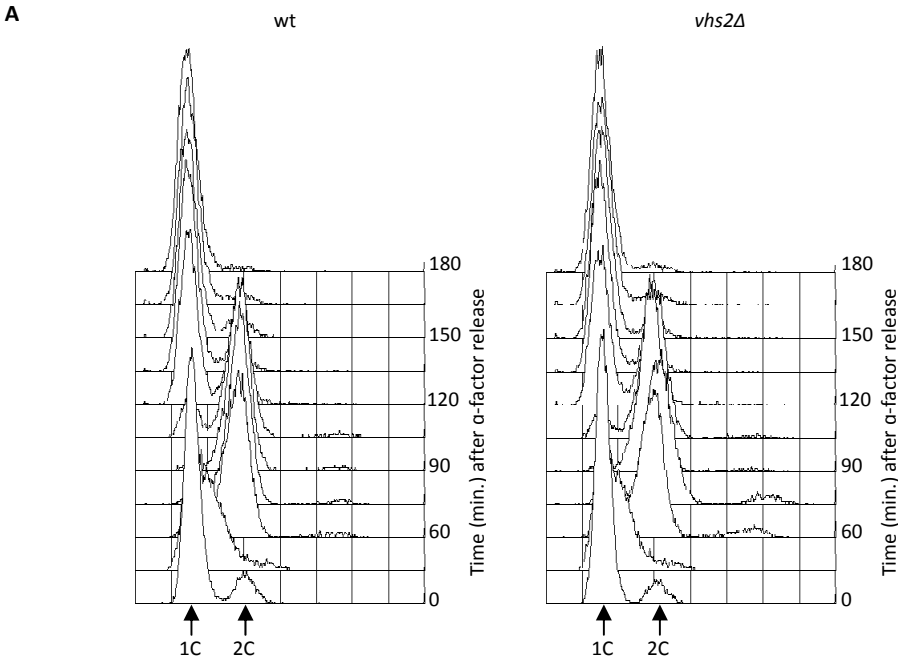

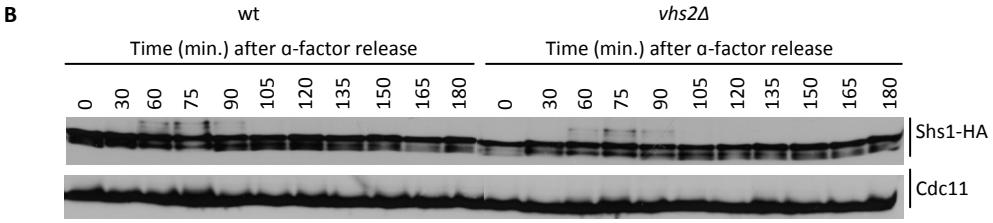

Figure 27. The lack of Vhs2 doesn't affects Shs1 phosphorylation.
(**A–B**) Exponentially growing coltures of *SHS1-HA* and *vhs2Δ SHS1-HA* cells were arrested in G1 by α-factor in YEPD at 25°C and released from G1 arrest at 25°C in fresh medium. At 75min after release α-factor was readded at 10μg/ml. At the indicated times, cell samples were taken for FACS analysis of DNA contents (**A**) and for determining Shs1 and Cdc11 levels and phosphorylation by wester blot analysis with anti-HA and anti-Cdc11 (loading control) antibodies (**B**).

Vhs2 levels and phosphorylation

Vhs2 was described as a multi-phosphorylated protein from high-throughput analysis (Oliveira et al., 2012) and it appears as multiple bands with different electroforetic mobility by TCA and native protein extracts of *VHS2-6HA* and *VHS2-8myc* cells (our data not shown). In order to clarify if the slowly migrating Vhs2 species were due to phosphorylation events we performed an *in vitro* phosphatase assay. Vhs2-6HA was purified from total extract of yeast cycling cells by immunoprecipitation using proteinA-sepharose resin and antibodies α-HA. The purified Vhs2-6HA was subjected to lambda phosphatase treatment for 7min at 30°C. Most of Vhs2 species disappeared after incubation (Fig. 28A), indicating that Vhs2 is subjected to phosphorylation events during the cell cycle.

Once it was established that, at least in part, the slowly migrating forms of Vhs2 were due to phosphorylations, we analyzed if its total levels and modifications could change during an unperturbated cell cycle.

VHS2-6HA cells were inoculated in YEPD, arrested in G1 with α-factor and released in fresh medium. When about 90-95% of the cells were budded, we readded α-factor in order to analyze a single cell cycle. Samples were taken at different time points after release to monitor the kinetics of DNA replication (Fig. 28B), budding, nuclear division (data not shown) and Vhs2 levels and modifications by western blot analysis (Fig. 28C). The analyzed cells progressed normally through the cell cycle (Fig. 28A). By western blot analysis of cycling cells extract Vhs2 appear as multiple bands (Fig. 28A). Vhs2-6HA protein is always present throughout the cell cycle (Fig. 28C), appeared to be mostly dephosphorylated in G1, then the phosphorylated forms accumulated during S-G2-M and decreased at the beginning of cell division (Fig. 28C).

Thus, Vhs2 is subjected to post-translational modifications that alter its electrophoretic mobility during the cell cycle and these modifications decrease concomitantly with the beginning of cytokinesis.

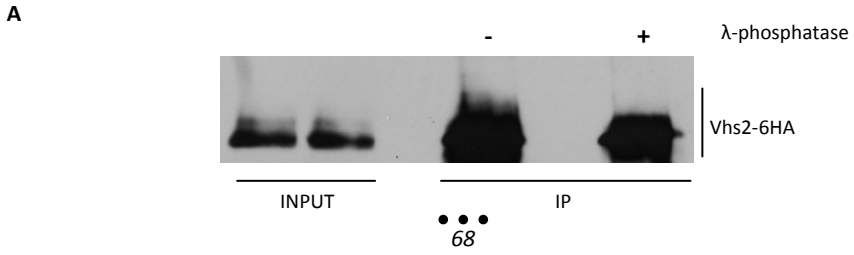

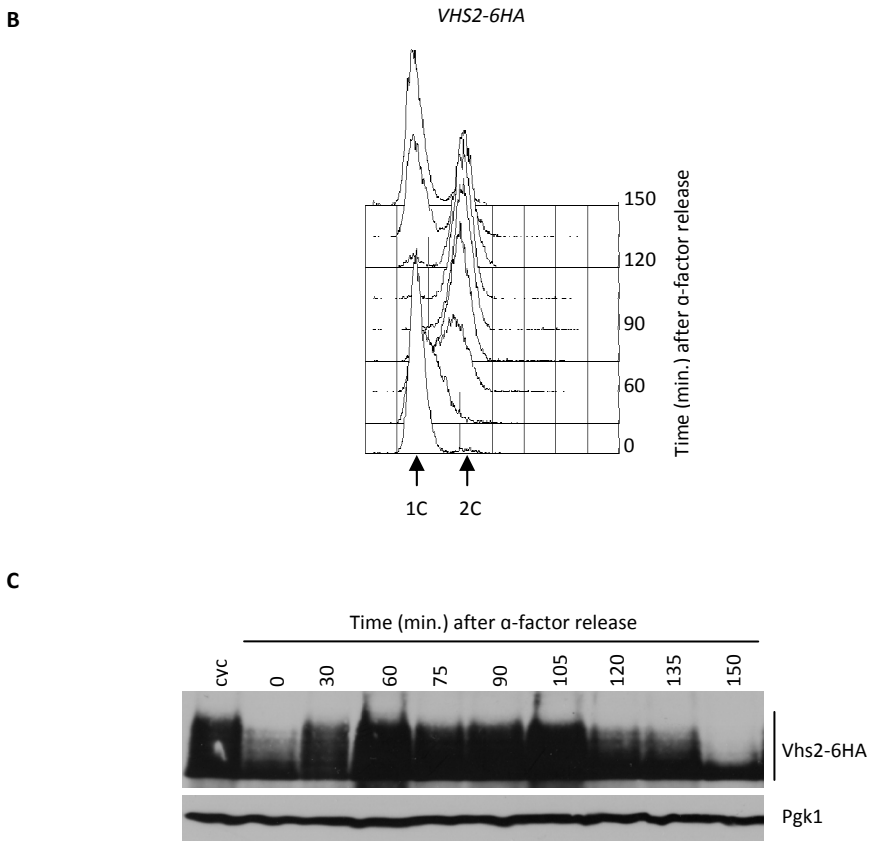

Figure 28. Vhs2 levels and phosphorylation.
(**A**) Total protein extract of *VHS2-6HA* cells in exponentially phase (input) were immunoprecipitated with anti-HA antibodies and the immunoprecipitate was incubated for 7min at 30°C with 20 unit/µl λ-phasphatase (+) or with reaction buffer only (-). (**B–C**) Exponentially growing cultures of *VHS2-6HA* cells were arrested in G1 by α-factor in YEPD αt 25°C and released from G1 arrest αt 25°C in fresh medium. At 75min after release α-factor was readded at 10µg/ml. At the indicated times, cell samples were taken for FACS analysis of DNA contents (**B**) and for determining Shs1 levels and phosphorylation by western blot analysis with anti-HA and anti-Pgk1 (loading control) antibodies (**C**).

Since Vhs2 appears to be phosphorylated during S-G2-M phases and dephosphorylated at the beginning of cytokinesis, in order to better understand the dephosphorylation timing of Vhs2 we performed a release of G2 arrested cells. *VHS2-6HA* cells were inoculated in YEPD, arrested in G2 with nocodazole and released in fresh medium containing α-factor in order to analyze kinetics of Vhs2 dephosphorylation during a single division. Samples were taken at different time points after release to

monitor the kinetics of cell division (Fig. 29A, B) and Vhs2 modifications by western blot analysis (Fig. 29C).
Vhs2 seemed to be hyperphosphorylated in G2 and the slow migrating bands seemed to disappear after 60min from nocodazole release, concomitantly with the beginning of cell division (Fig. 29B, C).

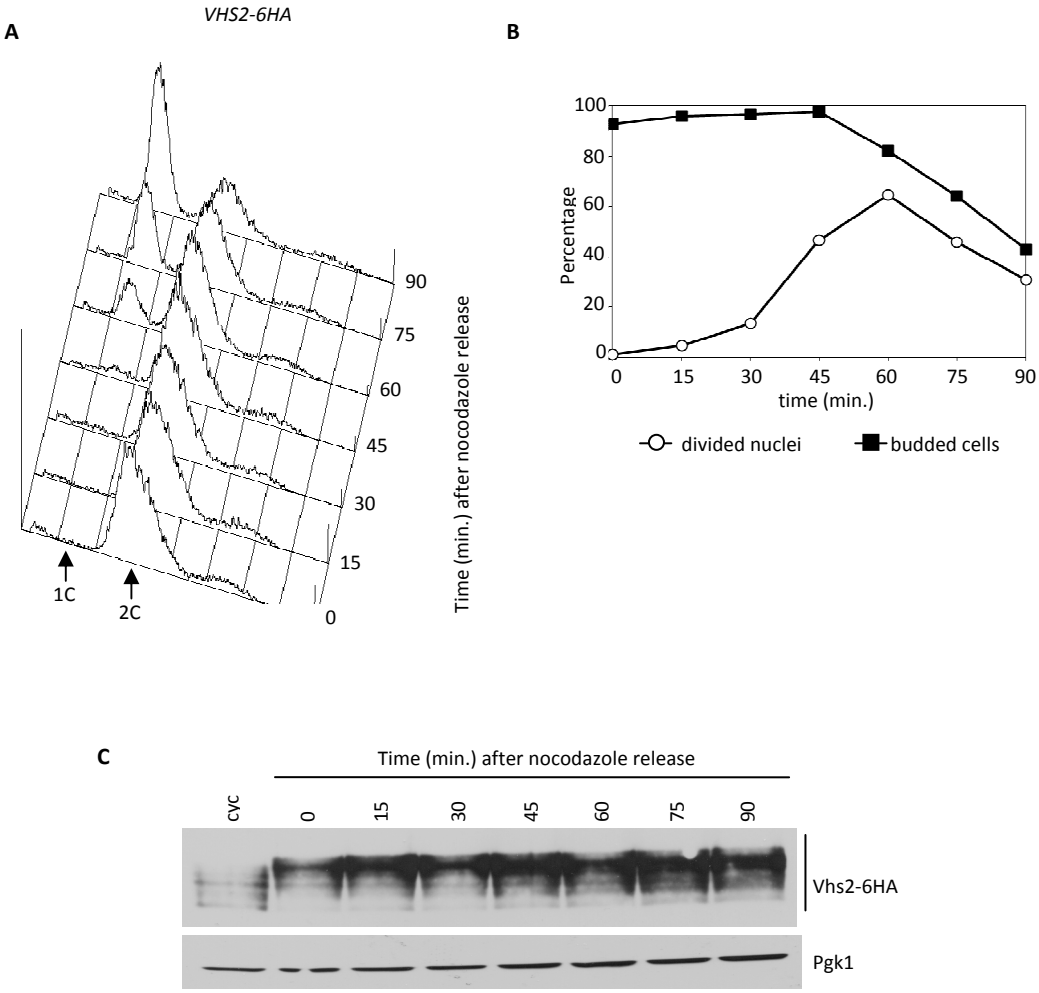

Figure 29. Vhs2 phosphorylation decreases during cytokinesis.
(**A–C**) Exponentially growing cultures of *Vhs2-6HA* cells were arrested in G2 by nocodazole αt 25°C and released from G2 arrest at 25°C in fresh medium containing α-factor []. At the indicated times, cell samples were taken for FACS analysis of DNA contents (**A**), for scoring budding and nuclear division (**B**) and for determining Vhs2 levels and phosphorylation by western blot analysis with anti-HA and anti-Pgk1 (loading control) antibodies (**C**).

These data prompted us to analyze the effect of hyperactivation or inactivation of different kinases and phosphatases, known to be involved in cytokinesis, on the phosphorylation state of Vhs2.
The most important phosphatase known to function during cytokinesis is Cdc14. Moreover, data from high-throughput screening analysis indicated that Vhs2 appeared to be phosphorylated by Dbf2 protein kinase that function during mitotic exit and cytokinesis (Mah et al., 2005; Ptacek et al., 2005), among other proteins; so we analyzed if Vhs2 levels and phosphorylation could change when these two enzymes were hyperactivated or inactivated.
To this purpose we constructed yeast strains containing both *VHS2-6HA* and thermo-sensitive alleles of Dbf2 or Cdc14 that are inactive at the restrictive temperature of 37°C (*dbf2-2* and *cdc14-1*). *VHS2-6HA*, *VHS2-6HA dbf2-2* and *VHS2-6HA cdc14-1* cells were grown in YEPD at 25°C and then shifted to 37°C for 2h. Cell samples were taken for FACS analysis (data not shown) and Vhs2 modifications analysis by western blot (Fig. 30A). As shown in figure 30, Vhs2 seemed to be hyperphosphorylated when Dbf2 kinase or Cdc14 phosphatase are inactivated. These data suggest that Dbf2 is not responsible for Vhs2 phosphorylation, while Cdc14 might regulate its dephosphorylation directly or indirectly. The fact that Vhs2 is not fully in its phosphorylated form following Cdc14 inactivation lead us to hypothesize that other kinases and phosphatases regulate the post-translational modification of this protein during the cell cycle.
In order to better understand if Vhs2 could be dephosphorylated directly by Cdc14, we analyzed the phosphorylation state of Vhs2 in *GAL1-CDC14* and *GAL1-cdc14C283A* (phosphatase dead allele) expressing strains.
VHS2-6HA, *VHS2-6HA GAL1-CDC14* and *VHS2-6HA GAL1-cdc14C283A* cells were grown in YEPR at 25°C and then shifted in YEPRG medium for 1 or 2 hours to induce *GAL1* promoter activation. Cell samples were taken for FACS analysis and Vhs2 modifications analysis by western blot (Fig. 30B).
As shown in figure 30, when Cdc14 is overproduced Vhs2 seemed to migrate as bands with higher electrophoretic mobility compared to the wild-type control conversely, when the phosphatase dead version of Cdc14 is overproducted, Vhs2 seemed to migrate as bands with lower electrophoretic mobility. These data are in agreement with the previous (Fig. 30A) which led us to hypothesize a role of Cdc14 phosphatase on Vhs2 dephosphorylation.

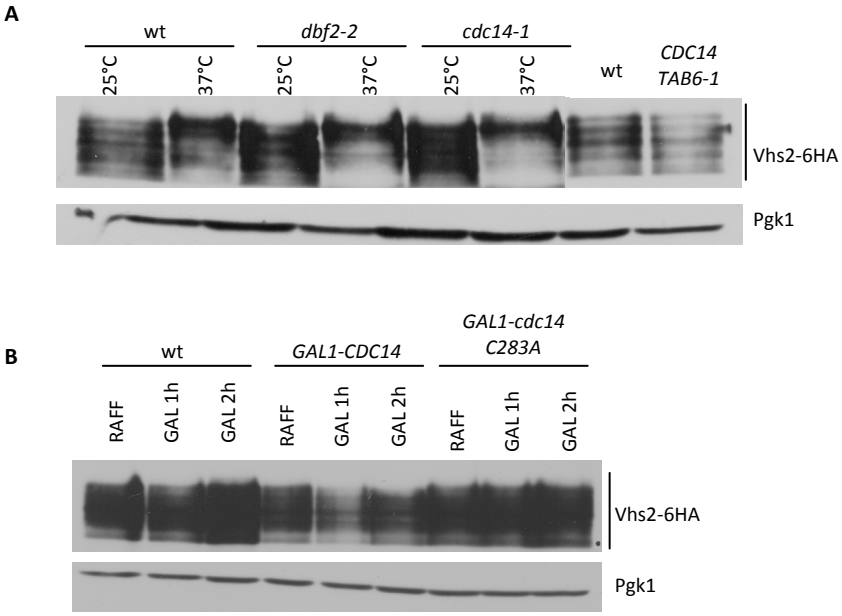

Figure 30. Vhs2 phosphorylation is altered in Cdc14 and Dbf2 mutants.
(**A**) Cell cultures of *VHS2-6HA*, *dbf2-2 VHS2-6HA* and *cdc14-1 VHS2-6HA* strains were grown in YEPD medium at 25°C to exponentially phase and then shifted to 37°C for 2h. Cell samples were taken for determining Vhs2 levels and phosphorylation by wester blot analysis with anti-HA and anti-Pgk1 (loading control) antibodies. (**B**) Cell coltures of *VHS2-6HA*, *GAL1-CDC14 VHS2-6HA* and *GAL1-cdc14-C283A VHS2-6HA* strains were grown in YEPR medium at 25°C to exponentially phase and then shifted in YEPRG at 25°C for 2h. Cell samples were taken for determining Vhs2 levels and phosphorylation by western blot analysis with anti-HA and anti-Pgk1 (loading control) antibodies.

Discussion

Saccharomyces cerevisiae Dma proteins participate in cytokinesis by controlling two different pathways

The events leading to cytokinesis must be tightly controlled and coordinated with nuclear division in order for a single eukaryotic cell to generate two identical daughter cells at the end of the mitotic cell cycle. Genetic studies revealed the existence of two partially redundant pathways that allow cytokinesis completion in budding yeast. The first pathway leads to the assembly of a functional AMR and requires Tem1, Iqg1, Bni1, Myo1, and actin. The second pathway controls septum formation and involves a number of proteins, among which Cyk3, Hof1, and Inn1. This feature ensures that cytokinesis is completed even in the absence of some proteins important for one of the two pathways, thus allowing cell survival.
In previous studies, Dma1 and Dma2 were shown to have redundant roles in mitotic spindle orientation, mitotic checkpoints, regulation of septin ring dynamics (Frachini et al., 2004; Merlini et al., 2012), and septin organization and function (Chahwan et al., 2013). The results of this work indicate that the Dma proteins participate in both pathways that control cytokinesis (Fig. 31). In particular, their lack alters the timing of AMR contraction with respect to mitotic spindle disassembly, causes a partial cytokinesis defect in *cyk3Δ* cells, and impairs proper PS deposition. In addition, Dma2 appears to function as a cytokinesis inhibitor, as we show that its moderate overproduction impairs both symmetric AMR contraction and PS formation, likely by acting on specific targets in these two cytokinesis pathways. These findings are consistent with published data on orthologs of the Dma proteins in other organisms. In particular, human *RNF8* overexpression caused adelay in cytokinesis (Plans et al., 2008), and ectopic expression of *S. pombe* Dma1 was shown to inhibit septum formation, leading to generation of elongated and multinucleate cells (Murone et al., 1996; Guertin 2002). Timely AMR contraction is brought about by a signaling network that includes Tem1-Iqg1 complex formation, which has been proposed to be an essential step (Shannon et al., 1999). Both Tem1 and Iqg1 are subjected to several levels of regulation, but how Tem1-Iqg1 interaction is controlled is unknown. We show here that Tem1 undergoes cell cycle-regulated ubiquitylation, and that the amount of

ubiquitylated Tem1 decreases concomitantly with cells undergoing AMR contraction. These data are very important per se, as Tem1 ubiquitylation has never been shown before. Unfortunately, we could not observe any effect of the absence of the Dma proteins on Tem1 ubiquitylation. On the other hand, the amounts of Tem1 ubiquitylated forms increase in the presence of Dma2 excess, which also inhibits Tem1-Iqg1 interaction, both *in vitro* and by two-hybrid assay, and causes defective AMR contraction. Based on the mobility shift of its ubiquitylated forms, Tem1 is likely polyubiquitylated. However,this post-translational modification is unlikely to signal Tem1 degradation, as total Tem1 levels do not decrease in response to Dma2 overproduction (data not shown), although the latter increases the amounts of Tem1 ubiquitylated forms. We cannot exclude that Tem1 polyubiquitylation might lead to a local degradation that cannot be detected by western blot analysis, but we favor the hypothesis that Tem1 ubiquitylation may regulate its activity, its subcellular localization, and/or its interaction with other cytokinesis factors. We could not evaluate whether Dma2 excess interferes with other possible Tem1 post-translational modifications, because none has been described in the literature so far. However, we observed that moderate Dma2 overproduction did not change the mobility of the Tem1-3HA doublet in SDS-PAGE (data not shown). In addition, we tried to analyze the Dma proteins' role in Tem1 localization at the division site, but we could never visualize Tem1 at the bud neck even in wild-type cells, and indeed this localization has never been described in the literature. Anyhow, it must be pointed out that moderate Dma2 overproduction did not affect Tem1 activity either in promoting mitotic exit, septin dynamics, or SPB localization (our unpublished observations). Altogether, these findings tempt us to propose that ubiquitylation of Tem1 might inhibit Tem1 binding to Iqg1, which, in turn, will not be competent to promote AMR contraction. Subsequent Tem1 deubiquitylation would allow Tem1-Iqg1 interaction, thus promoting AMR contraction. Whether the Dma proteins play a physiological role in this control still remains unaddressed. Proper PS formation requires bud neck recruitment and concerted action of Cyk3, Hof1, Inn1, and Chs2. We found that Dma2 excess causes asymmetric PS

deposition, likely by interfering with Chs2 and Cyk3 dynamics at the bud neck.

Indeed, we observed that the Chs2 ring contracts asymmetrically in GAL1-DMA2 cells. In addition, Dma2 can block Cyk3 localization at the bud neck without perturbing either Cyk3 total levels or phosphorylation, which is important for its recruitment at the division site (Meitinger et al., 2010). Unfortunately, we could not obtain reproducible results for Cyk3 ubiquitylation, and we can only speculate that the Dma proteins might regulate a still unknown factor(s) that controls Cyk3 function before its recruitment at the bud neck (Fig. 31). However Dma2 overproduction does not alter Inn1 bud neck localization, whose lack is known to cause a complete cytokinesis block (Jendretzki et al., 2009), and indeed Dma2-overproducing cells are viable and form a PS, likely due to the presence of Hof1. In fact, the presence of Dma2 excess, which causes defective AMR contraction, lack of Cyk3 localization at the bud neck, and asymmetric PS deposition is lethal for cells that lack Hof1, and Dma2-overproducing *hof1Δ* cells cannot complete cytokinesis and do not localize Inn1 at the bud neck. These data are in agreement with the existence of partially overlapping cytokinesis pathways and with the observation that *HOF1* or *CYK3* deletions have no effect on AMR assembly, but their combination causes synthetic lethality (Nishihama et al., 2009), and each one leads to severe growth defect in cells lacking Myo1 (Vallen et al., 2000; Korinek et al., 2000). As Hof1 and Cyk3 cooperate to recruit Inn1 (Jendretzki et al., 2009; Nishihama et al., 2009), the negative effect of Dma2 excess on Cyk3 might completely impede Inn1 recruitment to the bud neck in the absence of Hof1, thus causing cell lethality. In agreement with the findings above, the lack of the Dma proteins results in partial defects in the timing of AMR contraction with respect to mitotic spindle breakdown as well as in Cyk3 localization at the bud neck, and causes abnormally shaped PS formation. However, these defects do not either block cell division or impair viability of *dma1Δ dma2Δ* cells, likely due to the redundancy of cytokinesis controls. Importantly, the lack of the Dma proteins causes a sick phenotype and cytokinesis defects in *cyk3Δ* cells. Indeed, improper AMR contraction might be toxic for Cyk3-lacking cells that are already impaired in PS formation, as

expected based on the known central role for Cyk3 in a cytokinesis rescue mechanism acting in the absence of functional AMR.

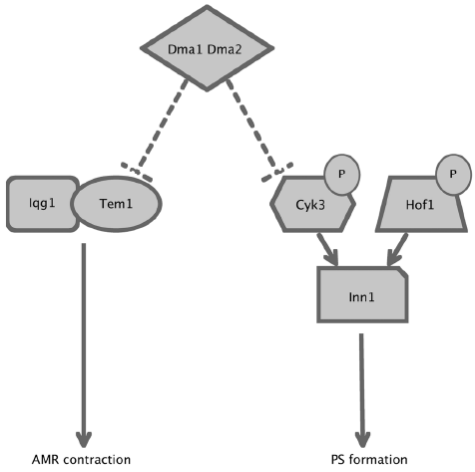

Figure 31. A model for the role of Dma proteins in cytokinesis control.
Dma1 and Dma2 participate, directly or indirectly, in the control of Tem1-Iqg1 interaction and Cyk3 localization, which are critical events for AMR contraction and PS formation, respectively (see text for details).

In summary, our findings shed new light on the biological role of the Dma proteins and reveal a new level of complexity in cytokinesis regulation. In particular, the Dma proteins seem to control both AMR contraction and symmetric PS deposition, thus acting as new cytokinesis inhibitors and contributing to couple mitotic exit with the cytokinetic events. Since their lack is not essential for cytokinesis completion, their function is likely redundant with other factor(s) that control cytokinesis. A challenging goal for the future will be the identification of cytokinesis proteins directly controlled by Dma1 and Dma2.

Tem1 ubiquitylation role in AMR contraction

Tem1 is a 245aa Ras-like GTP-ase, supposedly active in the GTP-bound state. Tem1, like other MEN factors, was found to localize at the spindle pole bodies (SPBs) during mitosis (Gunenberg et al., 2000) and then to the bud neck after mitotic exit (Lippincott et al., 2001). Therefore, this protein seems to play a role in the regulation of cytokinesis in addition to its role in the MEN cascade (Lippincott et al., 2001). Tem1 is not required for the assembly of actin and myosin at the bud neck but it is required for the contraction of the actomyosin ring (Lippincott et al., 2001). Moreover Tem1 can bind directly to the GRD domain of Iqg1 and this domain, like Tem1, is required for actomyosin ring contraction, but not for its assembly (Shannon and Li, 1999). These observations suggest that an interaction between Tem1 and the GRD domain of Iqg1 may trigger AMR contraction.
As described in the results, for the first time we showed that Tem1 undergoes cell cycle-regulated ubiquitylation. Interestingly, the amount of ubiquitylated Tem1 decreases concomitantly with cells undergoing AMR contraction (Cassani et al.,2013), leading us to hypothesize that this post-translational modification can inhibit Tem1 function in this process.
In order to understand the physiological relevance of Tem1 ubiquitylation, we studied the effects of Tem1 variants in which lysine residues were replaced by arginine residues, thus becoming not ubiquitylable.
In particular, we analized the kinetics of AMR contraction in cells that express high levels of Dma2 and different Tem1 K-R variants. With this we found that lysines 112, 133 and 219 seem to be important for Dma2's AMR contraction inhibition. Also lack of lysines 39 and 47 led to a partial effect. In particular, we observed that their substitution with arginine allows AMR contraction in the presence of high Dma2 levels indicating that ubiquitylation of these lysine residues is involved in AMR contraction inhibition. Surprisingly our analysis showed that also the lack of lysines 33, 59, 61, 170 causes a slight improvement of AMR contraction. In summary each Tem1K-R variant causes an improvement, more or less strong, of the AMR contraction of *GAL1-DMA2* cells, thus the substitution of several lysines in arginines has an effect. This phenotype has already been described in literature for other ubiquitylation mutants.

This analysis *in vivo* could be supported by the identification of Tem1 ubiquitylated residues by mass spectroscopy analysis *in vitro*.
It was important to determine if arginine substitution of lysines 112, 133 and 219 decreased Tem1 ubiquitylation *in vivo*. We tried to test this but with our protocol of detection of ubiquitin conjugates *in vivo* we could not detect Tem1 ubiquitylated forms when the protein is expressed from a centromeric plasmid. A challenging goal for the future will be to integrate the different *tem1K-R* alleles in the genome of wild type yeast cells in order to detect ubiquitin conjugates *in vivo* and to better characterize the role of Tem1 ubiquitylation in the regulation of the timing of AMR contraction by time lapse microscopy.
The obvious question is: can the Dma proteins ubiquitylate Tem1? Despite the amounts of Tem1 ubiquitylated forms increase in the presence of Dma2 excess, which also inhibits Tem1-Iqg1 interaction and causes defective AMR contraction (Cassani et al., 2013), we could not observe any effect of the absence of the Dma proteins on Tem1 ubiquitylation. It is therefore unlikely that Dma2 directly ubiquitylates Tem1. However, we can hypotesize that Dma2 could activate some Tem1 pro-ubiquitylation factor(s) or inactivate some anti-ubiquitylation factor(s) (Fig. 32). This can happen in response to precise stimuli or in each cell cycle in order to maintain the correct timing of AMR contraction respect to nuclear division, to ensure that the mother cell and daughter cell are both viable after cell separation.

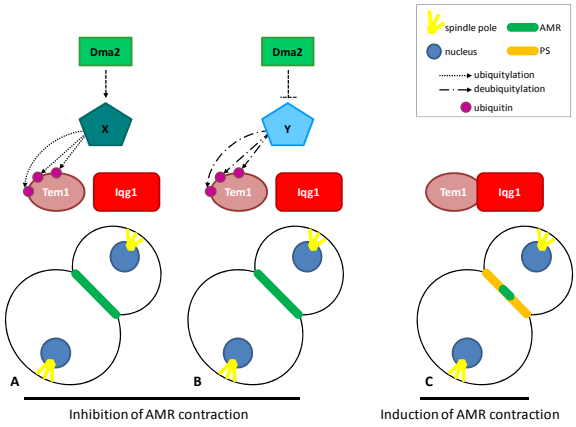

Figure 32. A model for the role of Dma2 in Tem1 ubiquitylation regulation.
Dma2 could regulate Tem1 ubiquitylation by activating an ubiquitin ligase (X) that can ubiquitylate Tem1 in order to inhibit the Tem1-Iqg1 interaction, a key event for the AMR contraction signalling; or by inhibiting an deubiquitylating enzyme (Y) that can deubiquitylate Tem1 in order to allow Tem1-Iqg1 interaction. See text for details.

Dma1 and Dma2 role in the NoCut pathway

Spindle-midzone defect and/or unsegregated chromatin over the spindle-midzone lead to inhibition of abscission in yeast and this process depends on Ipl1/Aurora and the anillin-related proteins Boi1 and Boi2. These proteins belong to the NoCut pathway, a checkpoint whose activation prevents chromosome breakage during cell division that could cause loss of cell viability (Nordern et al., 2006; Mendoza et al., 2009). It is not clear what primary signal is being monitored by this checkpoint. Similarly, it is unknown how the NoCut pathway inactivation allows abscission. It has been proposed that NoCut monitors the clearance of chromatin from the cleavage plane and that the spindle midzone is a sensor in this process (Norden et al., 2006), but other molecular mechanisms might be involved.
We were interested to understand if the Dma proteins could be activated by particular stimuli during cytokinesis in order to inhibit abscission.
Here we report evidences that the Dma proteins could be implicated in a checkpoint that blocks abscission.
First: the lack of Dma protein cause a "Cut phenotype" (Yanagida, 1998; Mendoza et al., 2009) in *ndc10-1* cells when shifted to 37°C. In fact cell wall digestion assay demostrated that *ndc10-1 dma1Δ dma2Δ* cells complete cytokinesis in the absence of chromosome segregation and hence cut the nucleus that is still lying on the cleavage plane, indicating a NoCut activation failure.
Second: drop test analysis showed that the lack of Dma1 and Dma2 causes a synthetic growth defect when combinated with the lack of Mre11. Mre11 is required to repair double-strand breaks (DSBs) through nonhomologous end hoining (NHEJ) that joins the ends of broken chromosomes irrespective of sequence homology (Krogh and Symington, 2004). So, if the lack of Dma proteins induces abscission in case of lagging chromosomes, *dma1Δ dma2Δ* cells strongly rely on NHEJ for survival. In agreement with this hypothesis, *dma1Δ dma2Δ* cells carriyng mutation in NHEJ genes, like *MRE11,* showed impaired growth compared to parental strains. This phenotype might be due to the fact that the absence of Dma1 and Dma2 could increase the frequency of chromosome breakage during cell division that in turn leads to a loss of cell viability.

Third: drop test analysis showed that the lack of Dma1 and Dma2 caused a synthetic growth defect when combinated with the lack of Boi1 and Boi2. Whereas the simultaneous lack of Dma proteins and Ipl1/aurora kinase did not cause any growth defect.
These data prompted us to better characterize the role of Dma proteins in this checkpoint. Since Ipl1 and Boi1 Boi2 appear to act in the same pathway (Norden at al., 2006), we hypothesize that Dma proteins work in the same pathway of Ipl1 but in parallel to Boi proteins to inhibit ascission.
This hypotesis is supported by the finding that *dma1Δ dma2Δ boi1Δ boi2Δ* cells showed a higher chromosome segregation defect than control strains at 25°C and this defect increases when cells are grown at 37°C.
These finding could be explained if the amount of chromosome segregation defects might be due to the increase of growth rate of the quadruple mutant that results in a less time for check the presence of defects that cannot be corrected due to the failure of the NoCut activation.
Furthermore we can hypothesize that the Dma proteins could act as sensors of spindle-midzone defects. Since a high temperature could compromise spindle stability and dynamics, and because Dma proteins were previously implicated in sensing of spindle position defect (Fraschini et al., 2004), the growth defect of *dma1Δ dma2Δ boi1Δ boi2Δ* cells at high temperature might be due to an inhability of these cells to sense and correct spindle defects that can lead to breakage of some lagging chromosomes.
We conclude speculating that, in order to inhibit abscission, Ipl1 monitors the presence of unsegregated chromatin on the spindle-midzone and activates the Boi proteins while, in a parallel pathway, the Dma proteins could sense the presence of defects in spindle-midzone regions (Fig. 33).
For the future it would be interesting to study deeper the molecular role of Dma proteins in the NoCut pathway and the connections with other proteins that act in this pathway. Other experiments will be required in order to clarify if Dma proteins work as sensor of spindle/spindle-midzone defects and at which level they act in order to activate the checkpoint.

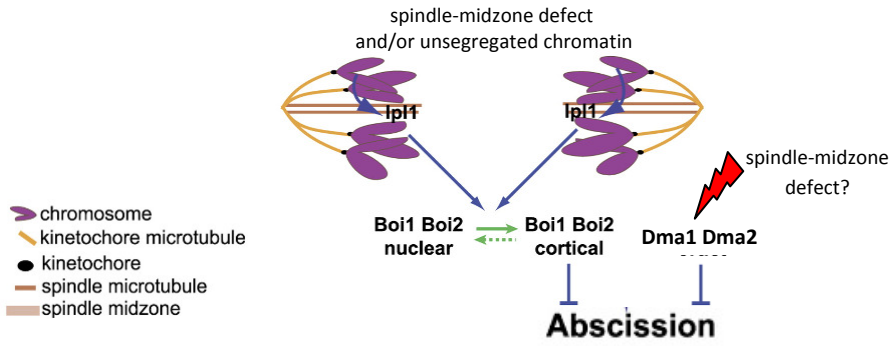

Figure 33. A model for the role of Dma proteins in the NoCut pathway.
Dma1 and Dma2 participate in the activation of the NoCut checkpoint in parallel to Boi proteins in order to inhibit abscission in response to spindle-midzone defect or unsegregated chromatin at the bud neck. See text for details. Picture modified from Norden et al., 2006).

Search for new players in cell division control

We started to study the biological function of Vhs2 in the cell cycle because we found this gene during a genetic screening performed in order to find high copy number suppressors of *GAL1-DMA2 hof1Δ* lethality.
Vhs2 is a protein of 436aa that was isolated as *gic1 gic2* suppressor (Gandhi et al., 2006). The authors described that Vhs2 is implicated in actin polarization together with Mlf3 and their primary sequences share 30% identity and 42% similarity (Gandhi et al., 2006). The function of this protein has not been characterized and its sequence provides no obvious clues regarding its cellular function.
Notwithstanding that high levels of Vhs2 did not suppress the synthetic lethality of the *GAL1-DMA2 hof1Δ* combination, in our laboratory we have collected evidences which suggest a role of this protein in septin ring stability.
Septins are conserved GTP-binding proteins that assemble into hetero-oligomeric complexes and higher-order structures such as filaments, rings, hourglasses or rings. Septins are usually associated with a discrete region of the plasma membrane and function as a cellular scaffold or diffusion barrier to effect cytokinesis, cell polarity, and many other cellular functions (Oh and Bi 2011). Septins undergo different post-translational modifications that regulate their structure during cell cycle.
The first evidence of the involvement of Vhs2 in septins regulation is provided by genetic analysis. Combining different mutant alleles that cause septin ring instability (*cdc3-1, cdc12-6, shs1Δ* and *shs1-100*) with the lack of Vhs2 we observed a synthetic growth defect, index of a possible role of Vhs2 in the regulation of septin ring dynamics. We demonstrated that this growth defect is not reconducible to an actin polarization defect despite the strange shape of the cells of some double mutant.
Another evidence of the involvement of Vhs2 in this process has been provided by the analysis of septin ring dynamics of *vhs2Δ* cells by *in situ* immunofluorescence. Interestingly, in the absence of Vhs2 cells disassemble the septin ring earlier than in wild type cells, i. e. when the spindle is long but not yet disassembled (30,7% of the analyzed cells). During cytokinesis in budding yeast the split septin rings sandwich the AMR

and other cortical factors at the division site. After cytokinesis and cell separation, the old septin ring at the division site is disassembled and a new septin ring is formed adjacently (Younghoon Oh and Erfei Bi 2011).
The viability of *vhs2Δ* cells, notwithstanding the defect in septin ring stability, could be explained by the fact that septin diffusion barrier is dispensable for cytokinesis in budding yeast in our genetic background (Wloka et al., 2011). Therefore it would be interesting to analyze if the deletion of Vhs2 in another genetic background could cause evident defect in cytokinesis progression.
One of our intentions for the future is to analyze septin ring disassembly through time lapse analysis in *vhs2Δ* cells for better characterize *in vivo* the timing of this process respect to wild-type cells. How Vhs2 regulates septin ring organization is unknown at the moment.
We analyzed the phosphorylation of Shs1 in *vhs2Δ* cells because this modification causes a destabilization of septin ring structure, in particular it induces the split of the septin collar (Bi and Park, 2012). However, we found that the lack of Vhs2 do not affects Shs1 phosphorylation. These data is in agreement whit our hypotesis suggesting that Vhs2 could inhibits a downstream passage respect to collar split, that is the septin ring disassembly.
Multiple mutations in septin SUMOylation sites prevents the disappearence of septin ring from old bud sites, leading to the proposal that SUMOylation of septins promotes disassembly of the septin ring, either directly or indirectly, by preventing/inducing other post-translational modifications, such as ubiquitination (Johnson and Blobel, 1999). Based on the genetic data collected and on failure of *vhs2Δ* cells to mantain septin ring at the division site between mitotic exit and cytokinesis, in the future it will be newsworthy to investigate whether septins have a variation in SUMOylation profile in the absence of Vhs2 respect to the wild type. Will also be interestingly to analyze whether the lack of Vhs2 can somehow allow septin ring disappearence in SUMOylation mutants.
We then focused our attention on Vhs2 regulation. Vhs2 appears as a multi-phosphorylated protein. Its levels seem constant but its phosphorylation profile changes during the cell cycle. In particular, by western blot analysis, Vhs2 seems to be hypo-phosphorylated during G1

and its phosphorylation accumulates starting from S phase and reaching maximum levels before the beginning of cell cycle division.
Based on these data we searched for kinases and phosphatases that function during mitotic exit or cytokinesis.
Since from high-throughput screening Dbf2 seems to phosphorylate Vhs2 and since Cdc14 is the main phosphatase that acts during mitotic exit and cytokinesis, we tested whether these two enzymes could act as regulators of Vhs2. Interestingly, we observed that Vhs2 is hyper-phosphorylated when Dbf2 is inactivated so, Vhs2 is likely phosphorylated by protein kinase/s that act upstream of Dbf2 and Dbf2 kinase activity does not seem to be required fot its phosphorylation. Data from high-throughput screening indicate that Vhs2 can be phosphorylated by Cdc28 on serine 301 (Holt et al., 2009), it will be interesting to validate this data *in vivo* by the use of a catalitically inactive Cdc28 and by site directed mutagenesis of serine 301.
In addition we observed that Vhs2 is hyper-phosphorylated when Cdc14 is inactivated and that Vhs2 phosphorylated forms are reduced in the presence of high level of Cdc14 but are constant if Cdc14 phosphatase activity is impaired. So, Vhs2 phosphorylation seems to be regulated by Cdc14 directly during mitotic exit/cytokinesis (Fig. 34).
At the moment we don't know the biological function of Vhs2 phosphorylation, nor the residues subjected to this modification.
In the end we can conclude that Vhs2 has a role in septin ring stabilization by acting directly or indirectly on factor(s) that regulate this structure and we can say that Vhs2 phosphorylation levels are regulated at least in part, by the action of Cdc14. Other experiments will be required in order to clarify the role and the regulation of this new player in septins dynamics.

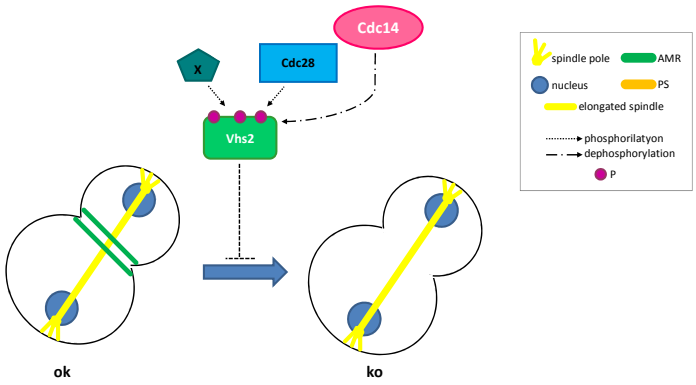

Figure 34. A model for the role of Vhs2 in septin ring stabilization.
Vhs2 partecipate in the controls of septin ring stability and its phosphorylation profile is regulated by Cdc14. See text for details.

Material and methods

ABBREVIATIONS

aa: Aminoacid
BFB: Bromophenol Blue
bp: Base Pairs
BSA: Bovine Serume Albumine
DAPI: 4,6-Diamidino-2-phenylindole
DMSO: Dimetilsolfossido
DTT: Dithiothreitol
EDTA: Ethylene Diamine Tetraacetic Acid
EGTA: Ethylene Glycol Tetraacetic Acid
GTP: Guanosine-5'-triphosphate
HEPES: 2-[4-(2-hydroxyethyl)piperazin-1-yl]ethanesulfonic acid
kDa: Kilodalton
Kphos: Phosphate buffer
NOC: Nocodazole
OD: Optical Density
O/N: Over Night
PEG: Polyethylene glycol
rpm: Rounds Per Minute
SDS: Sodium Dodecil Sulphate
TCA: Trichloroacetic acid
TRIS: Tris(hydroxymethyl)-aminomethane
X-gal: 5-bromo-4-chloro-3-indolyl-β-D-galactopyranoside
YNB: Yeast Nitrogen Base

BACTERIAL AND YEAST STRAINS

Bacterial strains

E. coli DH5α™ (F^-, Φ 80dlacZΔM15, ΔlacZTA-argF, U169, deoR, recA1, endA1, hsdR17, (rK^-, mK^+), supE44, thi-1, gyrA96, relA1 λ-) strain is used as bacterial hosts for plasmid manipulation and amplification. DH5α cells competent to transformation are purchased from Invitrogen.

E. coli BL21 strain (BF^-, ompT, hsdS, (rB^-, mB^+), gal, dmc) was used for bacterial expression and purification of yeast proteins used for *in vitro* assay.

Yeast strains

Strain genotypes used for this work are listed in table 3.

Table 3. yeast strain used in this work.

Name	***Relevant genotype***
yRF41	*MATa, dma2::LEU2, dma1::TRP1*
yRF63	*MATa, ade2, ade3, ura3, leu2, ase1::URA3*
yRF99	*MATa, ura3::URA3::GAL1-DMA2 (single integration)*
yRF214	*MATa, TEM1::HA3::KlURA3*
yRF490	*MATa, hof1::KanMX*
yRF663	*MATa, hof1::KanMX, ura3::URA3::GAL1-DMA2 (single integration)*
yRF700	*MATa, [YEp13]*
yRF701	*MATa, hof1::KanMX, ura3::URA3::GAL1-DMA2 (single integration), [YEp13]*
yRF729	*MATa, ade2-1, trp1-1, can1-100, leu2-3,112, his3-11,15, ura3, GAL, psi+, hof1::KanMX, dma2::LEU2, dma1::TRP1*
yRF850	*MATa, iqg1::IQG1-GFP::LEU2*
yRF851	*MATa, CYK3-GFP::URA3*
yRF903	*MATa, CYK3-3HA::SpHIS5*
yRF938	*MATa, dma2::LEU2, dma1::TRP1, CYK3-3HA::SpHIS5*
yRF942	*MATa, hof1::KanMX, ura3::URA3::GAL1-DMA2 (single integration), [YEp-CHS2]*
yRF966	*MATa, hof1::KanMX, ura3::URA3::GAL1-DMA2 (single integration), [YEp-BNI5]*
yRF979	*MATa, hof1::KanMX, ura3::URA3::GAL1-DMA2 (single integration), [YEp-CYK3]*
yRF997	*MATa, hof1::KanMX, ura3::URA3::GAL1-DMA2 (single integration), [YEplac181]*
yRF999	*MATa, hof1::KanMX, ura3::URA3::GAL1-DMA2 (single integration), [YEplac112]*

yRF1000	*MATa, [YEplac112]*
yRF1002	*MATa, [YEplac181]*
yRF1052	*MATa, ndc10-1, trp1, ura3, omns*
yRF1083	*MATa, ura3::URA3::GAL1-DMA2 (single integration), iqg1::IQG1-GFP:LEU2*
yRF1085	*MATa, ura3::URA3::GAL1-DMA2 (single integration), CYK3-3HA::SpHIS5*
yRF1103	*MATa, ura3::URA3::GAL1-DMA2 (single integration), CYK3-GFP::URA3*
yRF1138	*MATa, [YEp96 CUP1-6HIS-UBI4]*
yRF1163	*MATa, ade2-1, trp1-1, can1-100, leu2-3,112, his3-11,15, ura3, GAL, psi+ , dma2::LEU2, dma1::TRP1, ndc10-1.*
yRF1246	*MATa, dma2::HPHMx, dma1::LEU2kl, CYK3-8x GFP::URA3*
yRF1156	*MATa, iqg1-1, ura3::URA3::GAL-DMA2 (single integration)*
yRF1157	*MATa, hof1::KanMX, ura3::URA3::GAL1-DMA2 (single integration), bub2::HIS3*
yRF1234	*MATa, hof1::KanMX, ura3::URA3::GAL1-DMA2 (single integration), [pRS315 Dbf2-1c]*
yRF1268	*MATa, INN1-GFP-klTRP1*
yRF1271	*MATa, MYO1-CHERRY-hphNT1*
yRF1285	*MATa, ura3::URA3::GAL1-DMA2 (single integration), MYO1-CHERRY-hphNT1*
yRF1286	*MATa, ura3::URA3::GAL1-DMA2 (single integration), INN1-GFP-klTRP1*
yRF1308	*MATa, TEM1::HA3::KlURA3, [YEp96 CUP1 6HIS-UBI4]*
yRF1310	*MATa, hof1::KAN, ura3::URA3::GAL1-DMA2 (single integration), INN1-GFP-klTRP1*
yRF1333	*Mata, ade2-1, ura3-52, trp1del63, his3del200, leu2del1, ura3::URA3::GAL-DMA2 (single integration), MYO1-CHERRY-hphNT1, tem1::URA3, tem1K33R-HA3 (CEN HIS)*
yRF1351	*Mata, ade2-1, ura3-52, trp1del63, his3del200, leu2del1, ura3::URA3::GAL-DMA2 (single integration), MYO1-CHERRY-hphNT1, tem1::URA3, tem1K112R, K213R -HA3 (CEN HIS)*
yRF1355	*MATa, [YEp96 CUP1-UBI4*
yRF1359	*MATa, TEM1::HA3::KlURA3, [YEp96 CUP1-UBI4]*
yRF1364	*Mata, ade2-1, ura3-52, trp1del63, his3del200, leu2del1, ura3::URA3::GAL-DMA2 (single integration), MYO1-CHERRY-hphNT1, tem1::URA3, tem1K39R,K112-HA3 (CEN HIS)*
yRF1381	*Mat a, ade2-1, ura3-52, trp1del63, his3del200, leu2del1, ura3::URA3::GAL-DMA2 (single integration), MYO1-CHERRY-hphNT1, tem1::URA3, tem1K59R,K170R -HA3 (CEN HIS)*
yRF1383	*Mat a, ade2-1, ura3-52, trp1del63, his3del200, leu2del1, ura3::URA3::GAL-DMA2 (single integration), MYO1-CHERRY-hphNT1, tem1::URA3, tem1K154R,K208R-HA3 (CEN HIS)*
yRF1390	*Mat a, ade2-1, ura3-52, trp1del63, his3del200, leu2del1, ura3::URA3::GAL-DMA2 (single integration), MYO1-CHERRY-hphNT1, tem1::URA3, tem1K184R,K227R-HA3 (CEN HIS)*

yRF1400	*MATa, ura3::URA3::GAL1-DMA2 (single integration), TEM1::HA3::KlURA3*
yRF1412	*MATa, IQG1-3HA::klTRP1, cdh1::LEU2*
yRF1414	*MATa, ura3::URA3::GAL1-DMA2 (single integration), TEM1::HA3::KlURA3,[YEp96 CUP1-6HIS-UBI4]*
yRF1415	*MATa, ura3::URA3::GAL1-DMA2 (single integration), TEM1::HA3::KlURA3, [YEp96 CUP1-UBI4]*
yRF1420	*Mat a, ade2-1, ura3-52, trp1del63, his3del200, leu2del1, ura3::URA3::GAL-DMA2 (single integration), MYO1-CHERRY-hphNT1, tem1::URA3, tem1K133R,K219R-HA3 (CEN HIS)*
yRF1430	*Mat a, ade2-1, ura3-52, trp1del63, his3del200, leu2del1, ura3::URA3::GAL-DMA2 (single integration), MYO1-CHERRY-hphNT1, tem1::URA3, tem1K184R,K206R-HA3 (CEN HIS).*
yRF1436	*Mat a, ade2-1, ura3-52, trp1del63, his3del200, leu2del1, ura3::URA3::GAL-DMA2 (single integration), MYO1-CHERRY-hphNT1, tem1::URA3, tem1K47 -HA3 (CEN HIS)*
yRF1437	*Mata, ade2-1, ura3-52, trp1del63, his3del200, leu2del1, ura3::URA3::GAL-DMA2 (single integration), MYO1-CHERRY-hphNT1, tem1::URA3, tem1K61R-HA3 (CEN HIS)*
yRF1444	*Mata, ade2-1, ura3-52, trp1del63, his3del200, leu2del1, ura3::URA3::GAL-DMA2 (single integration), MYO1-CHERRY-hphNT1, tem1::URA3, tem1K112R-HA3 (CEN HIS).*
yRF1471	*Mata, ade2-1, ura3-52, trp1del63, his3del200, leu2del1, ura3::URA3::GAL-DMA2 (single integration), MYO1-CHERRY-hphNT1, tem1::URA3, tem1K133R-HA3 (CEN HIS).*
yRF1457	*MATa, his3, ura3, trp1, 6lexAOP-LEU2, [pSH18-34], [pEG202-p53], [pJG4-5-SV40]*
yRF1465	*MATa, TEM1::HA3::KlURA3, MYO1-CHERRY-hphNT1, [YEp96 CUP1-6HIS-UBI4]*
yRF1480	*Mata, ade2-1, ura3-52, trp1del63, his3del200, leu2del1, ura3::URA3::GAL-DMA2 (single integration), MYO1-CHERRY-hphNT1, tem1::URA3, tem1K39R-HA3 (CEN HIS).*
yRF1484	*Mata, ade2-1, ura3-52, trp1del63, his3del200, leu2del1, ura3::URA3::GAL-DMA2 (single integration), MYO1-CHERRY-hphNT1, tem1::URA3, tem1K170R-HA3 (CEN HIS)*
yRF1496	*Mata, ade2-1, ura3-52, trp1del63, his3del200, leu2del1, ura3::URA3::GAL-DMA2 (single integration), MYO1-CHERRY-hphNT1, tem1::URA3, tem1K59R -HA3*
1447	*Mata, ade2-1, ura3-52, trp1del63, his3del200, leu2del1, ura3::URA3::GAL-DMA2 (single integration), MYO1-CHERRY-hphNT1, tem1K219R-HA3 (CEN HIS)*
yRF1541	*MATa, ura3::URA3::GAL1-DMA2 (single integration), MYO1-CHERRY-hphNT1, cdc12-1*
yRF1563	*MATa, his3::TUB1-GFP::HIS3, MYO1-CHERRY-hphNT1*

yRF1564	*MATa, ura3::URA3::GAL1-DMA2 (single integration), MYO1-CHERRY-hphNT1, his3::TUB1-GFP::HIS3*
yRF1575	*MATa, boi1::LEU2, boi2:: URA3*
yRF1584	*MATa , dma1::TRP1, dma2::HPHMx, MYO1-CHERRY-hphNT1*
yRF1585	*MATa, dma1::TRP1, dma2::HPHMx, MYO1-CHERRY-hphNT1, his3::TUB1-GFP::HIS3*
yRF1588	*MATa, cyk3::natNT2*
yRF1589	*MATa, dma2::LEU2, dma1::TRP1, cyk3::natNT2*
yRF1595	*MATa, ade2-1, trp1-1, can1-100, leu2-3,112, his3-11,15, ura3, GAL, psi+ , dma2::LEU2, dma1::TRP1, chs2::natNT2*
yRF1601	*MATa, ade2-1, trp1-1, can1-100, leu2-3,112, his3-11,15, ura3, GAL, psi+, mre11::HIS3.*
yRF1603	*MATa, boi1::LEU2, boi2:: URA3, dma1::TRP1, dma2::HPHMx*
yRF1625	*MATa, ade2-1, trp1-1, can1-100, leu2-3,112, his3-11,15, ura3, GAL, psi+, mre11::HIS, boi1::LEU2, boi2:: URA3*
yRF1650	*MATa, his3, ura3, trp1, 6lexAOP-LEU2, [pSH18-34], [pEG202-TEM1], [pJG4-5-IQG1]*
yRF1654	*Mata, ade2-1, trp1-1, can1-100, leu2-3,112, his3-11,15, ura3, dma1::TRP1, dma2::HPHMx, mre11::HIS3*
yRF1651	*MATa, his3, ura3, trp1, 6lexAOP-LEU2, [pSH18-34], [pEG202], [pJG4-5-IQG1]*
yRF1652	*MATa, his3, ura3, trp1, 6lexAOP-LEU2, [pSH18-34], [pEG202-TEM1], [pJG4-5]*
yRF1663	*MATa, hof1::KanMX, [p425GAL1- DMA1-2HA]*
yRF1667	*MATa, his3, ura3, trp1, 6lexAOP-LEU2, [pSH18-34], [pEG202-TEM1], [pJG4-5-IQG1], [p425GAL1- DMA2-2HA]*
yRF1677	*MATa, dma2::HPHMx, dma1::LEU2kl, iqg1-1*
yRF1749	*MATa, cyk3:: natNT2, ura3::URA3::GAL1-DMA2 (single integration)*
yRF1750	*MATa, chs2:: natNT2, ura3::URA3::GAL1-DMA2 (single integration)*
yRF1795	*MATa, ura3::URA3::GAL1-DMA2 (single integration), MYO1-CHERRY-hphNT1, [pRS315 CHS2-GFP]*
yRF1796	*MATa, MYO1-CHERRY-hphNT1, [pRS315 CHS2-GFP]*

All yeast strains (Table 3) were derivatives of W303 (*ade2⁻1,trp1-1, leu2-3,112, his3-11,15, ura3, ssd1*) or were backcrossed at least three times to W303, except yRF1457, yRF1650, yRF1651, yRF1652, yRF1667 that were derivatives of EGY48 (*Mata his3 ura3 trp1 6lexAOP-LEU2*; *lexAOP-lacZ* reporter on plasmid pSH18–34). All the *GAL1-DMA2* strains carry a single copy of the *GAL1-DMA2* construct (Fraschini et al., 2006) integrated at the *URA3* locus.

GROWTH MEDIA

All media were sterilized with autoclave and stored at room temperature.

Media for E. coli

LD	1%	bactotryptone
	0.5%	yeast extract
	0.5%	NaCl (pH7.25)

LD + AMP LD + ampicillin (2.5g/L)

Agar to 1% was added in order to obtain solid medium.

Media for S. cerevisiae

YEP	1%	yeast extract
	2%	bactopeptone
	50mg/L	adenine (pH5.4)

Just before use YEP was supplemented with the appropriate carbon source: 2% glucose (YEPD), 2% raffinose (YEPR), 2% raffinose and 1% galattose (YEPRG). Agar to 2% was added in order to obtain solid medium.

Synthetic medium (S) 0.7% yeast nitrogen base without aa (pH5)

Before using, S medium was supplemented with the appropriate carbon source, 2% glucose or 2% raffinose or 2% raffinose and 1% galattose, and 25g/ml of all aminoacids and nitrogen bases (synthetic complete medium), unless differently indicated. Agar to 2% was added in order to obtain solid medium.

Sporification medium (VB)	1.36% $CH_3COONa\ 3H_2O$
	0.19% KCl
	0.0035% $MgSO_4 7H_2O$
	0.12% NaCl
	pH7

Agar to 2% was added in order to obtain solid medium.

BUFFERS AND SOLUTIONS

Transfer buffer: 1% Glycine
20mM TRIS-HCl
20% methanol

SDS-PAGE running buffer 5X: 2M glycin
0.25M TRIS
0.02M SDS
pH8.3

TBS 10X: 1.5M NaCl
0.5M TRIS-HCl
pH8

Laemmli buffer: 0.62M TRIS
2% SDS
10% glycine
0.001% BFB
100Mm DTT

ECL solution: 100mM Tris pH8.5
3mM H_2O_2
0.2mM P-coumaric acid
1,25mM Luminol

BSA/PBS: BSA 1%, K_2HPO_4 0.4M, KH_2PO_4 0.01M, NaCl 0.15M

MOLECULAR BIOLOGY TECHNIQUES

Genetic manipulation

Standard techniques were used for genetic manipulations (Maniatis et al., 1992; Sherman 1991). Gene deletions were generated by one-step gene replacement (Wach et al., 1994). *mre11Δ* was a kind gift of M. P. Longhese, *boi1Δ boi2Δ* and *rts1Δ* were a kind gift of Y. Barral, ase1Δ was a kind gift of D. Pellman. *ndc10-1* (Goh and Kilmartin, 1993), ipl1-321, cdc12-6 mutants were a kind gift of Y. Barral. cdc3-1, *cdc10-1*, *shs1-100* mutants were a kind gift of M. Iwase. *cdc12-1* was a kind gift of K. Nashmyth. *cdc14-1* mutant was a kind gift of S. Yoshida. *dbf2-2* was a kind gift of S. Irniger. *GAL-CDC14* and *GAL-CDC14C283A* were a kind gift of E. Schiebel. One-step tagging techniques were used to create 3HA-tagged or 6HA-tagged proteins variant (Janke et al., 2004). Iqg1-3HA-expressing strain was a kind gift from C. Price (Lancaster University). Cyk3-3HA expressing strain was a kind gift from A .Jendretzki (University of Osnabrück). GFP-Iqg1 and GFP-Cyk3 expressing strains were a kind gift of M. Iwase (University of Pennsylvania School of Medicine). GFP-Inn1 and Myo1-Cherry expressing strains were a kind gift of G. Pereira (German Cancer Research Center). The pRS315 *CHS2-GFP* and the RF28 TEM1-GST in pGEX-2KT (AMRAD)(inducible by IPTG and used for expression in *E. coli*) plasmids were a kind gift of R. Li. All gene replacements and tagging were controlled by PCR-based methods or Southern blot analysis.

Generation of diploid strains and sporulation

Diploid strains were generated by crossing the appropriate haploid strains on YEPD plates. After 24 hours, diploids were transferred to VB plates to induce sporulation, and incubated for two days at 25°C. Asci were digested with 0.025mg/ml zymolyase. Tetrads were dissected with a micromanipulator on the appropriate plates.

Synchronization with α-factor

MATa strains were inoculated in appropriate medium to reach a concentration of 5 x 10^6 cells/ml. α-factor was added to a final concentration of 2µg/ml. When more than 95% of cells arrested in G1 as unbudded (about 2 hours after α-factor adding), the pheromone was removed and cells were washed once with opportune fresh medium and

resuspended and incubated in the opportune fresh medium. Unless differently stated, synchronization were performed at 25°C and galactose, when requested, was added 30 minutes before α-factor release.

Synchronization with nocodazole

Strains were inoculated in appropriate medium to reach a concentration of 8.3 x 10^6 cells/ml. Nocodazole (Sigma) was added to a final concentration of 5µg/ml in DMSO 1% containing medium. When more than 95% of cells arrested in G2-M as largebudded (about 3 hours after nocodazole adding), the pheromone was removed and cells were washed once with opportune fresh medium containing 1% DMSO and resuspended and incubated in the opportune fresh medium. Unless differently stated, synchronization were performed at 25°C.

Drop test

Cell coltures were grown overnight at the appropriate temperature until they reached stationary phase. They were diluited to 1.25 x 10^6, 1.25 x 10^5, 1.25 x 10^4, 1.25 x 10^3 cells/ml. For each diluition, 5ml cell suspension were spotted on opportune plates and incubated at the appropriate temperatures.

FACS analysis

1.25 x 10^6 cells were collected each time point by centrifugation and resuspended in 1ml of 70% ethanol, prior to 1 hour of incubation at room temperature. Cells were than washed once with 50mM TRIS pH7.5 and 50µl of 10mg/ml RNAse was added to each sample. After incubation overnight at 37°C, cells were collected by centrifugation, pellets were resuspended in 0.5ml of 5ml/ml pepsin (freshly dissolved in 55mM HCl) and incubated at 37°C for 30 minutes. Cells were than washed once with FACS buffer (200mM TRIS pH7.5, 211mM NaCl, 78mM $MgCl_2$) and resusped in 0.5ml of FACS buffer containing 55µl of 0.5mg/ml propidium iodide. Samples were finally analyzed with Becton-Dickinson FACScan.

Two-hybrid assay

The yeast two-hybrid assay was performed using the B42/ lexA system with strain EGY48 (*Mata his3 ura3 trp1 6lexAOPLEU2*; *lexAOP-lacZ* reporter on plasmid pSH18-34) as the host strain (Gyuris et al., 1993). Bait plasmid

pEG202-Tem1 (RF35) for the two-hybrid assay, expressing a lexADB-Tem1 fusion, was obtained by amplifying the corresponding coding sequence of *TEM1* gene from genomic DNA and ligating the resulting fragment into BamHI-digested pEG202. Prey plasmid pJG4-5-Iqg1 (RF44), expressing a B42AD-Iqg1 fusion, was obtained by amplifying the corresponding coding sequence of *IQG1* from genomic DNA and ligating the resulting fragments into EcoRI-digested pJG4-5. The assay was performed on appropriate synthetic medium plates at pH 6.7 containing 5µg/ml X-gal.

Fluorescence microscopy and live imaging

For *in situ* immunofluorescence cells were fixed in 1ml of IF buffer(0.1M Kphos pH6.4, 0.5mM $MgCl_2$) containing 3.7% formaldehyde at 4°C ON. Samples were than washed three times with IF buffer and once with IF buffer containing 1.2M sorbitol. Cells were spheroplasted by incubating 10-30 minutes in 0.2ml of spheroplasting solution (0.1M Kphos pH6.4, 0.5mM $MgCl_2$, 1.2M sorbitol) containing 5µl of 10mg/ml 100T zymolyase and 0.2% β-mercatoethanol (only for ON fixed cells). Spheroplasts state were checked microscopically by mixing digested cells with an equal amount of 10% SDS. When cells are fully spheroplastized they were washed one time in IF buffer containing 1.2M sorbitol and resuspended in 0.2ml of the same solution. A 30 well slide was coated with 0.1% polylysine; a drop of cells resonably cloudy was added to each well and, after 5-10 minutes of incubation at RT, was removed. The slide was then removed from acetone bath and let dry. Primary antibody was added to each well and the slide was incubated at 4°C in the dark from 2 hours to ON. Then, the primary antibody was aspirated off and each well was washed three times with BSA/PBS, followed by the addition of the appropriate secondary antibody. Slides were incubaed at 4°C in the dark for 2 hours. Then, the secondary antibody was aspirated off and each well was washed three times with BSA/PBS. For nuclei staining, DAPI was diluited in ANTIFADE (0.1% phenylenediamine, 10% PBS pH8 in glycerol) to a final concentration of 0.05 µg/ml and added to each well. A coverslip was placed over and sealed using nail enamel. Slides were stored at -20°C in the dark until use.

Visualization of septin rings was performed using anti-Cdc11 polyclonal antibodies (1:200, sc-7170 Santa Cruz) followed by indirect immunofluorescence with Alexa Fluor 488-conjugated anti-rabbit antibody (1:100, Invitrogen). To detect spindle formation and elongation, anti-

tubulin immunostaining was performed with the YOL34 monoclonal antibody (1:100, Serotec) followed by indirect immunofluorescence using rhodamine-conjugated anti-rat Ab (1:500, Pierce Chemical Co). To detect actin ring, actin immunostaining was performed using anti-actin polyclonal antibodies (1:1000, A2066, Sigma-Aldrich) followed by indirect immunofluorescence using rhodamine-conjugated anti-rabbit Ab (1:50, Invitrogen).

To visualize Iqg1-GFP, Cyk3-GFP and sister chromatids separation, cells were fixed in cold ethanol and washed with Tris 50mM pH8. To visualize Inn1-GFP and Myo1-Cherry, cells were fixed in 4% formaldeyde and washed with PBS. For actin staining, cell were fixed adding 4% formaldehyde in the colture medium for 2 hours, cells were then washed with PBS and treated with PBS containing 20 unit rhodamine phalloidine (purchased by Sigma-Aldrich) for 2 hours. For chitin staining, cells were fixed in cold ethanol, washed with PBS, and treated with PBS containing 0.01mg/ml Calcofluor White (purchased by Sigma-Aldrich). Digital images were taken with a Leica DC350F chargecoupled device camera mounted on a Nikon Eclipse 600 and controlled by the Leica FW4000 software or with the MetaMorph imaging system software on a fluorescent microscope (Eclipse 90i; Nikon), equipped with a charge-coupled device camera (Coolsnap, Photometrics) with an oil 100X 0.5-1.3 PlanFluor oil objective (Nikon). For three-dimensional reconstruction of chitin staining, 30 Z-stacks at 0.2µm intervals were taken and projected onto a single image using MetaMorph imaging system software (Molecular Devices). For time-lapse movies cells were grown in synthetic complete medium + 2% glucose (or 2% raffinose for *GAL1-DMA2* experiment), then collected and imaged on agar in synthetic complete medium + 2% glucose (or 2% galactose for *GAL1-DMA2* experiment) using a Delta Vision Elite imaging system (Applied Precision) based on an IX71 inverted microscope (Olympus) with a camera CoolSNAP HQ2 from Photometrics, and a UPlanApo 60× (1.4 NA) oil immersion objective (Olympus). Every 3 minutes (unless otherwise stated) 3 Z-stacks at 1.2 micron intervals were taken for each fluorescent channel and projected onto a single image per channel using Fiji software (Schindelin et al., 2012).

Electron microscopy (TEM)

Samples were fixed by addition of glutaraldehyde (Sigma) directly to the culture medium to a final concentration of 2.5% for 10 minutes, centrifuged and incubated overnight at 4°C. After washes (3 × 10 minutes) in distilled water, pellet of cells were incubated in 4% $KMnO_4$ for 30 minutes, then washed in distilled water and transferred in a saturated solution of uranyl acetate for 30 minutes. After some washes in distilled water, samples were dehydrated in ethanol series, and, finally, in propylene oxide 100% for 20 minutes. Infiltration was subsequently performed with propylene–resin (Araldite-Epon, Sigma) mixture in volume proportions of 2:1 for 1 hour, 1:1 overnight. The pellets were left for 1 hour in volume proportions of 2:1 for 1 hour. Then the pellets were left for 4 hours in 100% pure resin and then shifted to 60°C for polymerization. Ultrathin sections of 80nm were made on an Ultracut E microtome (Reichert), post-stained in uranyl acetate and lead citrate and examined in a Leo912ab transmission electron microscope (Zeiss) at 80 KV. Digital images were acquired by Esivision CCD-BM/ 1K system.

Protein extracts and western blot analysis

For all the experiment performed in order to analyze protein levels or modifications (except for the analysis of Vhs2 levels during the cell cycle) total protein extracts were prepared by TCA precipitation. Briefly, cells were resuspended in 1ml of 20% TCA. After the addition of an equal amount of acid-treated glass-beads, cells were mechanically distrupted by vortexing 10 minutes on vortex at maximum power. Glass beads were washed once with 400µl of 5% TCA and the resulting extract was centrifuged for 10 minutes at 3000rpm. The pellet was resuspended in 100µl of Laemmli buffer 2X, neutralized by adding 50µl TRIS base, boiled for 3 minutes, and finally clarified by centrifugation for 5 minutes at 13000 rpm before loading on appropriate polyacrylamide gel. For monitoring Vhs2 levels during the cell cycle, total protein extracts were prepared by native extracts protocol. Briefly, cells were washed once whith 1ml Tris 10mM pH7.5 cold and then resuspended in two volumes of breaking buffer (Tris 50mM pH7.5 containing 120mM β-glycerophosphate and 2mM Na ortovanadate, supplemented with protease inhibitors (Complete Mini, purchased from Roche)) in ice.

Equal amounts of acid-treated glass-beads were then added to each suspension, and cells were broken mechanically by vortexing 5 minutes at 4°C on vortex at maximum power. Samples were then transferred into a new tubes and clarified by centrifugation. 1µl of each protein extract was diluited in 1ml of Biorad Protein Assay (Biorad) for spectrophotometric protein quantification at 935nm UV wavelength. Clarified extracts were resuspended in 50µl Laemmli buffer 3X, boiled for 3 minutes, and loaded on 10% polyacrylamide gel.
Proteins were separated based on their molecular weight on 10% or 12.5% polyacrylamide gel in SDS-PAGE. For western blot analysis, proteins were transferred to Protran membranes (Schleicher and Schuell) by 200mA ON. In order to preliminary quantify the total amount of transferred proteins, the filters were stained with Ponceau S (Sigma). After destaining with TBS 1X, filters were incubated for 1 hour at RT in non-fat 4% or 5% dust milk in TBS 1X and 0.2% Triton X-100. Filters were then probed with primary antibodies directly diluited in 4% or 5% milk. As primary antibodies were used monoclonal anti-HA (1:3000), anti-Pgk1 (1:40000) and anti-Cdc11 antibodies (1:2000) or with polyclonal anti-GST antibodies (1:2000) or anti-Clb2 antibodies (1:2000) for 2 hours. Filters were then washed three times in TBS 1X for 10 minutes, before incubating them for an hour at RT with properly diluited secondary antibodies (1:10000).
As secondary antibodies were used anti-mouse IgG, anti-rabbit IgG or anti-goat IgG purchased from Amersham, these antibodies are conjugated with the peroxydase enzyme. Filters were then washed three times in TBS 1X for 10 minutes, dried on 3MM paper and carefully dipped in ECL solution. After a new drying, the filters were exposed for different times to a film. Peroxydase, together with its reagents, catalyses a reaction wich emits light able to impress upon the film. The signal is detectable on the film after treatment with developing and fixing solutions.

Phosphatase assay

For the phosphatase treatment protein extract were made in the following breaking buffer: 50mM HEPES, 150mM NaCl, 20% glycerol, 5mM EDTA, 120mM β-glycerophosphate and 2mM Na ortovanadate, supplemented with protease inhibitors (Complete Mini, purchased from Roche). Vhs2-6HA was immunoprecipitated from 1µg of cleared extracts upon incubation with anti-HA antibodies for 1 hour at 4°C followed by incubation with

protein A-sepharose for 1 hour at 4°C. The slurry was washed three times in PBS, resuspended in 60 µl of phosphatase buffer containing 20units of lambda phosphatase (Biolabs) and 2mM $MnCl_2$ and incubated 7 minutes at 30°C before loading.

Expression and purification of recombinant proteins and in vitro binding

Experiment Tem1-Iqg1 binding assay was performed as described (Shannon et al., 1999). Briefly, Glutathione S-transferase (GST)-Tem1 fusion protein was produced in *Escherichia coli* carrying pKT5 plasmid (kind gift of Rong Li), grown in LD broth containing ampicillin at 37°C for 3 hours, transferred to 14°C for 1 hour and induced with 0.1 mM IPTG for 15 hours. Bacteria extract was prepared in lysis buffer (50mM TRIS-HCl pH8, 200mM NaCl, 2mM $MgCl_2$, 2mM DTT, 1mM GTP) supplemented with a cocktail of protease inhibitors. Cells were incubated with 1 mg/ml lisozyme in ice for 30 minutes, placed at 37 °C for 5 minutes and sonicated at 4°C. To prepare GST-Tem1 beads, the bacterial extracts containing GST-Tem1 were incubated with 40µl glutathione agarose beads (GE Healthcare) for 1 hour at 4°C. As negative control we used 40µl glutathione agarose beads incubated with an equal amount of lysis buffer. The beads were then washed 3 times in washing buffer (PBS containing 1mM DTT, 1mM GTP, and $MgCl_2$ 2mM). Yeast extracts were prepared by using acid glass beads in UB buffer (0.05M HEPES pH7.5, 0.1M KCl, 3mM $MgCl_2$, 1mM EGTA, 1mM DTT) supplemented with a cocktail of protease inhibitors. For Tem1-Iqg1 binding assay, Tem1 beads were incubated for 1 hour at 4°C with either total extract of wild-type cells or total extract of *GAL1-DMA2* cells induced for 2 hours with 1% galactose. The beads were washed 3 times in washing buffer and were then incubated with total extract of *IQG1-3HA* cells for 1 hour at 4°C. The beads were washed 3 times in washing buffer, resuspended after drying in Laemmli buffer with β-mercaptoethanol and boiled for 3 minutes at 100°C.

Detection of ubiquitin conjugates in vivo

For the experiments involving the expression of 6xHis-ubiquitin, cells were grown to log phase at 25°C in selective medium (synthetic medium lacking tryptophan) and untagged ubiquitin or 6xHis-ubiquitin production was induced by addition of 250µM $CuSO_4$ to each culture. After 3 further hours, yeast cells were washed in water, and protein extracts were prepared

under denaturing conditions. Cells were resuspended in 5ml of cold water and treated with 800µl of NaOH/BME solution (1.85M NaOH, 7.5% (v/v) 2-mercaptoethanol) for 20 minutes in ice. Then was addedd 800µl of 55% TCA for 20 minutes in ice. Cells were then collected by centrifugation at 8000rpm for 20 minutes (optimally at 4°C). The pellet of TCA precipitates was then resuspended at RT in 0.5ml buffer A (6M guanidine HCl, 100mM $NaPO_4$ pH8, 10mM TRIS-HCl pH8). Nickel pulldown was performed ON at RT using 40µl Ni-NTA agarose beads (Qiagen) for each samples. In the pulldown mixture were added 15mM imidazole and 0.05% Tween20. Pulldown samples were washed twice with buffer A containing 0.05% Tween20 and four times with Buffer C (8M urea, 100mM $NaPO_4$ pH6.3, 10mM TRIS-HCl pH 6.3) containing 0.05% Tween20 take care to remove as much of the liquid as possible after the last wash. The resin was then resuspended in HU buffer (8M urea, 200mM TRIS-HCl pH 6.8, 1mM EDTA, 5% SDS, 0.1% BFB, 1.5% DTT (added fresh)) and denaturated at 65°C for 10 minutes before loading. For the experiments involving *GAL1* induction, 1% galactose was added to the cell cultures 30 min before $CuSO_4$ addition.

Statistical analyses and other techniques

Standard deviations (SD) and standard mean errors (SEM) were calculated using Microsoft Excel software. The significance of the differences between AMR contraction dynamics and Chs2 dynamics was statistically tested by the Wilcoxon signed-ranksum test using MATLAB software, samples are significantly different if P value is $P < 0.05$. Flow cytometric DNA quantification was performed according to Fraschini et al., 1999 on a Becton-Dickinson FACScan.

References

Addinall S.G., Downey M., Yu M., Zubko M.K., Dewar J., Leake A., Hallinan J., Shaw O., James K., Wilkinson D.J., Wipat A., Durocher D., Lydall D.A. (2008). **Genomewide Suppressor and Enhancer Analysis of cdc13-1 Reveals Varied Cellular Processes Influencing Telomere Capping in Saccharomyces cerevisiae.** Genetics 180 (4) 2251-66 (2008).

Bembenek J., Kang J., Kurischko C., Li B., Raab J.R., Belanger K.D., Luca F.C., Yu H. (2005). **Crm1-mediated nuclear export of Cdc14 is required for the completion of cytokinesis in budding yeast.** Cell Cycle 2005; 4:961-71.

Bi E., Maddox P., Lew D.J., Salmon E.D., McMillan J.N., Yeh E., Pringle J.R. (1998). **Involvement of an actomyosin contractile ring in Saccharomyces cerevisiae cytokinesis.** J Cell Biol. 1998 Sep 7;142(5):1301-12.

Bi E. (2001). **Cytokinesis in budding yeast: the relationship between actomyosin ring function and septum formation.** Cell Struct Funct. 2001; 26:529-37.

Bi, E. and Park H.O. (2012). **Cell polarization and cytokinesis in budding yeast**. Genetics. 191:347-387.

Bieganowski P., Shilinski K., Tsichlis P.N., Brenner C. (2004). **Cdc123 and checkpoint forkhead associated with RING proteins control the cell cycle by controlling eIF2gamma abundance.** J Biol Chem. 2004 Oct 22; 279(43):44656-66.

Blondel M., Bach S., Bamps S., Dobbelaere J., Wiget P., Longaretti C., Barral Y., Meijer L., Peter M.. (2005). **Degradation of Hof1 by SCF(Grr1) is important for actomyosin contraction during cytokinesis in yeast.** EMBO J 2005; 24:1440-52.

Bodenmiller B., Wanka S., Kraft C., Urban J., Campbell D., Pedrioli P.G., Gerrits B., Picotti P., Lam H., Vitek O., Brusniak M.Y., Roschitzki B., Zhang C., Shokat K.M., Schlapbach R., Colman-Lerner A., Nolan G.P., Nesvizhskii A.I., Peter M., Loewith R., von Mering C., Aebersold R. (2010). **Phosphoproteomic Analysis Reveals Interconnected System-Wide**

Responses to Perturbations of Kinases and Phosphatases in Yeast. Sci. Signal 2010; 3:1-8.

Bosl W.J., Li R. (2005). **Mitotic-exit control as an evolved complex system.** Cell. 2005 May 6;121(3):325-33.

Bouck D.C., Bloom K.S. (2005). **The kinetochore protein Ndc10p is required for spindle stability and cytokinesis in yeast.** Proc Natl Acad Sci U S A. 2005 Apr 12;102(15):5408-13.

Brooks L.3rd, Heimsath E.G.Jr, Loring G.L., Brenner C. (2008). **FHA-RING ubiquitin ligases in cell division cycle control.** Cell Mol Life Sci 2008; 65:3458-66.

Buvelot S., Tatsutani S.Y., Vermaak D., Biggins S. (2003). **The budding yeast Ipl1/Aurora protein kinase regulates mitotic spindle disassembly.** J Cell Biol. 2003 Feb 3;160(3):329-39.

Byrne K.P., Wolfe K.H. (2005). **The Yeast Gene Order Browser: combining curated homology and syntenic context reveals gene fate in polyploid species.** Genome Res. 2005 Oct;15(10):1456-61.

Callis J., Ling R. (2005). **Preparation, characterization, and use of tagged ubiquitins.** Methods Enzymol 2005; 399:51-64.

Caydasi A.K., Ibrahim B., Pereira G. (2010). **Monitoring spindle orientation: Spindle position checkpoint in charge.** Cell Div. 2010 Dec 11;5:28.

Cassani C., Raspelli E., Santo N., Chiroli E., Lucchini G., Fraschini R. (2013). **Saccharomyces cerevisiae Dma proteins participate in cytokinesis by controlling two different pathways.** Cell Cycle. 2013 Sep 1;12(17):2794-808.

Chan L.Y., Amon A. (2010). **Spindle position is coordinated with cell-cycle progression through establishment of mitotic exit-activating and -inhibitory zones.** Mol Cell. 2010 Aug 13;39(3):444-54.

Chahwan R., Gravel S., Matsusaka T., Jackson S.P. (2013). **Dma/RNF8 proteins are evolutionarily conserved E3 ubiquitin ligases that target septins.** Cell Cycle 2013; 12(6):1000-8.

Chin C.F., Bennett A.M., Ma W.K., Hall M.C., Yeong F.M. (2012). **Dependence of Chs2 ER export on dephosphorylation by cytoplasmic Cdc14 ensures that septum formation follows mitosis.** Mol Biol Cell. 2012; 23(1):45-58.

Colman-Lerner A., Chin T.E., Brent R. (2001). **Yeast Cbk1 and Mob2 activate daughter-specific genetic programs to induce asymmetric cell fates.** Cell. 2001 Dec 14;107(6):739-50.

Corbett M., Xiong Y., Boyne J.R., Wright D.J., Munro E., Price C. (2006). **IQGAP and mitotic exit network (MEN) proteins are required for cytokinesis and re-polarization of the actin cytoskeleton in the budding yeast, Saccharomyces cerevisiae.** Eur J Cell Biol 2006; 85:1201-15.

Costanzo M., Baryshnikova A., Bellay J., Kim Y., Spear E.D., Sevier C.S., Ding H., Koh J.L., Toufighi K., Mostafavi S., Prinz J., St Onge R.P., VanderSluis B., Makhnevych T., Vizeacoumar F.J., Alizadeh S., Bahr S., Brost R.L., Chen Y., Cokol M., Deshpande R., Li Z., Lin Z.Y., Liang W., Marback M., Paw J., San Luis BJ, Shuteriqi E., Tong A.H., van Dyk N., Wallace I.M., Whitney J.A., Weirauch M.T., Zhong G., Zhu H., Houry W.A., Brudno M., Ragibizadeh S., Papp B., Pál C., Roth F.P., Giaever G., Nislow C., Troyanskaya O.G., Bussey H., Bader G.D., Gingras A.C., Morris Q.D., Kim P.M., Kaiser C.A., Myers C.L., Andrews B.J., Boone C. (2010). **The genetic landscape of a cell.** Science. 2010 Jan 22;327(5964):425-31.

De Virgilio C., DeMarini D.J., Pringle J.R. (1996). **SPR28, a sixth member of the septin gene family in Saccharomyces cerevisiae that is expressed specifically in sporulating cells.** Microbiology. 1996 Oct;142 (Pt 10):2897-905.

Dobbelaere J., Gentry M.S., Hallberg R.L., Barral Y. (2003). **Phosphorylation-dependent regulation of septin dynamics during the cell cycle.** Dev Cell. 2003 Mar;4(3):345-57.

Epp J.A., Chant J. (1997). **An IQGAP-related protein controls actin-ring formation and cytokinesis in yeast.** Curr Biol. 1997 Dec 1;7(12):921-9.

Fang X., Luo J., Nishihama R., Wloka C., Dravis C., Travaglia M., Iwase M., Vallen E.A., Bi E. (2010). **Biphasic targeting and cleavage furrow ingression directed by the tail of a myosin II.** J Cell Biol. 2010 Dec 27;191(7):1333-50.

Fares H., Goetsch L., Pringle J.R. (1996). **Identification of a developmentally regulated septin and involvement of the septins in spore formation in Saccharomyces cerevisiae.** J Cell Biol. 1996 Feb;132(3):399-411.

Fededa J.P., Gerlich D.W. (2012). **Molecular control of animal cell cytokinesis.** Nat Cell Biol. 2012 May 2;14(5):440-7.

Finley D., Ulrich H.D., Sommer T., Kaiser P. (2012). **The ubiquitin-proteasome system of Saccharomyces cerevisiae.** Genetics. 2012 Oct;192(2):319-60.

Fraschini R, Formenti E, Lucchini G, Piatti S. (1999). **Budding yeast Bub2 is localized at spindle pole bodies and activates the mitotic checkpoint via a different pathway from Mad2.** J Cell Biol 1999; 145:979-91.

Fraschini R, Bilotta D, Lucchini G, Piatti S (2004). **Functional characterization of Dma1 and Dma2, the budding yeast homologues of Schizosaccharomyces pombe Dma1 and human Chfr.** Mol Biol Cell 2004; 15:3796-8106.

Fraschini R., D'Ambrosio C., Venturetti M., Lucchini G., Piatti S. (2006). **Disappearance of the budding yeast Bub2-Bfa1 complex from the mother-bound spindle pole contributes to mitotic exit.** J Cell Biol. 2006; 172:335-46.

Frenz L.M., Lee S.E., Fesquet D., Johnston L.H. (2000). **The budding yeast Dbf2 protein kinase localises to the centrosome and moves to the bud neck in late mitosis.** J Cell Sci. 2000; 19:3399-408.

Gandhi M., Goode B.L., Chan C.S. (2006). **Four novel suppressors of gic1 gic2 and their roles in cytokinesis and polarized cell growth in Saccharomyces cerevisiae.** Genetics. 2006 Oct;174(2):665-78.

Geymonat M., Spanos A., De Bettignies G., Sedgwick S.G. (2009). **Lte1 contributes to Bfa1 localization rather than stimulating nucleotide exchange by Tem1.** J Cell Biol 2009; 187:497-511.

Gruneberg U., Campbell K., Simpson C., Grindlay J., Schiebel E. (2000). **Nud1p links astral microtubule organization and the control of exit from mitosis.** EMBO J 2000; 19:6475-88.

Guertin D.A., Venkatram S., Gould K.L., McCollum D. (2002). **Dma1 prevents mitotic exit and cytokinesis by inhibiting the septation initiation network (SIN).** Dev Cell 2002; 3:779-90.

Gyuris J., Golemis E., Chertkov H., Brent R. (1993). **Cdi1, a human G1 and S phase protein phosphatase that associates with Cdk2.** Cell 1993; 75:791–803.

Holt L.J., Tuch B.B., Villén J., Johnson A.D., Gygi S.P., Morgan D.O. (2009). **Global analysis of Cdk1 substrate phosphorylation sites provides insights into evolution.** Science. 2009 Sep 25;325(5948):1682-6.

Huen M.S., Grant R., Manke I., Minn K., Yu X., Yaffe M.B., Chen J. (2007). **RNF8 transduces the DNA-damage signal via histone ubiquitylation and checkpoint protein assembly.** Cell. 2007 Nov 30;131(5):901-14.

Huh W.K., Falvo J.V., Gerke L.C., Carroll A.S., Howson R.W., Weissman J.S., O'Shea E.K. (2003). **Global analysis of protein localization in budding yeast.** Nature 425(6959):686-91.

Hwa Lim H., Yeong F.M., Surana U. (2003). **Inactivation of mitotic kinase triggers translocation of MEN components to mother-daughter neck in yeast.** Mol Biol Cell. 2003 Nov;14(11):4734-43. Epub 2003 Aug 22.

Janke C., Magiera M.M., Rathfelder N., Taxis C., Reber S., Maekawa H., Moreno-Borchart A., Doenges G., Schwob E., Schiebel E., Knop M. (2004). **A versatile toolbox for PCR-based tagging of yeast genes: new fluorescent proteins, more markers and promoter substitution cassettes.** Yeast. 2004 Aug;21(11):947-62.

Jendretzki A., Ciklic I., Rodicio R., Schmitz H.P., Heinisch J.J. (2009). **Cyk3 acts in actomyosin ring independent cytokinesis by recruiting Inn1 to the yeast bud neck.** Mol Genet Genomics 2009; 282:437-51.

Joazeiro C.A., Weissman A.M. (2000). **RING finger proteins: mediators of ubiquitin ligase activity.** Cell. 2000 Sep 1;102(5):549-52.

Johnson E.S., Blobel G. (1999). **Cell cycle-regulated attachment of the ubiquitin-related protein SUMO to the yeast septins.** J Cell Biol. 1999 Nov 29;147(5):981-94.

Ko N., Nishihama R., Tully G.H., Ostapenko D., Solomon M.J., Morgan D.O., Pringle J.R. (2007). **Identification of yeast IQGAP (Iqg1p) as an anaphase-promoting-complex substrate and its role in actomyosin-ring-independent cytokinesis.** Mol Biol Cell 2007; 18:5139-53.

Kolas N.K., Chapman J.R., Nakada S., Ylanko J., Chahwan R., Sweeney F.D., Panier S., Mendez M., Wildenhain J., Thomson T.M., Pelletier L., Jackson S.P., Durocher D. (2007). **Orchestration of the DNA-damage response by the RNF8 ubiquitin ligase.** Science. 2007 Dec 7;318(5856):1637-40.

Korinek W.S., Bi E., Epp J.A., Wang L., Ho J., Chant J. (2000). **Cyk3, a novel SH3-domain protein, affects cytokinesis in yeast.** Curr Biol 2000; 10:947-50.

Krogh B.O., Symington L.S. (2004). **Recombination proteins in yeast.** Annu Rev Genet. 2004;38:233-71.

Lee P.R., Song S., Ro H.S., Park C.J., Lippincott J., Li R., Pringle J.R., De Virgilio C., Longtine M.S., Lee K.S. (2002). **Bni5p, a septin-interacting protein, is**

required for normal septin function and cytokinesis in *Saccharomyces cerevisiae*. Mol Cell Biol. 2002 Oct;22(19):6906-20.

Lesage G., Shapiro J., Specht C.A., Sdicu A.M., Ménard P., Hussein S., Tong A.H., Boone C., Bussey H. (2005). **An interactional network of genes involved in chitin synthesis in Saccharomyces cerevisiae.** BMC Genet. 2005; 16, 6:8.

Lippincott J., Li R. (1998). **Dual function of Cyk2, a cdc15/PSTPIP family protein, in regulating actomyosin ring dynamics and septin distribution.** J Cell Biol 1998b; 143(7):1947-60.

Lippincott J., Shannon K.B., Shou W., Deshaies R.J., Li R. (2001). **The Tem1 small GTPase controls actomyosin and septin dynamics during cytokinesis.** J Cell Sci. 2001 Apr;114(Pt 7):1379-86.

Longtine M.S., DeMarini D.J., Valencik M.L., Al-Awar O.S., Fares H., De Virgilio C., Pringle J.R. (1996). **The septins: roles in cytokinesis and other processes.** Curr Opin Cell Biol. 1996 Feb;8(1):106-19.

Loring G.L., Christensen K.C., Gerber S.A., Brenner C. (2008). **Yeast Chfr homologs retard cell cycle at G1 and G2/M via Ubc4 and Ubc13/Mms2-dependent ubiquitination.** Cell Cycle. 2008 Jan 1;7(1):96-105.

Luca F.C., Mody M., Kurischko C., Roof D.M., Giddings T.H., Winey M. (2001). **Saccharomyces cerevisiae Mob1p is required for cytokinesis and mitotic exit.** Mol Cell Biol. 2001 Oct;21(20):6972-83.

Mah A.S., Elia A.E., Devgan G., Ptacek J., Schutkowski M., Snyder M., Yaffe M.B., Deshaies R.J. (2005). **Substrate specificity analysis of protein kinase complex Dbf2-Mob1 by peptide library and proteome array screening.** BMC Biochem. 2005 Oct 21;6:22.

Maniatis T., Fritsch E.F., Sambrook J. (1992). **Molecular cloning: a laboratory manual.** Cold Spring Harbor Laboratory Press, Cold Spring Harbor Laboratory, NY. 1992.

Mailand N., Bekker-Jensen S., Faustrup H., Melander F., Bartek J., Lukas C., Lukas J. (2007). **RNF8 ubiquitylates histones at DNA double-strand breaks and promotes assembly of repair proteins.** Cell. 2007 Nov 30;131(5):887-900.

Mazanka E., Alexander J., Yeh B.J., Charoenpong P., Lowery D.M., Yaffe M., Weiss E.L. (2008). **The NDR/LATS family kinase Cbk1 directly controls transcriptional asymmetry.** PLoS Biol. 2008 Aug 19;6(8):e203.

Meitinger F., Petrova B., Lombardi I.M., Bertazzi D.T., Hub B., Zentgraf H., Pereira G. (2010). **Targeted localization of Inn1, Cyk3 and Chs2 by the mitotic-exit network regulates cytokinesis in budding yeast.** J Cell Sci 2010; 123:1851-61.

Meitinger F., Boehm M.E., Hofmann A., Hub B., Zentgraf H., Lehmann W.D., Pereira G. (2011). **Phosphorylation-dependent regulation of the F-BAR protein Hof1 during cytokinesis.** Genes Dev. 2011 Apr 15;25(8):875-88.

Meitinger F., Palani S., Pereira G. (2012). **The power of MEN in cytokinesis.** Cell Cycle. 2012 Jan 15;11(2):219-28.

Meitinger F., Palani S., Hub B., Pereira G. (2013). **Dual function of the NDR-kinase Dbf2 in the regulation of the F-BAR protein Hof1 during cytokinesis.** Mol Biol Cell. 2013 May;24(9):1290-304.

Mendoza M., Norden C., Durrer K., Rauter H., Uhlmann F., Barral Y. (2009). **A mechanism for chromosome segregation sensing by the NoCut checkpoint.** Nat Cell Biol. 2009 Apr;11(4):477-83.

Menssen R., Neutzner A., Seufert W. (2001). **Asymmetric spindle pole localization of yeast Cdc15 kinase links mitotic exit and cytokinesis.** Curr Biol. 2001 Mar 6;11(5):345-50.

Meraldi P., Honda R., Nigg E.A. (2004). **Aurora kinases link chromosome segregation and cell division to cancer susceptibility.** Curr Opin Genet Dev. 2004 Feb;14(1):29-36. Review.

Merlini L., Fraschini R., Hess B., Barral Y., Lucchini G., Piatti S. (2012). **Budding yeast Dma proteins control septin dynamics and the spindle position checkpoint by promoting the recruitment of the Elm1 kinase to the bud neck.** PLoS Genet 2012; 8(4):e1002670.

Michaelis C., Ciosk R., Nasmyth K. (1997). **Cohesins: chromosomal proteins that prevent premature separation of sister chromatids.** Cell. 1997 Oct 3;91(1):35-45.

Moseley J.B., Goode B.L. (2006). **The yeast actin cytoskeleton: from cellular function to biochemical mechanism.** Microbiol Mol Biol Rev. 2006 Sep;70(3):605-45. Review.

Munoz I., Simón E., Casals N., Clotet J., Ariño J. (2003). **Identification of multicopy suppressors of cell cycle arrest at the G1-S transition in Saccharomyces cerevisiae.** Yeast 20(2):157-69.

Murone M., Simanis V. (1996). **The fission yeast dma1 gene is a component of the spindle assembly checkpoint, required to prevent septum formation and premature exit from mitosis if spindle function is compromised.** EMBO J 1996; 15:6605-16.

Nelson B., Kurischko C., Horecka J., Mody M., Nair P., Pratt L., Zougman A., McBroom L.D., Hughes T.R., Boone C., Luca F.C. (2003). **RAM: a conserved signaling network that regulates Ace2p transcriptional activity and polarized morphogenesis.** Mol Biol Cell. 2003 Sep;14(9):3782-803.

Nishihama R., Schreiter J.H., Onishi M., Vallen E.A., Hanna J., Moravcevic K., Lippincott M.F., Han H., Lemmon M.A., Pringle J.R., Bi E. (2009). **Role of Inn1 and its interactions with Hof1 and Cyk3 in promoting cleavage furrow and septum formation in S. cerevisiae.** J Cell Biol 2009; 185:995-1012.

Norden C., Mendoza M., Dobbelaere J., Kotwaliwale C.V., Biggins S., Barral Y. (2006). **The NoCut pathway links completion of cytokinesis to spindle midzone function to prevent chromosome breakage.** Cell. 2006 Apr 7;125(1):85-98.

Oh Y., Bi E. (2011). **Septin structure and function in yeast and beyond.** Trends Cell Biol. 2011 Mar;21(3):141-8.

Oh Y., Chang K.J., Orlean P., Wloka C., Deshaies R., Bi E. (2012). **Mitotic exit kinase Dbf2 directly phosphorylates chitin synthase Chs2 to regulate cytokinesis in budding yeast.** Mol Biol Cell. 2012 Jul;23(13):2445-56.

Oliveira A.P., Ludwig C., Picotti P., Kogadeeva M., Aebersold R., Sauer U., (2012). **Regulation of yeast central metabolism by enzyme phosphorylation.** Mol Syst Biol 8 623 (2012).

Palani S., Meitinger F., Boehm M.E., Lehmann W.D., Pereira G. (2012). **Cdc14-dependent dephosphorylation of Inn1 contributes to Inn1-Cyk3 complex formation.** J Cell Sci. 2012 Jul 1;125(Pt 13):3091-6.

Pan F., Malmberg R.L., Momany M. (2007). **Analysis of septins across kingdoms reveals orthology and new motifs.** BMC Evol Biol. 2007 Jul 1;7:103.

Piatti S., Böhm T., Cocker J.H., Diffley J.F., Nasmyth K. (1996). **Activation of S-phase-promoting CDKs in late G1 defines a "point of no return" after which Cdc6 synthesis cannot promote DNA replication in yeast.** Genes Dev. 1996; 10:1516-31.

Plans V., Guerra-Rebollo M., Thomson T.M. (2008). **Regulation of mitotic exit by the RNF8 ubiquitin ligase.** Oncogene 2008; 27:1355-65.

Pollard TD. (2010). **Mechanics of cytokinesis in eukaryotes.** Curr Opin Cell Biol 2010; 22:50–6.

Ptacek J., Devgan G., Michaud G., Zhu H., Zhu X., Fasolo J., Guo H., Jona G., Breitkreutz A., Sopko R., McCartney R.R., Schmidt M.C., Rachidi N., Lee S.J.,

Mah A.S., Meng L., Stark M.J., Stern D.F., DeVirgilio C., Tyers M., Andrews B., Gerstein M., Schweitzer B., Predki P.F., Snyder M. (2005). **Global analysis of protein phosphorylation in yeast.** Nature 438 (7068) 679-84 (2005).

Raspelli E., Cassani C., Lucchini G., Fraschini R. (2011). **Budding yeast Dma1 and Dma2 participate in regulation of Swe1 levels and localization.** Mol Biol Cell. 2011; 22:2185-97.

Ruchaud S., Carmena M., Earnshaw W.C. (2007). **Chromosomal passengers: conducting cell division.** Nat Rev Mol Cell Biol. 2007 Oct;8(10):798-812.

Sanchez-Diaz A., Marchesi V., Murray S., Jones R., Pereira G., Edmondson R., Allen T., Labib K. (2008). **Inn1 couples contraction of the actomyosin ring to membrane ingression during cytokinesis in budding yeast.** Nat Cell Biol 2008; 4:395-406.

Segal M. (2011). **Mitotic exit control: a space and time odyssey.** Curr Biol. 2011 Oct 25;21(20):R857-9.

Schindelin J. Arganda-Carreras I., Frise E., Kaynig V., Longair M., Pietzsch T., Preibisch S., Rueden C., Saalfeld S., Schmid B., Tinevez J.Y., White D.J., Hartenstein V., Eliceiri K., Tomancak P., Cardona A. (2012). **Fiji: an open-source platform for biological-image analysis.** Nat Methods 2012; 9(7):676-82.

Scolnick D.M., Halazonetis T.D. (2000). **Chfr defines a mitotic stress checkpoint that delays entry into metaphase.** Nature. 2000 Jul 27;406(6794):430-5.

Shannon K.B., Li R. (1999). **The multiple roles of Cyk1p in the assembly and function of the actomyosin ring in budding yeast.** Mol Biol Cell. 1999 Feb;10(2):283-96.

Sherman F. (1991). **Getting started with yeast.** Methods Enzymol 1991; 194:3-21.

Song S., Grenfell T.Z., Garfield S., Erikson R.L., Lee K.S. (2000). **Essential function of the polo box of Cdc5 in subcellular localization and induction of cytokinetic structures.** Mol Cell Biol 2000; 20:286-98.

Stegmeier F., Amon A. (2004). **Closing Mitosis: The Functions of the Cdc14 Phosphatase and Its Regulation.** Annu Rev Genet 2004; 38:203-232.

Steigemann P., Wurzenberger C., Schmitz M.H., Held M., Guizetti J., Maar S., Gerlich D.W. (2009). **Aurora B-mediated abscission checkpoint protects against tetraploidization.** Cell. 2009 Feb 6;136(3):473-84.

Shaw J.A., Mol P.C., Bowers B., Silverman S.J., Valdivieso M.H., Durán A., Cabib E. (1991). **The function of chitin synthases 2 and 3 in the Saccharomyces cerevisiae cell cycle.** J Cell Biol. 1991 Jul;114(1):111-23.

Sullivan M., Morgan D.O. (2007). **Finishing mitosis, one step at a time.** Nat Rev Mol Cell Biol. 2007 Nov;8(11):894-903.

Tuttle R.L., Bothos J., Summers M.K., Luca F.C., Halazonetis T.D. (2007). **Defective in mitotic arrest 1/ring finger 8 is a checkpoint protein that antagonizes the human mitotic exit network.** Mol Cancer Res. 2007 Dec;5(12):1304-11.

Vallen E.A., Caviston J., Bi E. (2000). **Roles of Hof1p, Bni1p, Bnr1p, and myo1p in cytokinesis in Saccharomyces cerevisiae.** Mol Biol Cell. 2000 Feb;11(2):593-611.

van der Waal M.S., Hengeveld R.C., van der Horst A., Lens S.M. (2012). **Cell division control by the Chromosomal Passenger Complex.** Exp Cell Res. 2012 Jul 15;318(12):1407-20.

Visintin R., Craig K., Hwang E.S., Prinz S., Tyers M., Amon A. (1998). **The phosphatase Cdc14 triggers mitotic exit by reversal of Cdk-dependent phosphorylation.** Mol Cell. 1998 Dec;2(6):709-18.

Wach A., Brachat A., Pohlmann R., Philippsen P. (1994). **New heterologous modules for classical or PCR-based gene disruptions in Saccharomyces cerevisiae.** Yeast 1994; 10:1793-808.

Weiss E.L. (2012). **Mitotic exit and separation of mother and daughter cells.** Genetics. 2012 Dec;192(4):1165-202.

Wloka C., Nishihama R., Onishi M., Oh Y., Hanna J., Pringle J.R., Krauss M., Bi E. (2011). **Evidence that a septin diffusion barrier is dispensable for cytokinesis in budding yeast.** Biol Chem. 2011 Aug;392(8-9):813-29.

Wloka C., Bi E. (2012). **Mechanisms of cytokinesis in budding yeast.** Cytoskeleton (Hoboken). 2012 Oct;69(10):710-26.

Xu S., Huang H.K., Kaiser P., Latterich M., Hunter T. (2000). **Phosphorylation and spindle pole body localization of the Cdc15p mitotic regulatory protein kinase in budding yeast.** Curr Biol 2000; 10:329-32

Yaffe M.P., Schatz G. (1984). **Two nuclear mutations that block mitochondrial protein import in yeast.** Proc Natl Acad Sci U S A. 1984; 81:4819-23.

Yanagida M. (1998). **Fission yeast cut mutations revisited: control of anaphase.** Trends Cell Biol. 1998 Apr;8(4):144-9. Review.

Yeong F.M. (2005). **Severing all ties between mother and daughter: cell separation in budding yeast.** Mol Microbiol. 2005; 55:1325-31.

Yoshida S., Asakawa K., Toh-e A. (2002). **Mitotic exit network controls the localization of Cdc14 to the spindle pole body in Saccharomyces cerevisiae.** Curr Biol. 2002 Jun 4;12(11):944-50.

Zachariae W., Schwab M., Nasmyth K., Seufert W. (1998). **Control of cyclin ubiquitination by CDK-regulated binding of Hct1 to the anaphase promoting complex.** Science. 1998 Nov 27;282(5394):1721-4.